The Dissertation Committee for Timothy John Young

certifies that this is the approved version of the following dissertation:

Supercritical Fluid Spray Processes for Microencapsulation and Formation of Submicron Aqueous Dispersions of Pharmaceutical Compounds

Committee:

Keith P. Johnston, Supervisor

Robert O. Williams III

C. Buddie Mullins

Brian A. Korgel

William J. Koros

Supercritical Fluid Spray Processes for Microencapsulation and Formation of Submicron Aqueous Dispersions of Pharmaceutical Compounds

by

Timothy John Young, B.S.Ch.E.

Dissertation

Presented to the Faculty of the Graduate School of

The University of Texas at Austin

in Partial Fulfillment

of the Requirements

for the Degree of

Doctor of Philosophy

The University of Texas at Austin

December, 2003

Dedication

To the memory of

William P. Young

Charles Metzler

Acknowledgements

First, I would like to thank my advisor, Dr. Keith P. Johnston, for his invaluable assistance and guidance throughout this effort. I would also like to thank Dr. Robert Williams III, Dr. C. Mullins, Dr. Brian Korgel, and Dr. William Koros for their contributions as members of my dissertation committee. Also, I would like to thank Dr. Stephen Webber for his assistance and numerous discussions surrounding particle size analysis.

I would like to thank the members of the supercritical fluid group, especially Matt Yates, Sandro da Rocha, Petros Psathas, Xiaoxia Chen, Ted Lee, Kirk Ziegler, Jae-Jin Shim, Gunilla Jacobson, and Lourdes Calvo. Your friendship and companionship was greatly appreciated. I would also like to thank members of other groups who provided support, contributions, and collaborations during my graduate studies: Melisa Barron, True Rogers, Jiahui Hu, Melanie Batarseh, Stefan Martula, Paul Atkinson, and Kim Ebers.

I would like to thank the members of the Chemcial Engineering Dept. staff, especially Mark Smith, Durrell Haynes, Eddie Oliver, Eddie Ibarra, "T" Stockman, Chris Bailor for helping me with all the things I couldn't do on my own. I'd also like to thank John Mendenhall for teaching me everything I know about TEM/SEM.

I would like to acknowledge support from RTP Pharma, Inc., the Separations Research Program at the University of Texas at Austin, and the National Science Foundation. I would also like to thank ISCO corporation.

Finally, many thanks to my family: Mom, Dad, Li'l Sis, and Grandma. Without your love and support, this would never have been possible. This thesis is dedicated to my grandfathers, who taught me the meaning of the word "perseverance."

Supercritical Fluid Spray Processes for Microencapsulation and Formation of Submicron Aqueous Dispersions of Pharmaceutical Compounds

Publication No._____

Timothy John Young, Ph.D.

The University of Texas at Austin, 2003

Supervisor: Keith P. Johnston

Precipitation with a Compressed Fluid Antisolvent (PCA) and Rapid Expansion from Supercritical Solution (RESS) are two processes based on supercritical fluids that are capable of producing submicron particles. Novel variations of these basic processes have been examined to produce stable particles of various pharmaceutical compounds.

PCA is an antisolvent precipitation technique where an organic solution of drug + polymer in solvent is atomized (sprayed) into supercritical (SC) CO_2. Upon liquid mixing, the solute materials precipitate to form microparticles. A Vapor-over-Liquid technique has been used to produce larger, uniform particle sizes of biodegradable polymers. By suspending a protein in the solvent phase, the protein can be encapsulated/coated by the precipitating polymer.

RESS is a process by which a homogeneous solution at supercritical conditions is sprayed through an expansion nozzle to atmospheric conditions. The resultant change in phase leads to the precipitation of the solute materials. The production of extremely small particles (<50 nm) have been predicted but rarely demonstrated. Typically, particle growth occurs to form larger (~1 μm) particles. A novel adaptation was developed, dubbed RESAS (Rapid Expansion from Supercritical to Aqueous Solution), wherein the expansion is conducted within an aqueous environment. The aqueous phase can contain surfactant or lipid stabilizers to capture and preserve submicron particles of water-insoluble drug actives in the form of a suspension.

Table of Contents

List of Tables

List of Figures

CHAPTER 1

Introduction

The overall objective of this thesis is to use supercritical fluid-based spray methods to produce submicron materials of pharmaceutical compounds. This introductory chapter reviews the properties of supercritical CO_2 and two spray techniques used to make submicron particles. Also, an outline of individual topics to be discussed in later chapters is presented.

1.1 SUPERCRITICAL CO_2

A material is defined as being supercritical (SC) when the temperature and pressure of the system are above the critical point of the fluid. A supercritical fluid has properties between those of a gas and a liquid, and are often referred as having gas-like properties at liquid-like densities. A phase diagram for carbon dioxide (CO_2) is shown in Figure 1.1.

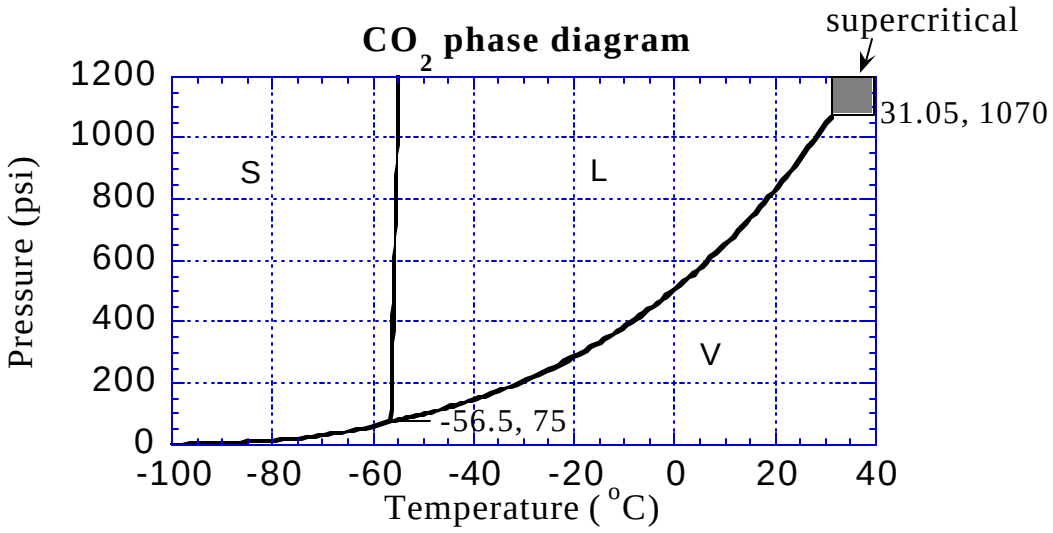

Figure 1.1 Pressure-temperature phase diagram for CO_2. The supercritical region is blocked out.

The physical properties of SC CO_2 can be demonstrated by examining the density as a function of temperature and pressure at and above the critical point, as is shown in Figure 1.2. At subcritical conditions the density changes only slightly until the phase change occurs from gas to liquid. At supercritical conditions, the density dramatically changes over a continuum from low to high density. The most dramatic change in density with pressure is seen just slightly above the critical temperature. As temperature increases, the effect of pressure lessens, and extremely high pressures are required to achieve liquid-like densities. Similar behavior is observed for other physical properties like viscosity, diffusivity, and solubility parameter.[1] When using SC CO_2 as a solvent, this dramatic change in density can be used to "tune" the solvent's properties.

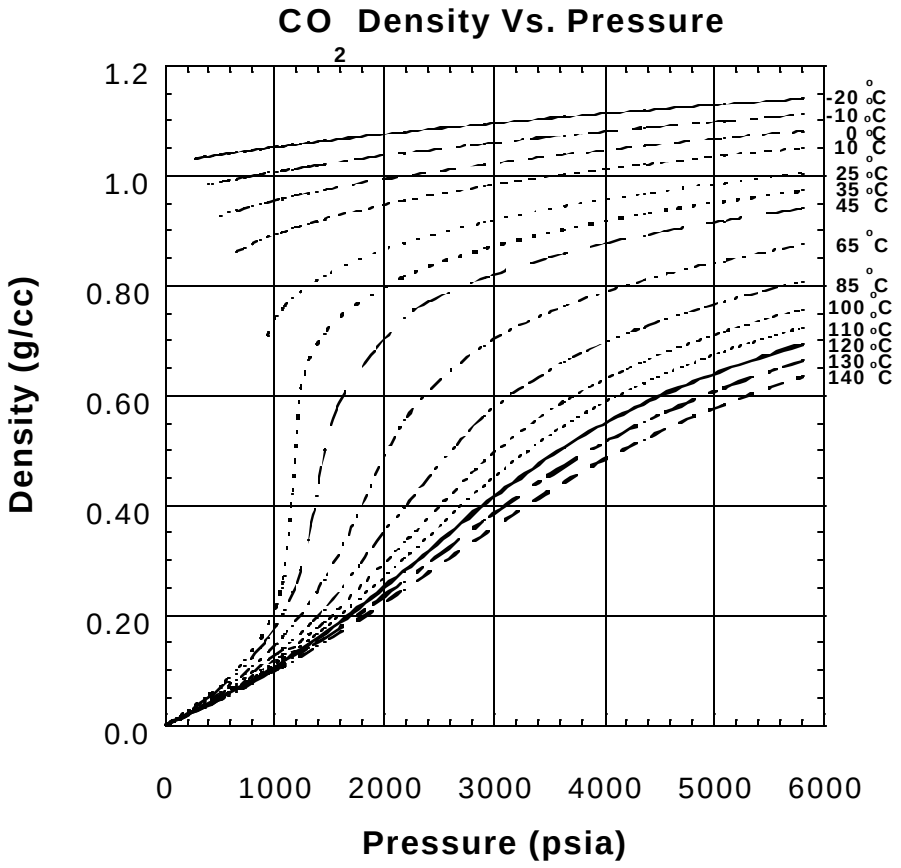

Figure 1.2 Density of CO_2 as a function of temperature and pressure.

There are several advantages of CO_2-based processes. CO_2 is being used to replace many traditional organic solvents and CFC's since it is essentially

nontoxic, inflammable, inexpensive, and environmentally friendly. It also has relatively mild critical conditions, Tc = 31 °C, Pc = 73.8 bar, and so allows processing at moderate temperatures to prevent thermal degradation. Because it is a gas at room temperature and atmospheric pressure, there is little or no residual solvent left in the materials after processing. Also, since diffusivities in CO_2 tend to be higher than for conventional liquids, higher degees of supersaturation can be achieved in precipitation techniques relying on solvent mixing.

1.2 PRECIPITATION WITH A COMPRESSED FLUID ANTISOLVENT (PCA)

Precipitation of a solute from solution to form microparticles by addition of a liquid antisolvent is well known. The liquid antisolvent is chosen such that it is miscible with the primary solvent, yet when combined with the solvent, results in a lowering of the solubility of the solute. Thus, the solute precipitates. The morphology of the resultant particles can be controlled by the conditions at which the antisolvent addition is carried out, i.e. temperature, rate, drop size, etc. Recently, as an alternative to conventional organic liquids, microparticles have been formed by precipitation with compressed CO_2 in the liquid and supercritical fluid states.[2-18] The PCA process consists of atomizing a solution into compressed liquid or supercritical fluid CO_2 as represented in Figure 1.3. The atomization process may be accomplished by spraying at high velocities through a small nozzle (typically 100 μm) or by sonication[14] through a larger nozzle. The organic solvent diffuses rapidly into the bulk CO_2 phase, while CO_2 diffuses into the droplets, thereby precipitating the polymer. The rate of diffusion in both

directions and thus the degree of supersaturation are higher than in the case of conventional liquid antisolvents, often resulting in submicron to micron-sized particles. A more in-depth analysis of the mechanism behind particle formation in the PCA process is given in Chapter 2. More viscous polymer solutions at higher polymer concentrations lead to fibers with micron-sized features.[4,8] Several studies have shown very low concentrations of residual solvent in the product materials, especially after a CO_2 extraction step upon completion of the spray.[19-22]

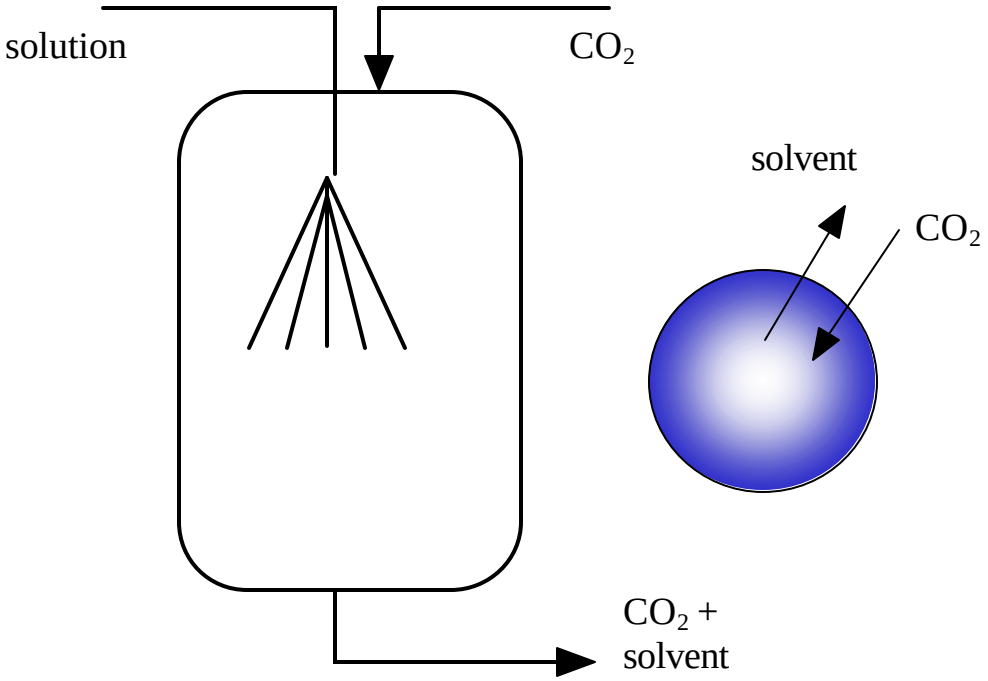

Figure 1.3 Schematic diagram of the Precipitation with a Compressed Fluid Antisolvent (PCA) process.

Microspheres may be formed for semicrystalline polymers like poly(l-lactic acid) (l-PLA) without flocculation and agglomeration at 40 °C.[19,23,9,11,13,15-16] Amorphous polymers, on the other hand, such as polystyrene (PS),[3,10,12] poly(methyl methacrylate) (PMMA),[10] and poly(dl-lactide-*co*-glycolide) (PGLA)[9] often flocculate and agglomerate. The loss of individual particles is a result of plasticization of the polymer by CO_2, which can be further influenced by residual solvent in CO_2. CO_2 can depress the T_g of PMMA by 100 °C below the normal value of 105 °C.[10,24] Upon exposure of PS to CO_2, the temperature at which stationary particles agglomerate corresponds closely with the depressed T_g.[5] For PGLA, agglomeration was present from 0 to 23 °C.[9] Severe agglomeration can occur when poly(d,l-lactide) microspheres precipitate from toluene solution by addition of isopropanol as the phase separating agent.[25] However, at temperatures between -40 °C and -100 °C the microspheres become sufficiently firm to avoid agglomeration.

1.3 RAPID EXPANSION FROM SUPERCRITICAL SOLUTION (RESS)

In rapid expansion from supercritical solution (RESS), nucleation and crystallization are triggered by reducing the solvent density, or solvent strength, through expansion to atmospheric conditions.[26-37] Typically, the solution is sprayed through a 10-50 μm i.d. nozzle with an aspect ratio (L/D) of 5-100. A schematic diagram representing the RESS process is provided in Figure 1.4. This process has been used successfully to form a variety of microparticles and microfibrils from polymers, drugs, and inorganic compounds. Dissolution rates

of poorly-water soluble drugs may be increased by reducing the particle size, to increase the surface area, and by inhibiting crystallization to form amorphous particles. Both of these factors may be achieved by RESS according to theoretical models of nucleation. The particle formation steps include nucleation, condensation of solute molecules about the nuclei and coagulation of particles in the free jet expansion. The particle morphology has been linked to the location of the occurrence of the precipitation conditions (i.e. density), whether in the preheater, nozzle entrance, nozzle body, or in the free jet expansion. Also, it is theorized that if coagulation can be minimized, it should be possible to produce 20-50 nm particles.[38-39] The inability to approach the theoretical lower limit is likely due to particle growth during collisions in the free jet.[38] In cases where a cosolvent is used, the particle size tends to be higher, either from a difference in supersaturation level or the presence of residual solvent "wetting" the particles. Recent work by Charoenchaitrakool et al.[40] has produced 2.5 μm particles by RESS with enhanced dissolution rates for the poorly water-soluble compound ibuprofen, likely due to both the reduction in particle size and crystallinity.[40] A summary of some recent work conducted with RESS of drug compounds is provided in Table 1.1.[30,31,37,41-43]

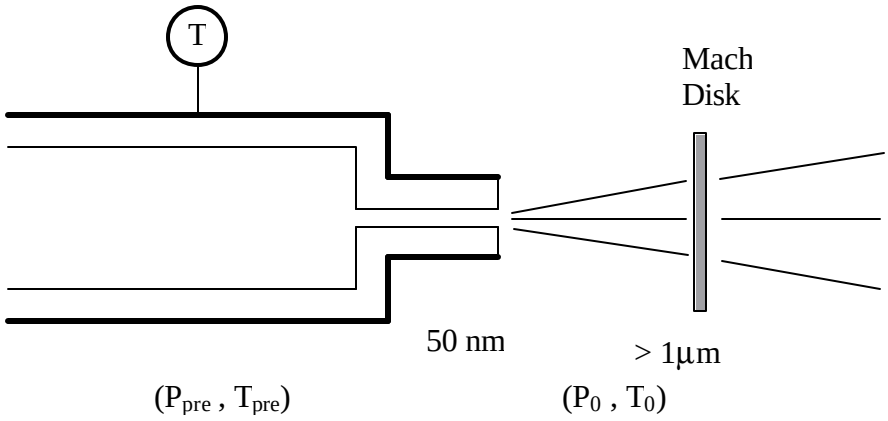

Figure 1.4 Schematic diagram of the Rapid Expansion from Supercritical Solution (RESS) process.

Table 1.1 Summary of solubilities and RESS studies of some pharmaceutical compounds in CO_2.

Solute	**Cosolvent**	**Solubility Mass fraction (10^4)**	**T (°C)**	**P (bar)**	**Mean particle Diameter (μm)**
Mevinolin		0.09-3.4	55	125-409	0.1-0.3
Mevinolin	5 % MeOH	10-45	40	103-379	10-50
Salicylic acid		2.6-21	60	115-325	2-20
Theophylline			65	225	0.4
Naproxen		0.4-0.5	60	138-180	1-15
Progesterone		0.6-52	60	115-240	4-9

1.4 THESIS OUTLINE

Chapter 1 covers work conducted using the Vapor-over-Liquid Precipitation with a Compressed fluid Antisolvent (V/L PCA) technique for encapsulation of active compounds into polymers. Lysozyme was encapsulated in biodegradable polymer microspheres which were precipitated from an organic solution by spraying the solution into carbon dioxide. The polymer, either poly(l-lactide) (l-PLA) or poly(dl-lactide-*co*-glycolide) (PGLA), in dichloromethane solution with suspended lysozyme was sprayed into a CO_2 vapor phase through a capillary nozzle to form droplets which solidified after falling into a CO_2 liquid phase. By delaying precipitation in the vapor phase, the primary particles became sufficiently large, from 5 to 70 μm, such that they could encapsulate the lysozyme. At an optimal temperature of -20 °C, the polymer solution mixed rapidly with CO_2, and the precipitated primary particles were sufficiently hard such that agglomeration was reduced markedly compared with higher temperatures. More uniform particles were formed by flowing CO_2 at high velocity in a coaxial nozzle to mix the droplets at the CO_2 vapor-liquid interface. This process offers a means to produce encapsulated proteins in poly(dl-lactide-*co*-glycolide) microspheres without earlier limitations of massive polymer agglomeration and limited protein solubility in organic solvents.

In Chapter 2, stable suspensions of submicron particles of cyclosporine, a water-insoluble drug, produced by Rapid Expansion from Supercritical to Aqueous Solution (RESAS) are discussed. To minimize growth of the

cyclosporine particles, which would otherwise occur in the free jet expansion, the solution was sprayed into an aqueous Tween-80 (Polysorbate-80) solution. Steric stabilization by the surfactant impedes particle growth and agglomeration. The particles were an order of magnitude smaller than those produced by RESS into air without the surfactant solution. Concentrations as high as 38 mg/mL for 400-700 nm particles were achieved in a 5.0 % (w/w) Tween-80 solution.

In Chapter 3, RESAS has been used to form stable suspensions of submicron particles of cyclosporine A with new surfactant systems based on phospholipid vesicles to suspend the particles and minimize growth due to particle coagulation during the expansion process. The ability for the surfactant molecules to orient at the surface of the particles and provide steric stabilization could be manipulated by changing process variables including temperature and suspension concentration. Suspensions with high payloads (up to 54 mg/mL) could be achieved with a mean diameter of 500 nm and particle size distribution ranging from 40-920 nm.

1.5 REFERENCES

(1) McHugh, M. A.; Krukonis, V. J. *Supercritical Fluid Extraction Principles and Practice*; 2nd ed.; Butterworths: Stoneham, MA, **1994**

(2) Dixon, D. J. *Formation of Polymer Materials by Precipitation with a Compressed Fluid Antisolvent*; University of Texas at Austin: Austin, Texas **1992.**

(3) Dixon, D. J.; Johnston, K. P.; Bodmeier, R. P. *AIChe Journal* **1993**, 39, 127-139.

(4) Dixon, D. J.; Johnston, K. P. *Journal of Applied Polymer Science* **1993**, 50, 1929-1942.

(5) Dixon, D. J.; Luna-Barcenas, G.; Johnston, K. P. *Polymer* **1994**, 35, 3998 - 4005.

(6) Yeo, S. D.; Lim, G. B.; Debenedetti, P. G.; Bernstein, H. *Biotechnology and Bioengineering* **1993**, 41, 341-346.

(7) Yeo, S.-D.; Debenedetti, P. G.; Radosz, M.; Schmidt, H.-W. *Macromolecules* **1993**, 26, 6207-6210.

(8) Luna-Barcenas, G.; Kanakia, S. K.; Sanchez, I. C.; Johnston, K. P. *Polymer* **1995**, 36, 3173-3182.

(9) Bodmeier, R. P.; Wang, H.; Dixon, D. J.; Mawson, S.; Johnston, K. P. *Pharmaceutical Research* **1995**, 12, 1211-1217.

(10) Mawson, S.; Johnston, K. P.; Betts, D. E.; McClain, J. B.; DeSimone, J. M. *Macromolecules* **1997**, 30, 71-77.

(11) Mawson, S. *The Formation and Characterization of Polymeric Materials Precipitated by CO2-Based Spray Processes*; University of Texas at Austin: Austin,Texas **1996**.

(12) Mawson, S.; Kanakia, S.; Johnston, K. P. *Journal of Applied Polymer Science* **1997**.

(13) Mawson, S.; Kanakia, S.; Johnston, K. P. *Polymer* **1997**, 38, 2957-2967.

(14) Falk, R.; Randolph, T.; Meyer, J. D.; Kelly, R. M.; Manning, M. C. *Journal of Controlled Release* **1997**, 44, 77-85.

(15) Winters, M. A.; Knutson, B. L.; Debenedetti, P. B.; Sparks, H. G.; Przybycien, T. M.; Stevenson, C. L.; Prestrelski, S. J. *Journal of Pharmaceutical Sciences* **1996**, 85, 586-594.

(16) Bleich, J.; Kleinebudde, P.; Müller, B. W. *International Journal of Pharmaceutics* **1994**, 106, 77-84.

(17) Bleich, J.; Müller, B. W. *Journal of Microencapsulation* **1996**, 13, 131-9.

(18) Fischer, W.; Müller, B. W. United States 5043280, **1991**

(19) Randolph, T. W.; Randolph, A. J.; Mebes, M.; Yeung, S. *Biotechnology Progress* **1993**, 9, 429-435.

(20) Steckel, H.; Thies, J.; Müller, B. W. *International Journal of Pharmaceutics* **1997**, 152, 99-110.

(21) Ruchatz, F.; Kleinebudde, P.; Müller, B. W. *Journal of Pharmaceutical Sciences* **1997**, 86, 101-5.

(22) Falk, R. F.; Randolph, T. W. *Pharmaceutical Research* **1998**, 15, 1233-7.

(23) Chou, Y. H.; Tomasko, D. L. *GAS Crystallization of Polymer-Pharmaceutical Composite Particles*; International Society for the Advancement of Supercritical Fluids: Sendai, Japan, **1997**; Vol. A, pp 55-7.

(24) Condo, P. D.; Paul, D. R.; Johnston, K. P. *Macromolecules* **1994**, 27, 365-371.

(25) Fong, J. W. United States 4166800, **1979**

(26) Subramaniam, B.; Rajewski, R. A.; Snavely, K. *Journal of Pharmaceutical Sciences* **1997**, *86*, 885-90.

(27) Phillips, E. M.; Stella, V. J. *International Journal of Pharmaceutics* **1992**, *94*, 1-10.

(28) Tom, J. W.; Debenedetti, P. G. *The Journal of Supercritical Solutions* **1994**, *7*, 9-29.

(29) Mawson, S.; Johnston, K. P.; Combes, J. R.; DeSimone, J. M. *Macromolecules* **1995**, *28*, 3182-3191.

(30) Alessi, P.; Cortesi, A.; Kikic, I.; Foster, N. R.; Macnaughton, S. J.; Colombo, I. *Industrial and Engineering Chemistry Research* **1996**, *35*, 4718-4726.

(31) Mohamed, R. S.; Halverson, D. S.; Debenedetti, P. G.; Prud'homme, R. K. in *Supercritical Fluid Science and Technology*; Johnston, K. P. and Penninger, J. M. L., Ed.; American Chemical Society: Washington D.C., **1989**; Vol. 406, pp 355-78.

(32) Matson, D. W. *Chemtech* **1989**, *19*, 480-6.

(33) Chang, C. J.; Randolph, A. D. *AIChE Journal* **1989**, *35*, 1876-82.

(34) Domingo, C.; Berends, E.; van Rosmalen, G. M. *Journal of Supercritical Fluids* **1997**, *10*, 39-55.

(35) Lele, A. K.; Shine, A. D. *Ind. Eng. Chem. Res.* **1994**, *33*, 1476-1485.

(36) Krukonis, V. J. in *Supercritical Fluid Extraction and Chromatography: Techniques and Applications*; Chapentier, B. A. and Sevenants, M. R., Ed.; American Chemical Society: Washington, D.C., **1988**; Vol. 366, pp 26-43.

(37) Kim, J. H.; Paxton, T. E.; Tomasko, D. L. *Biotechnology Progress* **1996**, *12*, 650-61.

(38) Debenedetti, P.G. In *Supercritical Fluids: Fundamentals for Application* (Vol. 273) (Kiran, E. and Levelt Sengers, J.M.H., eds.), **1994**, pp. 719-729, Kluwer Academic Publishers

(39) Weber, M. and Thies, M. **2001,** *Personal Communication*

(40) Charoenchaitrakool, M. et al. *Ind. Eng. Chem. Res.* **2000**, 39 (4794-802)

(41) Larson, et al. *Biotechnol. Prog*. **1996**

(42) Reverchon, et al. *J. Supercrit. Fluids* **1993**, *6*, pp.241-8

(43) Subra, et al. *High Pressure Chemical Engineering* **1996**, *12* pp.49-54

CHAPTER 2

Encapsulation of Lysozyme in a Biodegradable Polymer by Precipitation with a Vapor-Over-Liquid Antisolvent

2.1 INTRODUCTION

Microencapsulation of pharmaceutical compounds in biodegradable polymer particles is of great interest for controlled-release in oral, inhalation or injection methods of delivery. Typical methods of microencapsulation include emulsion-solvent-extraction, spray-drying, and phase-separation techniques.[1-7] Potential drawbacks associated with these techniques include the use of toxic organic solvents for solubility, residual solvent in the microspheres, low encapsulation efficiencies due to partitioning of the pharmaceutical compound between two immiscible phases, and denaturation. The biodegradable homopolymers poly(l-lactic acid), poly(dl-lactic acid), poly(glycolic acid), and copolymers of these have been of particular interest as carrier substances.[8-13]

Several supercritical fluid processes have been utilized to form microparticles of polymers and pharmaceutical compounds. To manipulate particle morphology, the solvent power of compressed CO_2 can be changed by adjusting the temperature and pressure.[14-15] The critical conditions of CO_2 are

easily attainable, i.e. T_C = 31 °C and P_C = 73.8 bar. This environmentally benign solvent is essentially non-toxic, non-flammable, and inexpensive. Phase separation techniques based upon supercritical fluids include: rapid expansion from supercritical solution (RESS),[13,16-27] gas antisolvent recrystallization (GAS),[27-30] and precipitation with a compressed fluid antisolvent (PCA),[31-43] also known as aerosol solvent extraction system (ASES)[44-47] or supercritical antisolvent technique (SAS).[44] RESS is useful for materials which are soluble in CO_2. Unfortunately, CO_2, with no dipole moment and a very low polarizability, is a very weak solvent and dissolves very few polymers.[48-49] RESS of a highly soluble polymer, poly(1,1,2,2-tetrahydroperfluorodecylacrylate), from CO_2 produced submicron particles and fibers.[24]

Recently, microparticles have been formed by precipitation with compressed CO_2 in the liquid and supercritical fluid states.[31-47] The PCA process consists of atomizing a solution into compressed liquid or supercritical fluid CO_2. The atomization process may be accomplished by spraying at high velocities through a small nozzle (typically 100 μm) or by sonication[43] through a larger nozzle. The organic solvent diffuses rapidly into the bulk CO_2 phase, while CO_2 diffuses into the droplets, thereby precipitating the polymer. The rate of diffusion in both directions and thus the degree of supersaturation are higher than in the case of conventional liquid antisolvents, often resulting in submicron to micron-sized particles. More viscous polymer solutions at higher polymer concentrations lead to fibers with micron-sized features.[33,37] Several studies have shown very

low concentrations of residual solvent in the product materials, especially after a CO_2 extraction step upon completion of the spray.[29,50-52]

Microspheres may be formed for semicrystalline polymers like poly(l-lactic acid) (l-PLA) without flocculation and agglomeration at 40 °C.[29-30,38, 41,43,45-46] Amorphous polymers, on the other hand, such as polystyrene (PS),[32,39,41] poly(methyl methacrylate) (PMMA),[39] and poly(dl-lactide-*co*-glycolide) (PGLA)[38] often flocculate and agglomerate. The loss of individual particles is a result of plasticization of the polymer by CO_2, which can be further influenced by residual solvent in CO_2. CO_2 can depress the T_g of PMMA by 100 °C below the normal value of 105 °C.[39,53] Upon exposure of PS to CO_2, the temperature at which stationary particles agglomerate corresponds closely with the depressed T_g.[34] For PGLA, agglomeration was present from 0 to 23 °C.[38] Severe agglomeration can occur when poly(d,l-lactide) microspheres precipitate from toluene solution by addition of isopropanol as the phase separating agent.[54] However, at temperatures between -40 °C and -100 °C the microspheres become sufficiently firm to avoid agglomeration.

A novel variation of the PCA process was used to form hollow spheres (microballoons) of polystyrene from polystyrene in toluene solutions with concentrations above 6 wt.%. [34] In this case the cell was filled only partially with liquid CO_2, with its equilibrium vapor phase above it. The solution was atomized in the vapor phase and the droplets subsequently fell into the liquid phase where they solidified. By delaying precipitation in the vapor phase hollow microspheres were formed. The microballoons were slightly larger than the diameter of the

nozzle, and it is conceivable that they could be used to encapsulate a pharmaceutical compound.

A key challenge in the PCA process is to maintain the biological activity of proteins, peptides, and enzymes.[35] The dissolution of insulin, lysozyme, and trypsin into a typical solvent for PCA, like DMSO, denatures these proteins, probably due to a change in conformation.[55] Each of these materials remained denatured after processing via PCA. The bioactivity of certain proteins such as insulin and lysozyme recover upon redissolution into an aqueous environment, suggesting the interactions causing denaturation can be partially reversible.[44,56] A recent study also suggests that long-term storage of proteins which have been denatured by supercritical fluid processing, such as lysozyme, does not severely alter the stability and ability to recover bioactivity.[57]

The objective of this study was to encapsulate chicken egg-white lysozyme into uniform 50-100 μm poly(dl-lactide-*co*-glycolide) (PGLA) spheres. Smaller particles would be too small to encapsulate a significant number of 5-10 μm protein particles for controlled-release purposes. Larger particles would be undesirable for certain administration methods, for example parenteral administration requires particles <100 μm in diameter.[58] The first part of this study examines the particle morphology for PGLA particles formed by PCA without any protein present. To produce larger primary particles than the 1-5 μm particles typically produced by PCA in liquid or supercritical CO_2,[31-32,35-36,38-42,44-45,59] we chose to delay precipitation by spraying into a CO_2 vapor phase above a CO_2 liquid phase. Another goal was to achieve high enough local concentrations

of polymer in the droplets striking the CO_2 liquid phase to allow significant particle growth, while avoiding agglomeration. To attempt to minimize agglomeration caused by plasticization of the polymer by CO_2, the temperature was varied from 23 to -40 °C. The effects of nozzle diameter, solution flowrate, CO_2 flowrate, and solution concentration were also evaluated. In the second part, we address microencapsulation of chicken egg-white lysozyme into the polymer particles. Lysozyme was suspended in dichloromethane, in contrast with earlier studies where a protein was dissolved in an organic solvent.[27,30,38,43,46] Suspensions may be formed for a broad range of peptides and proteins, many of which are insoluble in organic solvents. Suspension of a protein in an organic solvent typically produces less denaturation than dissolution. The knowledge gained from the study of PGLA particle formation in the first part was utilized to encapsulate lysozyme in non-agglomerated particles with diameters in the 50-100 μm range as desired. In both parts of this study, separate sections are presented to delineate between experiments in static (non-flowing) and flowing CO_2.

2.2 EXPERIMENTAL

2.2.1 Materials

Semicrystalline poly(l-lactic acid) (l-PLA) (MEDISORBTM 100L, Stolle-Dupont Co. Cincinnati, OH) had a M_W of 94,100 and a M_W/M_n of 1.85. Poly(dl-lactide-co-glycolide) (PGLA) was purchased from Birmingham Polymers, Inc. (Birmingham, AL) and had a M_W of 30,000. Chicken egg-white lysozyme

(Sigma, St. Louis, MO) was spray-dried from aqueous solution to form 1-10 μm particles. Ruthenium tetroxide (Electron Microscopy Sciences, Fort Washington, PA), reagent grade dichloromethane and bone dry grade CO_2 were used as received.

2.2.2 Apparatus

The apparatus for precipitation with compressed CO_2, shown in Figure 2.1, is based upon earlier designs.[32,39] The solutions were sprayed into a 1.27 cm. i.d. sapphire tube with a volume of 13 mL. This tube allowed visual observation of skin formation in falling droplets, jet dynamics and polymer precipitation. Visual observations proved invaluable in optimizing the PCA process. A thermostated water bath was utilized for experiments performed above 0 °C, while a dry ice-ethanol bath was used for subzero temperatures. For all experiments, the CO_2 level inside the cell was maintained 1 cm. below the tip of the spray nozzle. The CO_2 inlet line (30 feet long, 0.030 inch i.d. by 1/16 inch o.d.) was immersed in the bath to equilibrate the CO_2 temperature prior to introduction into the cell.

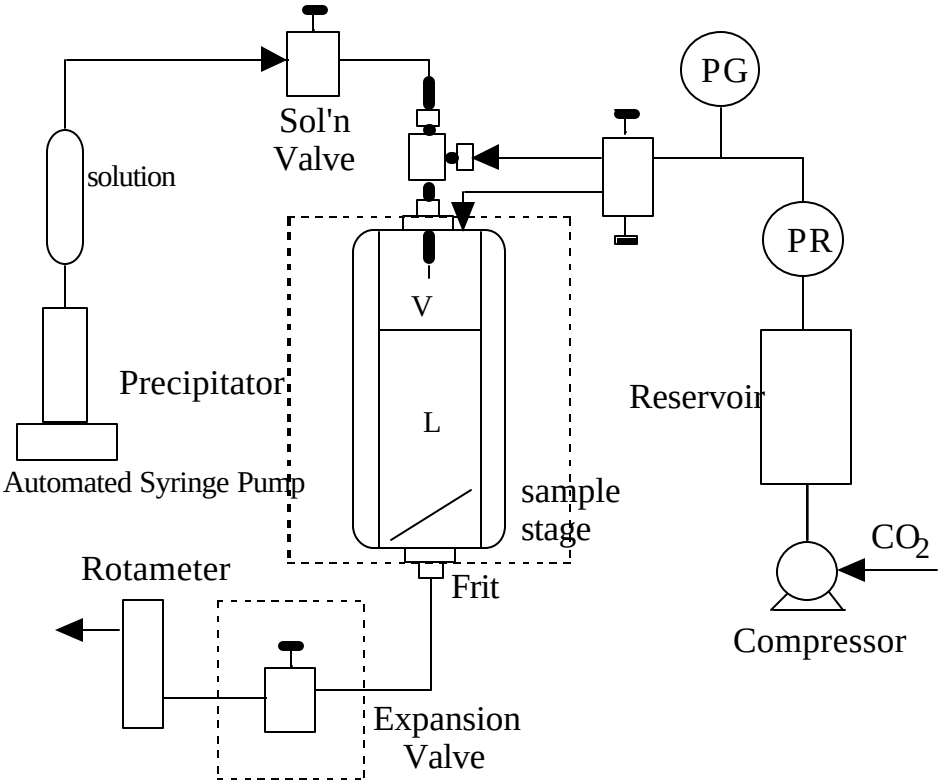

Figure 2.1. Schematic of the apparatus for precipitation with a vapor-over-liquid compressed fluid antisolvent.

A cylindrical tube (1" o.d. by 11/16" i.d. by 8" long, Autoclave Engineers, model CNLX 1608-316) rated up to 689 bar equipped with a piston was used to pressurize the polymer solution. This tube was pressurized with dichloromethane by using a computer-controlled syringe pump (ISCO, model 260D). The polymer solution was sprayed into the cell via a 100 µm i.d. fused silica capillary tube or a 0.030" i.d. stainless steel tube. In all cases, the nozzle length was 6 1/2". Nozzles smaller than 100 µm could not be used because they were plugged by the

suspended lysozyme particles. To insure smoothness, the capillary tips were inspected with a microscope. The lysozyme was suspended in the polymer solution by using an ultrasonic bath.

To collect particles, two small rectangular glass plates (1" by 1/4"), slanted at an angle of 60 degrees, were stacked in the bottom of the cell with approximately 5 mm between them. These glass plates were partially covered with double-sided carbon conductive tape. Also, a 1/4" diameter 0.5 μm filter was placed in the CO_2 effluent line at the base of the precipitation cell.

The solution flow rate was controlled with the automated syringe pump, and in most cases the solution was dripped into the cell at 0.1-1.0 mL/min. The solution was injected into a vapor CO_2 phase residing above a liquid CO_2 phase. In some cases, the solution flowrate was increased to ~1.8 mL/min where the solution no longer dripped, but instead streamed into the cell. This stream subsequently broke up into smaller droplets upon contacting the CO_2 liquid surface. For most cases, the CO_2 was not flowing. In experiments with flowing CO_2, the CO_2 entered the cell either through a port in the top of the cell or through an annular region in a coaxial nozzle, described in detail elsewhere.[41] The CO_2 flow rate was controlled by a needle valve (Whitey, SS-21RS4) in the effluent line and measured by a rotameter (Omega, model FLT-40ST). To prevent freezing due to CO_2 expansion, the valve was heated in a water bath to greater than 50 °C. Upon completion of solution injection, the cell was filled with liquid CO_2 to a pressure of 103 bar. Liquid CO_2 was swept through the cell for

10 minutes to remove the dichloromethane and further dry the particles. After drying, the cell depressurized over a 15 minute span.

2.2.3 Characterization

Scanning Electron Microscopy (SEM) (Jeol JSM-35C) was used to analyze the morphology of the polymer particles. The glass slides were mounted on a SEM stage and coated to an approximate thickness of 200 Angstroms (Pelco Model 3 Sputter Coater).

To detect lysozyme within the particles, two techniques were used. In the first method, the lysozyme was stained by ruthenium tetroxide prior to suspension in the polymer solution, and the product was observed with an optical microscope (Olympus VANOX-T or Olympus C-35AD-2)) and compared with SEM images of the same particles. Energy dispersive spectroscopy (EDS) was used as the second method (Kevex Analyst 8000 Microanalyzer). Two of the amino acids present in lysozyme, cysteine and methionine, contain sulfur, which is not present in the polymer, and can be detected by this technique.

2.3 Results And Discussion

2.3.1 Effect of CO_2-Dichloromethane Mixtures on Morphology of Polymers

For the CO_2 antisolvent process to be successful, the polymer must be highly insoluble in the CO_2-organic solvent mixture, and this mixture must not cause too much agglomeration of the polymer. Previously, it was shown that

lower molecular weight l-PLA is only slightly soluble in CO_2-cosolvent mixtures.[18] CO_2 does not cause l-PLA particles to agglomerate, since they are semi-crystalline.[38] L-PLA has a melting temperature (T_m) of 173-178 °C and a glass transition temperature (T_g) of 60-65 °C (manufacturer's data). The amorphous biodegradable polymer poly(dl-lactide-co-glycolide) (PGLA), however, is highly plasticized by CO_2. PGLA has a T_g of 45-50 °C.

Experiments were performed to determine if CO_2 causes PGLA particles to agglomerate. PGLA, as a powder, and in some cases dichloromethane, as a liquid, were fed into a high-pressure cell equipped with a sapphire window, which has been described previously.[60] The cell was sealed, and then liquid CO_2 was injected slowly into the cell. From ambient temperature down to 0 °C, PGLA powder quickly gels into a viscous mass when in the presence of liquid CO_2 for concentrations from 0.01 to 1.0 wt %. At these concentrations, very little polymer dissolved, even with up to 5 wt % CH_2Cl_2 as a potential cosolvent. The cosolvent concentrations were chosen to mimic conditions used in the PCA process. Upon depressurization, the polymer foamed. At -20 °C, the polymer powder occasionally stuck to the wall of the cell, but was also partially suspended throughout the cell. At temperatures below -40 °C the polymer remained as a free-flowing non-sticky powder. Since CO_2 acts as a plasticizer, it can lower the Tg of the polymer. The T_g of PGLA containing dissolved CO_2 could easily be as low as -40 °C, or even lower, based upon other systems mentioned previously.[34,39,53-54]

2.3.2 Organic Solvent-CO_2 Miscibility and Mixing

Dichloromethane is highly miscible with CO_2 at ambient temperature and pressures above 61 bar. In our investigations, concentrations as high as 73 wt % CH_2Cl_2 were miscible with liquid CO_2 at temperatures from 23 °C down to -46 °C. The mixing behavior of CH_2Cl_2 and CO_2 was observed inside the sapphire cell. The cell was filled partially with liquid CO_2 and equilibrated at the desired temperature and pressure. Pure dichloromethane was then injected into the cell through the 100 µm i.d. capillary nozzle. For conditions where the cell was only partially filled with liquid CO_2, i.e. vapor and liquid CO_2 phases were both present, the solvent was injected at flow rates of 0.5 mL/min or slower. This flow rate range prevented the solvent stream from atomizing, and allowed the solvent to drip into the liquid phase. At temperatures ranging from ambient to -20 °C, the drops quickly dispersed into the liquid CO_2 phase upon contact. At colder temperatures (-30 °C and below) however, the drops were seen to fall about 1 cm through the liquid CO_2 phase before breaking up. Operating at temperatures at or below -30 °C therefore may be expected to delay precipitation of the polymer and/or lead to agglomeration due to insufficient mixing between the drop and liquid phases. While the solvent is still miscible with CO_2 at low temperatures, the rate of mixing decreases significantly.

2.3.3 Polymer particles formed in static vapor-over-liquid CO_2

As shown in Table 2.1, the concentration of the polymer solution, temperature, solution flow rate and CO_2 flow rate were manipulated to observe

the effect on particle formation. In this section, the CO_2 was static (non-flowing). Since both a vapor and a liquid phase are present in each experiment, the initial pressure was simply the vapor pressure of CO_2 at a given temperature. At 0 °C the pressure was 35 bar, and at -20 °C it was 20 bar. As the solution was injected, the pressure decreased slightly, corresponding to the pressure of the CO_2/CH_2Cl_2 mixture. The liquid CO_2 level was maintained at 1 cm below the tip of the nozzle to allow droplet formation and release from the tip before contact with the liquid phase. With the low flow rate and low shear through the vapor phase, ~200 µm drops were formed at a frequency of approximately one per second.

L-PLA is a semi-crystalline polymer which has been used many times in PCA to form microparticles without agglomeration.[13,29,38,41,43,45-46] Therefore, we first present results for l-PLA to serve as a basis for understanding the more challenging experiments with amorphous PGLA. When a 1.0 % solution of l-PLA in dichloromethane was dripped into vapor-over-liquid CO_2 at 0.5 mL/min and 20 °C, the result was microspheres 1-4 µm in diameter, as shown in Figure 2.2 (top) and Table 2.2. On the basis of visual observation, it appeared that little precipitation occurred before each droplet contacted the liquid phase. After the droplet fell into the liquid CO_2 phase, rapid mass transfer led to intense nucleation resulting in the small

Table 2.1. Morphology of particles produced by dripping homogeneous solutions of amorphous poly(dl-lactide-co-glycolide) and semi-crystalline poly(l-lactide) in dichloromethane into vapor-over-liquid carbon dioxide.

Poly-mer	**$C_{sol'n}$ (wt%)**	**Temp (°C)**	**$Q_{sol'n}$ (mL/min)**	**Q_{CO2} (mL/min)**	**Spray time (min)**	**Part. size (µm)**	**Comments**
PGLA	1.0	-20	0.22	0.0	0.35	0.5-5	particles
	5.0	-20	0.22	0.0	0.17	5-70	particles
	5.0	1	0.10	0.0	1.37	10-50	some 500 µm agglomerates
	5.0	5	0.10	0.0	0.35	5-15	some 500 µm agglomerates
	10.0	-20	4.0	0.0	0.33	---	1000 µm agglomerates
	1.0	-30	0.21	0.0	0.36	---	1000 µm agglomerates
	5.0[a]	-20	0.13	0.0	4.66	---	1000 µm agglomerates
	5.0[b]	-18	0.5	17.5	1.68	3-25	particles
	5.0[b,c]	0	0.5	35	0.35	10-50	some 500 µm agglomerates
l-PLA	1.0	20	0.5	0.0	0.45	1-4	particles
	5.0[c]	24	0.5	0.0	0.58	250-500	particles

[a] 750 µm i.d. nozzle

[b] CO_2 flow through coaxial nozzle

[c] 0.5 wt. % lysozyme also present

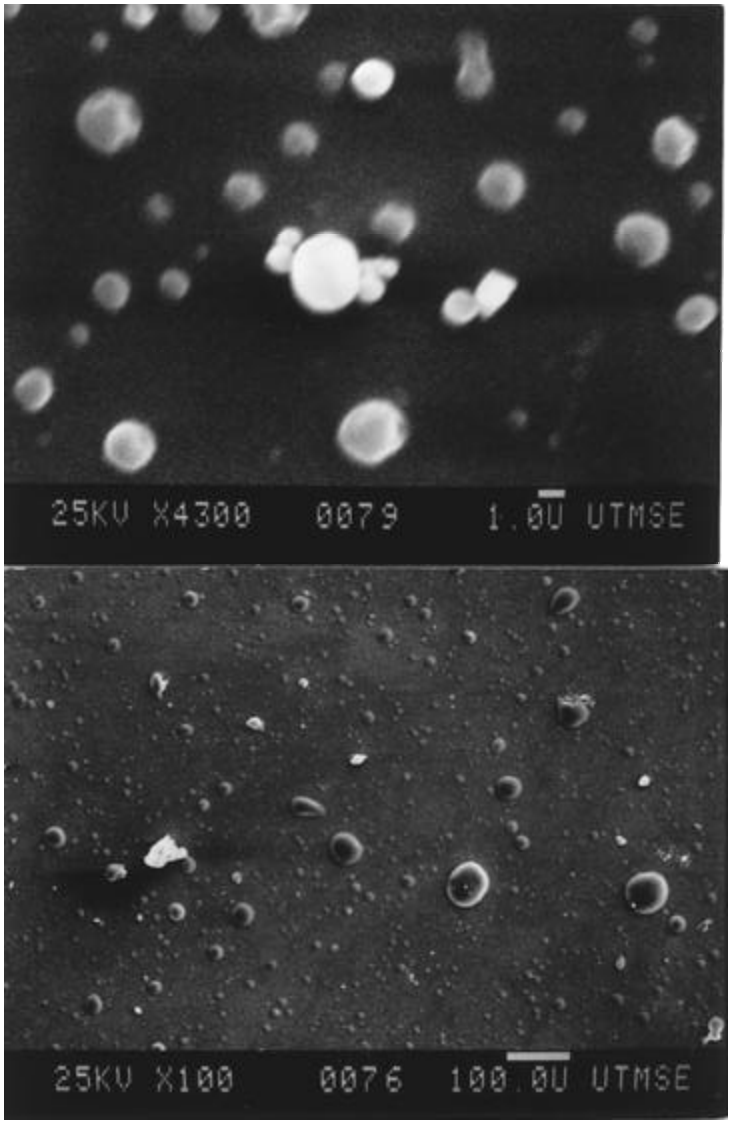

Figure 2.2. SEM micrographs of l-PLA microspheres (top) formed by spraying a 1.0 wt % l-PLA in dichloromethane (CH_2Cl_2) solution at 0.5 mL/min at 20 °C and PGLA microspheres (bottom) formed by spraying a 5.0 wt % PGLA in CH_2Cl_2 solution at 0.22 mL/min (T= -20 °C), both through a 100 μm capillary nozzle into static CO_2.

microspheres. This result indicates atomization does not play as important a role in achieving small particles as suggested previously.[41] The particles formed a free-flowing powder and could be sprayed for several minutes with no agglomeration even as solvent accumulated inside the cell.

Figure 2.3 is a schematic of a ternary phase diagram consisting of a polymer, organic solvent, and compressed CO_2.[32] The mass transfer pathways are shown only for the lower liquid CO_2 phase. Two of the binary systems are completely miscible at most conditions in this study, but the polymer-CO_2 binary system is only slightly miscible. The binodal (coexistence) curve separates the one-phase and two-phase regions in the ternary system. Between the binodal and spinodal curves is the metastable region. The system is stable to small concentration fluctuations in this region, and phase separation will be by nucleation and growth. Upon crossing the binodal curve for dilute polymer solutions, a polymer-rich phase will nucleate and grow within a solvent-rich continuous phase.

For a 5.0 % solution of l-PLA sprayed at similar conditions, we observed skin formation on the backlit droplet while it was in the vapor-phase, and the resulting particles were 250-500 μm in diameter. It was easy to observe that the liquid droplet became opaque as it fell through the CO_2 vapor. A viscous skin appeared to form on the surface of the drop, and the drop did not break up upon contact with the liquid CO_2. This observation of skin formation is entirely consistent with SEM micrographs, which indicated that the particles were the same size as the droplets. In other experiments, at lower concentrations, where a

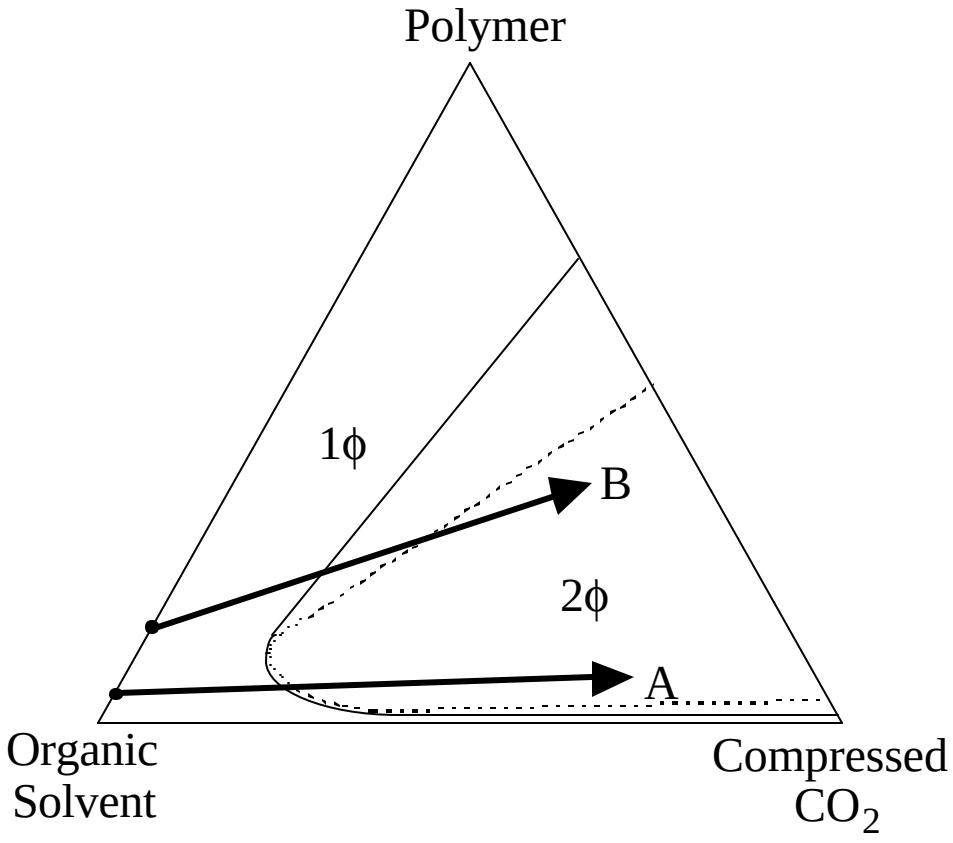

Figure 2.3. Schematic ternary phase diagram comparing mass transfer pathways for precipitation with a compressed fluid antisolvent: (———) binodal curve, (- - - - - -) spinodal curve.

skin did not form, a clear transparent droplet fell through the vapor. With the higher polymer concentration, the dissolution of CO_2 into the droplet forms a skin on the droplet while it is still in the vapor phase. At this concentration for l-PLA, the mass transfer pathway on the phase diagram in Figure 2.3 passes above the critical point on the binodal curve (curve B), thus a solvent-rich phase nucleates and grows within a polymer-rich phase causing skin formation. The polymer entanglement and viscosity in the skin are sufficient to maintain the integrity of the droplet as it solidifies in the liquid CO_2, as was observed in a similar system, as shown in Figures 4-10 of reference 34. Here, the final particle size produced in each droplet is larger than the nozzle diameter, 100 μm, which was also the case for PS in toluene solutions sprayed into vapor over liquid CO_2 [34]

In vapor-over-liquid PCA when drops fall through vapor and atomization is not present, mass transfer is still fast enough in dilute solutions and is fast enough to produce 1-4 μm l-PLA particles, apparently following mass transfer pathway A in Figure 2.3. However, in a previous study with intense atomization into liquid CO_2 at a high density of 0.96 g/mL, the primary particle sizes were even smaller, from 0.1 to 1 μm.[41] Not only was atomization more intense producing smaller droplets, but the phase boundary was reached more quickly from the faster mass transfer. In addition, the polymer solidified more rapidly leading to smaller particles. Dilute solutions were not studied in the past for V/L CO_2, as, for example, the concentration was 6 wt. % or higher for PS solutions and particles were larger than 100 μm.[34]

For PGLA, the solution concentration was varied from 1.0 to 10.0 wt %. To prevent agglomeration, most experiments were performed at -20 °C to raise the polymer solution viscosity sufficiently, while maintaining high enough rates of CO_2-organic solvent mixing (on the basis of the above visual observations of mixing). Also, spray times were generally kept short, <30 sec, to avoid accumulating large concentrations of dichloromethane in the static CO_2, which causes agglomeration. As the polymer concentration and thus the solution viscosity increased, it became necessary to raise the solution flow rate to maintain a constant droplet size. The size was chosen to be slightly larger than the nozzle's inner diameter. At 1.0 wt % and -20 °C, small 0.5-5 μm particles were formed by dripping the solution at a flow rate of 0.22 mL/min into CO_2. These non-agglomerated particles were similar to the l-PLA microspheres shown in Figure 2.2 (top). The same experiment conducted at 0 °C and above produced some small (0.5-5 μm) primary particles but mostly large (>500 μm) solid agglomerates. Therefore, the polymer particles are significantly more viscous and less susceptible to agglomeration at -20 °C.

As shown in Figure 2.2 (bottom), a 5.0 wt.% solution resulted in 5-70 μm microspheres. At this higher concentration, larger particles may be expected because of the higher solution viscosity. When the large droplet strikes the liquid surface, the more viscous solution mixes more slowly with the surrounding liquid CO_2 and mass transfer rates are slower. With slower mixing and mass transfer, the degree of supersaturation is lower than with less viscous solutions (lower concentrations), resulting in fewer nuclei per weight of polymer. Because most of

the nuclei tend to be formed in a small volume where the droplet falls, coalescence of primary particles is more prevalent than for the experiments with lower polymer concentrations, where faster mixing occurs. With the reduction in nucleation rate and higher polymer concentrations (which produces faster agglomeration), especially in a local volume where the drop falls, larger particles are formed.

Unlike previous studies for polystyrene with the same vapor-over-liquid technique, these particles are much smaller than the initial droplet size, which was ~ 200 μm. For 6 wt % polystyrene (200,000 MW) in toluene solutions, 300 μm diameter microballoons are formed with a 151 μm nozzle.[34] A skin, about 20 μm thick, forms on the droplet while still in the vapor phase which then hardens upon contact with the liquid phase. The polymer entanglement and viscosity in the skin are sufficient to maintain the integrity of the droplet as it solidifies in the liquid CO_2. The PGLA in this study has a much lower molecular weight (~30,000) and the solutions are much less viscous. Also, the miscible region in the phase diagram in Figure 2.3 is larger for PGLA-dichloromethane-CO_2 than for PS-toluene-CO_2 because of the lower molecular weight for PGLA versus PS and the lower solubility parameter of dichloromethane versus toluene. Consequently, it will take longer for PGLA to precipitate on the mass transfer pathway on the phase diagram (Figure 2.3), delaying skin formation.[34] Without any visual indication of skin formation in the vapor phase, smaller particles are produced, as the droplet breaks up on contact with the liquid phase.

At dilute concentrations, PGLA does not appear to form a skin when contacting CO_2 vapor, and the particles do not form until the large droplet has begun to disperse in the liquid CO_2 phase. When the solution concentration is increased to 10 wt. %, the solution becomes extremely viscous and individual particles are not formed, only large agglomerates, >1000 μm. Here, a thin skin is visible on the droplets while they are being formed in the vapor phase, although the microscopic structure of the skin could not observed with the naked eye. The formation of a skin was confirmed by examination of the samples with SEM (not shown). Skin formation is favored by the higher solution viscosity and high concentration, which may shift the mass transfer pathway above the critical point (see Figure 2.3). This shift would cause solvent-rich domains to nucleate and grow within a polymer-rich domain.[34,37] The thin skin is weak, since it contains a high concentration of dissolved CO_2, and it was easy to observe visually that the skin immediately ruptures upon hitting the CO_2 liquid surface. The ruptured skin appeared as large agglomerates or films when examined by SEM (not shown). The mixing and diffusion of solvent away from the droplet are very slow due to the high polymer concentration and viscosity, resulting in severe agglomeration.

When a polymer solution is sprayed at 1.0 mL/min into flowing liquid CO_2 (without a CO_2 vapor phase) we found that fibers are produced for PGLA concentrations above 1.0 wt.%. Fibers are formed from the jet due to the rapid nucleation, high solution concentration, high solution viscosity (to prevent atomization) and skin formation.[33] In experiments with vapor-over-liquid CO_2, the large droplets are formed instead of a jet (at the same flow rate) due to much

higher interfacial tension because of the low CO_2 density . The precipitation in the droplets is slower than in the case of a jet due to the larger dimensions of the solution phase and lower miscibility between the phases for CO_2 vapor compared with CO_2 liquid. As a result, fibers are not formed.

The opposing effects of temperature on particle growth, coalescence, and mixing between the phases must be properly balanced to produce large non-agglomerated particles. As temperature is decreased the polymer solution becomes more viscous, which will cause coalescence to be less prevalent. Some coalescence, however, will aid the formation of the desired 50-100 μm particles rather than the typical 1-5 μm particles. As mentioned earlier, decreasing the temperature below -20 °C slows the mixing between the solvent and CO_2 phases. When a 1.0 % solution of PGLA in dichloromethane was dripped into liquid CO_2 at -30 °C, no distinct particles were formed, only large agglomerates, due to the slow mixing. When the solution droplets fell, they initially formed a pool at the liquid surface, and then penetrated the surface. The polymer began to precipitate at the interface, forming a film, and occasionally droplets fell through the film and agglomerated. Previously, we showed that PGLA particles exposed to CO_2 do not tend to agglomerate at -40 °C, indicating hard particles or even a glassy state. Unfortunately, the rate of mixing between the organic solvent and the liquid CO_2 is too slow at -30 °C and -40 °C to disperse the polymer.

At temperatures higher than 0 °C, agglomeration also occurred readily. As seen in Figure 2.4 (top), a 5.0 wt.% solution dripped into liquid CO_2 at 1 °C yielded some distinct particles in the 10-50 μm range, but the polymer was

partially agglomerated. This occurred for every experiment at 0 °C or above since the polymer is excessively swollen by CO_2 and the viscosity is too low at these temperatures.

A 0.030" i.d. (~750 μm) stainless steel nozzle was used to form larger initial droplets in order to attempt to produce the desired particle size. For PGLA concentrations of 1.0 and 5.0 wt. %, and temperatures from -20 °C to 4 °C, the particles were always severely agglomerated with few, if any, distinct particles. The large drops formed more slowly, providing more time for precipitation to occur which allowed a thin skin to form on the large droplets while in the vapor phase. On the basis of visual observation, this skin was weak and ruptured upon impact with the liquid CO_2 surface. The larger droplet size produced a larger local concentration of polymer and solvent, which caused severe agglomeration of the polymer.

2.3.4 Polymer particles formed in flowing vapor-over-liquid CO_2

Experiments were performed with flowing CO_2 to minimize CH_2Cl_2 accumulation. CO_2 was passed through the annular region of a coaxial nozzle, described previously,[41] at high velocity (69-138 cm/s) to agitate the surface of the liquid phase to enhance mixing. Figure 2.4 (middle and bottom) shows PGLA particles formed by spraying a 5.0 wt % solution at 0.5 mL/min into the cell through a 100 μm capillary nozzle with CO_2 flowing at 17.5 mL/min and at -20 °C. Vigorous mixing was observed at the interface, such that particles nucleated and grew throughout the liquid phase rather than in a local region where the

droplets fell. The resulting spherical particles ranged in size from 3-25 μm in diameter with no agglomeration even after almost 2 minutes of spraying. The difference in results was dramatic compared to the case for static CO_2. The particles were suspended throughout the cell, but plugging of the frit in the effluent line at the bottom of the cell limited spray times. This problem could be reduced in the future with a larger filter. The increased mixing causes a higher degree of supersaturation, more nucleation, faster solvent removal and quenching, and less time for growth. The result was far less coalescence and agglomeration when compared to the case with static CO_2. Experiments were also run at higher temperatures to determine if the increased mixing was enough to prevent agglomeration. For all cases where the temperature was 0 °C or higher, some 10-50 μm particles were formed, but mostly large (>500 μm) agglomerates were formed. The particles were not sufficiently hard at the higher temperatures to prevent coalescence.

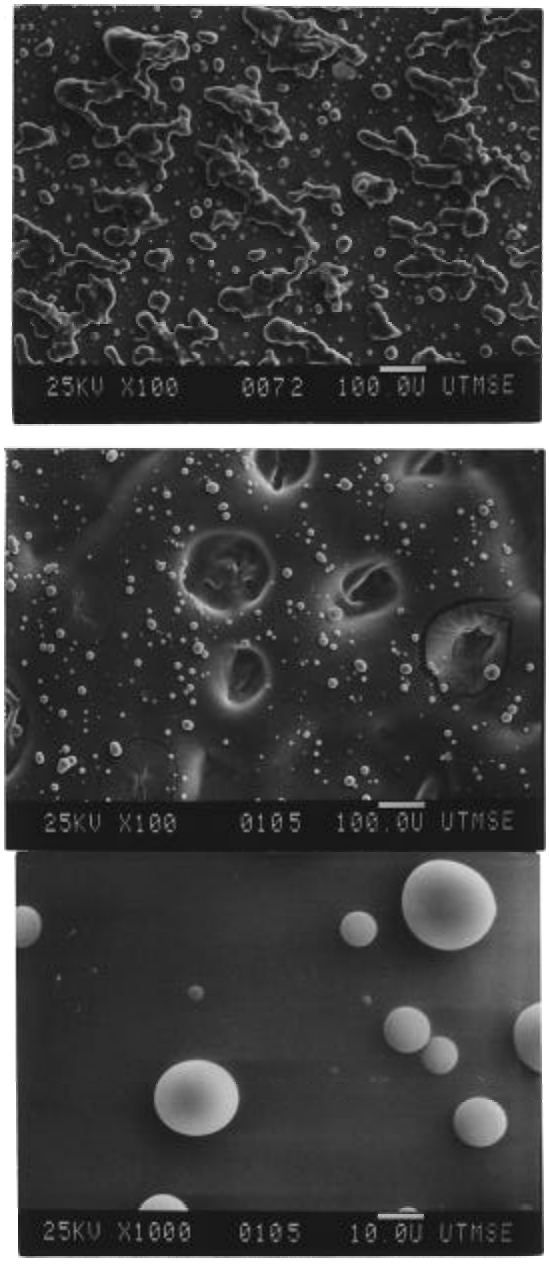

Figure 2.4. SEM micrographs of PGLA microspheres formed by spraying a 5.0 wt % PGLA in CH_2Cl_2 solution at 0.1 mL/min (T=1 °C) into static CO_2 (top) and at 0.5 mL/min into CO_2 flowing at 17.5 mL/min at -20 °C (middle and bottom) through a 100 μm capillary.

2.3.5 Encapsulation of lysozyme into PGLA with static CO_2

In control experiments, lysozyme suspensions in CH_2Cl_2 were sprayed into CO_2 through a 100 µm capillary nozzle at temperatures from 23 to 0 °C. The lysozyme suspensions were formed with an ultrasonic bath and were stable for hours. The suspension flowed smoothly through the capillary and the particle size (1-10 µm) and morphology of the product were identical to those of the original lysozyme, which is shown in Figure 2.5. The original spray-dried lysozyme particles and those removed after spraying into CO_2 were "bowl-shaped" when examined by SEM. Since the polymer particles discussed previously were spheres, it is easy to distinguish between polymer and protein particles.

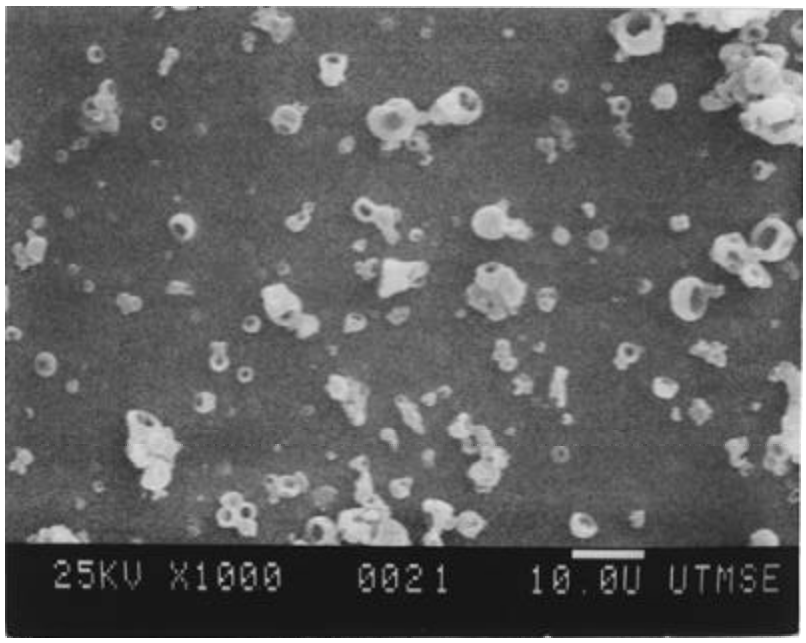

Figure 2.5. SEM micrograph of spray-dried lysozyme particles.

Table 2.2 summarizes results of encapsulating lysozyme into PGLA. Again, the temperature was chosen as -20 °C to strike a balance between mixing favored at high temperatures and formation of hard, non-sticky particles in CO_2 which is favored at low temperatures. An initial loading of 10:1 by weight of polymer to protein was maintained in each case. Figure 2.6 (top) shows the result of spraying a 1.0 wt. % solution of PGLA with lysozyme into static CO_2. The primary particle size was 0.5 - 5 μm in diameter with very little encapsulation of the similarly-sized protein particles. The solution was too dilute for polymer particles to encapsulate a significant fraction of the protein particles. This result was anticipated, since it was shown above that small 0.5-5 μm PGLA particles are formed by precipitation from a 1.0 wt. % solution, which are too small to coat the lysozyme particles.

For a PGLA concentration of 5.0 wt. %, the particles are in the 5-60 μm diameter range, and the encapsulation efficiency is substantial, as demonstrated in Figure 2.6 (bottom). Here, the magnification is high enough to examine a single particle. The craters or holes in the polymer particle represent protein particles for the following reasons. In identical experiments without protein, the craters were never present. Also, the size of the craters matches those of the pure protein particles. Further evidence that the craters represent protein particles is given below in the subsection on experiments with flowing CO_2.

Table 2.2. Morphology of particles produced by dripping homogeneous solutions of amorphous poly(dl-lactide-co-glycolide) and semi-crystalline poly(l-lactide) in dichloromethane containing suspended lysozyme into vapor-over-liquid carbon dioxide.

Poly-mer	**$C_{sol'n}$ (wt%)**	**Temp (°C)**	**$Q_{sol'n}$ (mL/ min)**	**Q_{CO_2} (mL/ min)**	**Spray time (min)**	**Particle size (μm)**	**Encapsulation**
PGLA / lyso.	1.0 /0.1[a]	-23	0.1	0.0	0.48	0.5-5	no
	5.0 / 0.5	-20	0.1	0.0	1.28	10-60	yes
	5.0 / 0.5	-20	0.5	0.0	0.63	10-50	yes
	5.0 / 0.5	-20	1.5	0.0	0.28	5-50	yes
	5.0 /0.5[b]	-20	1.8	0.0	0.18	5-60	yes
	5.0 /0.5[c]	-20	0.5	25	0.42	5-30	yes
	5.0 /0.5[d]	-21	0.5	35	0.82	>1000[e]	no
l-PLA / lyso.	1.0 / 0.1	20	0.1	0.0	3.23	0.5-2.5	no
	5.0 / 0.5	24	0.5	0.0	0.58	250-500	yes

[a]1.0 wt. % PGLA, 0.1 wt. % lysozyme
[b]onset of streaming due to high $Q_{sol'n}$
[c]CO_2 flow through coaxial nozzle
[d]CO_2 flow enters from top of cell
[e]agglomerates

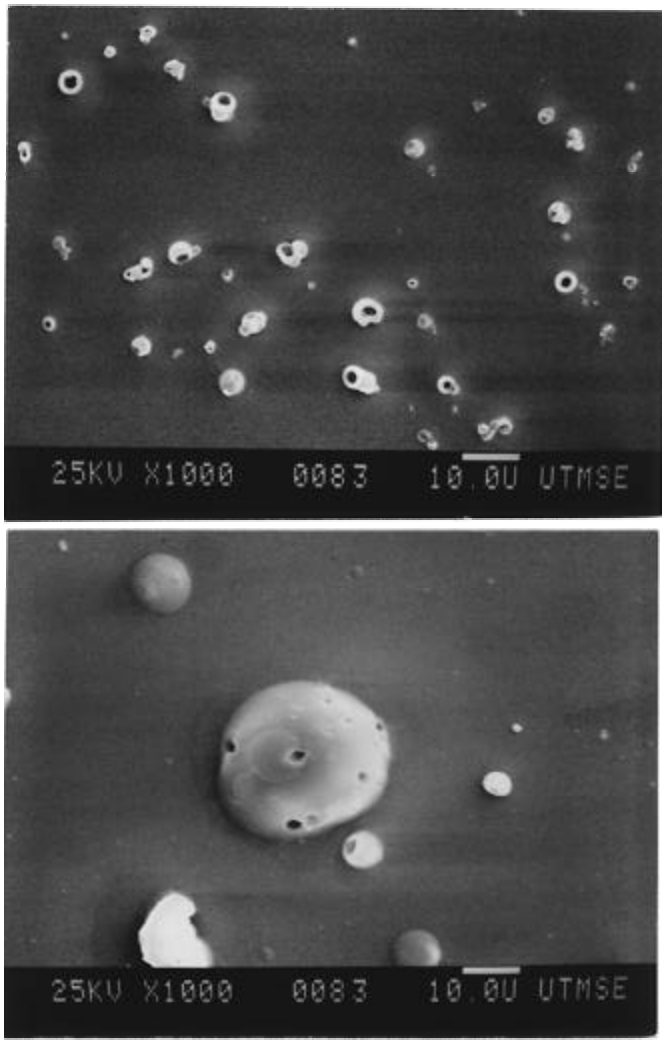

Figure 2.6. SEM micrographs of PGLA microspheres formed by spraying a 1.0/0.1 wt % (top) and a 5.0/0.5 wt % (bottom) PGLA/lysozyme suspension at 0.1 mL/min in CH_2Cl_2 through a 100 µm capillary nozzle into static CO_2 at -20 °C.

At lower magnifications, the particles looked similar to those shown in Figure 2.2 (bottom). Apparently, the presence of the small, encapsulated protein particles does not have a significant influence on the polymer particle size. The polymer particles are much larger than in the case of a 1.0 wt.% solution, and are large enough to encapsulate multiple protein particles. Also, since the solution is more concentrated, the probability of a polymer particle nucleating and growing next to a lysozyme particle is enhanced. Also, the protein has the potential to act as a nucleating agent for the polymer. The large droplets formed in the CO_2 vapor phase lead to relatively slow mixing when the droplets strike the liquid CO_2 phase. The high local concentrations of the sticky CO_2-swollen polymer and protein lead to a large amount of growth.

A desirable feature of this spray geometry is that a polymer-rich phase nucleates in the presence of the protein in the confined space of the droplets, which occupy a small volume fraction compared to the total volume. Such nucleation may be expected to produce higher encapsulation efficiencies than if the polymer nucleated throughout the total cell volume. This advantage of compartmentalization of polymer and protein is not present in the GAS process cited above where CO_2 is added to a liquid solution. A disadvantage of the V/L PCA process is that the primary mass transfer takes place at the vapor-liquid surface rather than throughout the entire volume, which can lower the production rate.

Varying the size of the droplets leaving the nozzle could potentially lead to a change in size of the polymer particles. As the flow rate of the polymer

solution increased, it was observed that the droplet size decreased. However, no significant change in particle morphology occurred when the solution flow rate was increased from 0.1 to 1.5 mL/min for a 5.0 wt.% solution at -20 °C. In each case, the particles appeared as those shown in Figure 2.6 (bottom). A complication of extremely slow flow rates is plugging of the nozzle, which occurred very often at 0.1 mL/min, but infrequently at 0.5 mL/min or higher. This plugging is likely a result of precipitation inside the nozzle, caused by CO_2 diffusing upwards into the nozzle, and/or entrapment of the solid protein particles.

The degree of agglomeration of the polymer product is dependent upon the solution flow rate and spray time. When conducting the spray, at a certain time large particles could easily be seen with the naked eye. When analyzed by SEM, these large particles were agglomerates and not simply large flocculates of small primary particles. At a solution flow rate of only 0.1 mL/min, the experiment could be run for 1 minute before agglomeration began to occur. For higher flow rates, the observed time where large particles appeared decreased accordingly to 40 and 20 seconds at flow rates of 0.5 and 1.5 mL/min, respectively. This agglomeration could potentially be avoided by either flowing CO_2 continuously through the cell as described in the next section or by spraying into a larger volume cell. At 1.8 mL/min, streaming of the solution begins to occur rather than dripping. Here, the range of particle sizes did not change, but there was a higher percentage of large particles compared to the previous cases at lower flow rates. Due to the large amount of solution flowing into the cell, agglomeration began to occur after only 10 seconds.

2.3.6 Encapsulation of lysozyme into PGLA with flowing CO_2

Figure 2.7 compares an optical micrograph and a SEM micrograph of polymer particles with protein particles visible on the surface. These particles were formed by spraying a 5.0 wt.% PGLA solution with suspended lysozyme at 0.5 mL/min along with CO_2 flowing in the annulus at a velocity of 138 cm/s. The SEM image (top) shows particles with craters or holes in their surfaces, which may be identified as the "bowl" shaped spray-dried lysozyme particles. The micrograph taken with the optical microscope (bottom) shows the same polymer particle with encapsulated stained protein particles. The stained protein directly corresponds to the craters observed in the SEM micrograph. This correspondence between optical and SEM photomicrographs was always observed where we compared images of particles formed by the vapor/liquid PCA process. Figure 2.8 (top) shows 40-70 μm particles with encapsulated lysozyme formed at the same conditions as Figure 2.7, except at a higher CO_2 flow rate. By varying the focal plane throughout the depth of the particle (not shown), we observed in the optical microscope that the protein particles were encapsulated throughout the PGLA particles and were not just on the surface. While there did not appear to be any protein particles that were not encapsulated, polymer particles without encapsulated protein were present.

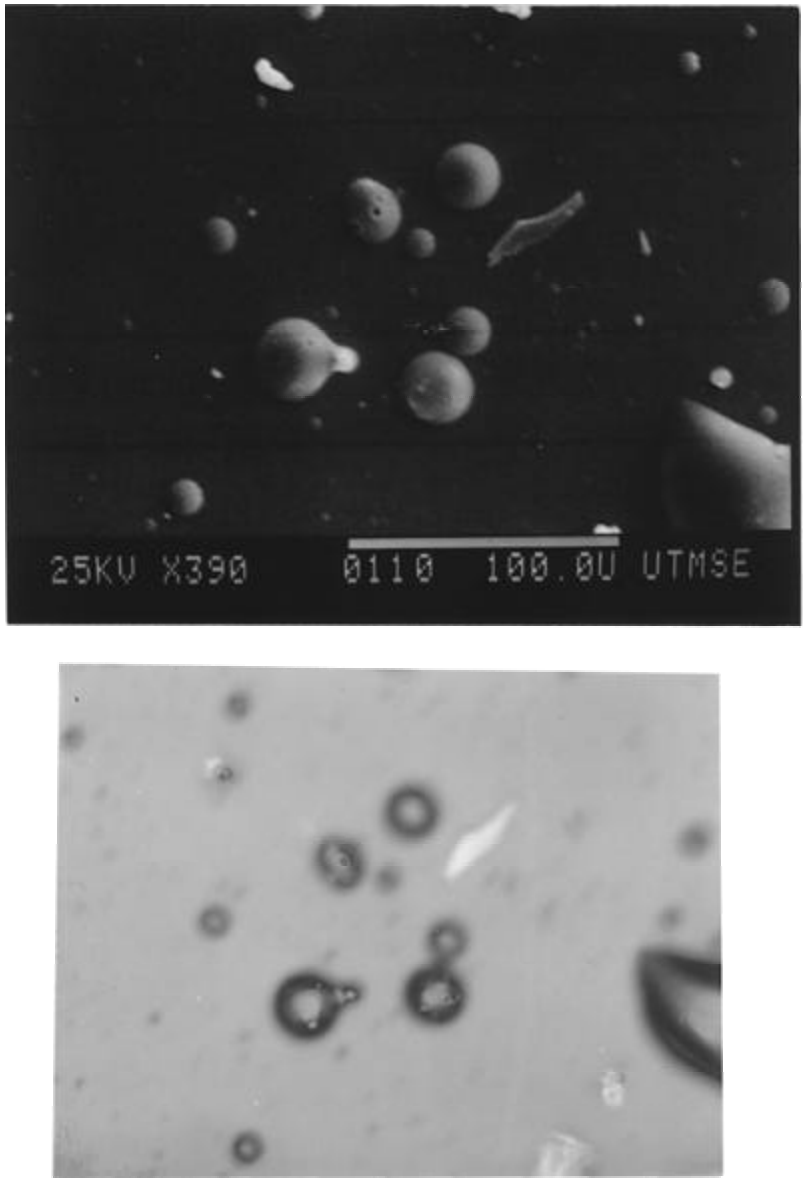

Figure 2.7. SEM micrograph (top) and optical micrograph (bottom) of PGLA microspheres formed by spraying a 5.0/0.5 wt % suspension of PGLA/lysozyme in CH_2Cl_2 at 0.5 mL/min through a 100 μm capillary nozzle into CO_2 flowing at 15 mL/min at -20 °C.

Flowing CO_2 at high velocity during the spray delayed the time at which large particles were observed visually in the tube. This time corresponded to the time where agglomeration was observed in the SEM micrographs. Flowing CO_2 through the annular region surrounding the nozzle at high velocity caused a large amount of mixing at the vapor/liquid interface and suspended the precipitated particles throughout the cell, yielding spherical, non-agglomerated particles. Spraying a 5.0%/0.5% PGLA/lysozyme solution at 0.5 mL/min into the cell at -20 °C with CO_2 flowing at 25 mL/min yielded spherical particles 5-30 μm in diameter, with encapsulation of the protein as seen in Figure 2.8 (bottom). These particles are more uniform in size and shape than those formed in static CO_2, and appear like those in Figure 2.4 (middle). The particle sizes are more uniform in this case due to better mixing at the vapor-liquid interface.

In another type of experiment, CO_2 was introduced into the cell through a large opening located in the top of the cell 1 cm above the tip of the nozzle. Here, the CO_2 velocity was relatively low and turbulence from the CO_2 did not have much effect on the solution stream or on the CO_2 vapor/liquid interface. The purpose of flowing CO_2 was to reduce the accumulation of solvent in the cell. Spraying a 5.0%/0.5% PGLA/lysozyme solution at 0.5 mL/min into CO_2 flowing at 35 mL/min at -21 °C yielded little change in particles size and failed to delay the onset of agglomeration, compared to the case with static CO_2. The same was true for higher CO_2 flow rates up to 52 mL/min. With this cell configuration, the CO_2 stream does not cause significant turbulence or mixing inside the cell. Since agglomeration occurred at the same time as in static CO_2 experiments, most of the

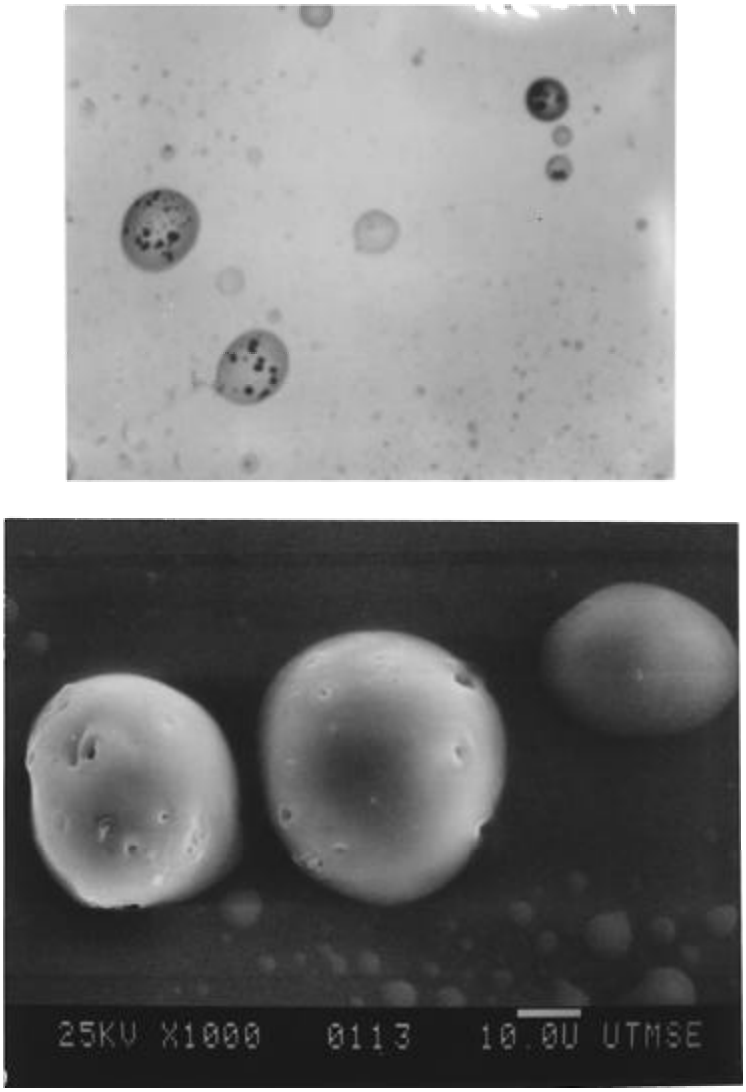

Figure 2.8. SEM micrograph (top) and optical micrograph (bottom) of PGLA microspheres formed by spraying at 0.5 mL/min a 5.0/0.5 wt % PGLA/lysozyme suspension in CH_2Cl_2 through a 100 µm capillary nozzle into CO_2 flowing at 25 mL/min at -20 °C.

agglomeration occurs immediately after precipitation and not after solvent buildup in the cell. In this case the particles were concentrated at the liquid-vapor interface and were not suspended throughout the liquid phase.

Elemental analysis via Energy Dispersive Spectroscopy (EDS) was also used to confirm the presence of lysozyme in the polymer particles. Lysozyme has 2 amino acid constituents containing sulfur, cysteine and methionine, which can be detected via EDS. Chicken egg white lysozyme is reported to contain 8 cysteine molecules and 2 methionine molecules per protein chain.[61-62] Both of these amino acids have one sulfur atom per molecule, resulting in 10 per lysozyme molecule. EDS scans of the pure protein (top) and particles with encapsulated protein (bottom) are shown in Figure 2.9. The analysis of the pure lysozyme shows peaks corresponding to the presence of phosphorus, chlorine, and potassium impurities as well as the sulfur. Analysis of the peaks is only qualitative, unfortunately, due to multiple scattering of the x-rays. Particles formed by spraying a 5.0% PGLA solution with suspended lysozyme were analyzed as shown in Figure 2.9 (bottom). The lower curve represents a polymer particle with no protein present, while the upper curve corresponds to a single polymer particle with entrapped lysozyme. The particles were collected on a section of a glass slide, thus explaining the presence of the silicon impurity peak. The presence of the other peaks, excluding silicon, indicates that lysozyme was encapsulated within the polymer particle examined.

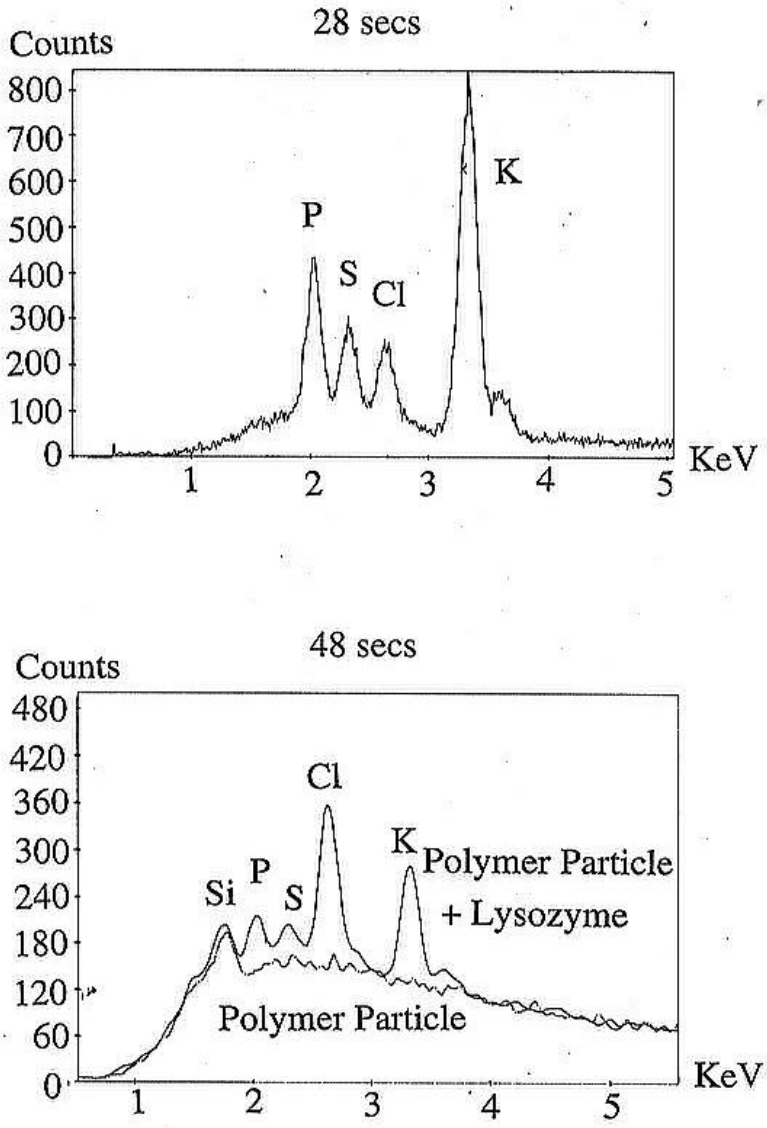

Figure 2.9 EDS scans of spray-dried lysozyme (top) and PGLA microspheres (bottom) formed by spraying a 5.0/0.5 wt % suspension of PGLA/lysozyme at 0.5 mL/min in CH2Cl2 through a 100 μm capillary nozzle into CO_2 flowing at 15 mL/min at –20 °C.

2.3.7 Encapsulation of lysozyme into l-PLA

When polymer particles are similar in size to the protein particles, little or no encapsulation is expected to occur. Figure 2.10 (top) shows particles formed by spraying a 1.0% l-PLA solution with suspended lysozyme at 0.1 mL/min and 20 °C. As shown, the 1-4 μm polymer particles do not tend to encapsulate the lysozyme particles. Therefore, the polymer precipitation occurs without requiring the protein as a nucleation site. Solutions with higher polymer concentrations will tend to form larger particles as evidenced earlier for PGLA. Spraying a 5.0% l-PLA solution at 0.5 mL/min and 24 °C resulted in particles 250-500 μm in diameter, Figure 2.10 (bottom). This polymer precipitates very rapidly and a polymer skin quickly forms on the droplet while still in the CO_2 vapor phase. The high solution viscosity caused the drop size to be larger than the nozzle inner diameter, and the resultant particle diameter was the same as the initial drop size. In this case the large polymer particles appeared to encapsulate all of the protein particles, as no individual protein particles were found on the sample slides.

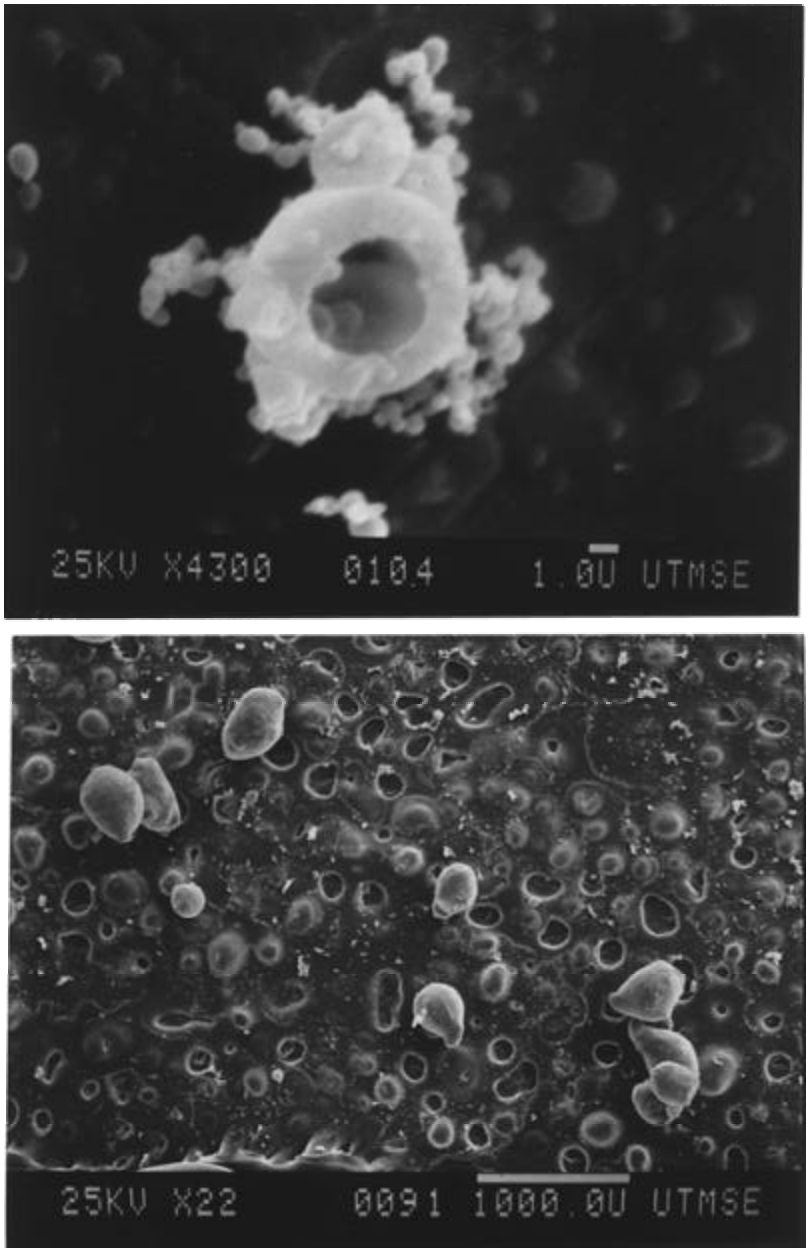

Figure 2.10. SEM micrographs of l-PLA microspheres formed by spraying a 1.0/0.1 wt % l-PLA/lysozyme suspension at 0.1 mL/min at 20 °C (top) and a 5.0/0.5 wt % l-PLA/lysozyme suspension at 0.5 mL/min at 24 °C (bottom) through a 100 μm capillary nozzle into static CO_2.

2.4 CONCLUSIONS

Several major challenges for the PCA process were overcome in order to encapsulate a protein into PGLA. The PGLA particles were large enough to encapsulate the protein and did not agglomerate. In contrast, the primary particles (0.5 to 5 μm) were too small for encapsulation when the solution was sprayed into liquid or supercritical CO_2; furthermore, the particles were highly agglomerated. By delaying precipitation in a vapor CO_2 phase over a liquid CO_2 phase, much larger primary particles were formed, from 5 to 70 μm. At an optimal temperature of -20°C, the polymer solution mixed rapidly with CO_2, and agglomeration of primary particles was minimal due to harder particles than at higher temperatures.

The amorphous polymer PGLA is highly plasticized by CO_2. Dissolution of CO_2 into PGLA depresses the T_g from the normal value of 45 °C to approximately -40 °C at 276 bar, based upon observation of particle agglomeration. Below -40°C, the polymer remains as a non-sticky free-flowing powder in the presence of CO_2 at 276 bar. Below -30°C, the rate of mixing between CH_2Cl_2 and liquid CO_2 decreases appreciably. At an optimal temperature of -20 °C, the highly viscous PGLA microspheres do not agglomerate, yet the temperature is high enough to achieve adequate mixing between liquid CO_2 and the organic solution. An additional benefit of operating at colder temperatures is the relatively low pressure. At -20°C, the saturation pressure of CO_2 is 19.7 bar, compared to 61.4 bar at 23 °C.

The vapor-over-liquid PCA process forms microspheres in the 5-70 μm range when a 5.0 % solution of PGLA in dichloromethane is sprayed at 0.22 mL/min through a 100 μm diameter nozzle into static CO_2 at -20 °C. Experimental temperatures of 0 °C or above, or below -30°C yielded only large (>1000 μm) agglomerates. At high temperatures the particles are too sticky due to dissolved CO_2, and at low temperatures, the organic solution and CO_2 mix too slowly. Lower concentrations yielded smaller primary particles whereas highly viscous concentrated solutions above 10.0 wt. % led to skin formation in the vapor phase and subsequent agglomeration in the liquid CO_2 phase. The thin skin is weak due to low molecular weight and dissolved CO_2, and hence rupturing occurs upon impact at the liquid interface leading to agglomeration. Particle sizes did not change appreciably with solution flow rate in the "dripping" regime. At the onset of streaming flow, there was a higher percentage of large particles, while the particle size range remained the same. The most spherical and uniform particles ranging in size from 3-25 μm in diameter were produced by flowing CO_2 at high velocity through an annular region in a coaxial nozzle to provide mixing at the interface.

Encapsulation of 1-10 μm lysozyme particles proved successful for the 5-70 μm PGLA microspheres for a 1:10 ratio by weight of protein to polymer and a 5 wt % polymer solution. The presence of lysozyme in the particles was demonstrated by SEM analysis, optical microscopy, and EDS. A high encapsulation efficiency for this process is favored by the fact that the protein and polymer precipitate together in small droplets. The use of protein suspensions

extends the applicability of the PCA process substantially, since many proteins are insoluble in organic solvents and are less likely to be denatured when suspended.

2.5 REFERENCES

(1) Mathiowitz, E.; Jacob, J. S.; Jong, Y. S.; Carino, G. P.; Chickering, D. E.; Chaturvedi, P.; Santos, C. A.; Vijayaraghavan, K.; Montgomery, S.; Bassett, M.; Morrell, C. *Nature* **1997**, 386, 410-4.

(2) Cavalier, M.; Benoit, J. P.; Thies, C. *Journal of Pharmacy and Pharmacology* **1986**, 38, 249-53.

(3) Leelarasamee, N.; Howard, S. A.; Malanga, C. J.; Ma, J. K. H .*Journal of Microencapsulation* **1988**, 5, 147-57.

(4) Spenlehauer, G.; Veillard, M.; Benoit, J. P. *Journal of Pharmaceutical Sciences* **1986**, 75, 750-5.

(5) Park, T. G.; Alonso, M. J.; Langer, R. *Journal of Applied Polymer Science* **1994**, 52, 1797-1807.

(6) Thanoo, B. C.; Doll, W. J.; Mehta, R. C.; Digenis, G. A.; DeLuca, P. P. *Pharmaceutical Research* **1995**, 12, 2060-4.

(7) Fong, J. W.. United States 4384975, 1983

(8) Domb, A. J.; Amselem, S.; Maniar, M. In *Polymeric Biomaterials*; Dumitrius, S., Ed.; Marcel Dekker, Inc.: New York, 1994, pp 399-433.

(9) Puisieux, F.; Barratt, G.; Couarraze, G.; Couvreur, P.; Devissaguet, J. P.; Dubernet, C.; Fattal, E.; Fessi, H.; Vauthier, C.; Benita, S. In *Polymeric Biomaterials*; Dumitrius, S., Ed.; Marcel Dekker, Inc.: New York, 1994, pp 749-94.

(10) Langer, R. *Chemical Engineering Communications* **1980**, 6, 1-48.

(11) Lewis, D. H. In *Biodegradable Polymers as Drug Delivery Systems*; Chasin, M. and Langer, R., Ed.; Marcel Dekker, Inc.: New York, 1990; Vol. 45, pp 1-41.

(12) Alonso, M. J. In *Microparticulate Systems for the Delivery of Proteins and Vaccines*; Cohen, S. and Bernstein, H., Ed.; Marcel Dekker, Inc.: New York, 1996; Vol. 77, pp 203-242.

(13) Knutson, B. L.; Debenedetti, P. G.; Tom, J. W. In *Microparticulate Systems for the Delivery of Proteins and Vaccines*; Cohen, S. and Bernstein, H., Ed.; Marcel Dekker, Inc.: New York, 1996, pp 89-125.

(14) Johnston, K. P.; Kim, S.; Combes, J. *Am. Chem. Soc. Symp. Ser.* **1989**, 406, 52-71.

(15) McHugh, M. A.; Krukonis, V. J. *Supercritical Fluid Extraction Principles and Practice*; 2nd ed.; Butterworths: Stoneham, MA, 1994.

(16) Matson, D. W.; Petersen, R. C.; Smith, R. D. *J. Mater. Sci.* **1987**, 22, 1919-1928.

(17) Matson, D. W.; Fulton, J. L.; Peterson, R. C.; Smith, R. D. *Ind. Eng. Chem. Res.* **1987**, 26, 2298-2306.

(18) Tom, J. W.; Debenedetti, P. G. *Biotechnolgy Progress* **1991**, 7, 403-411.

(19) Tom, J. W.; Debenedetti, P. G. *Journal of Aerosol Science* **1991**, 22, 555-584.

(20) Phillips, E. M.; Stella, V. J. *International Journal of Pharmaceutics* **1992**, 1-10.

(21) Boen, S. N.; Bruch, M. D.; Lele, A. K.; Shine, A. D. In *Polymer Solutions, Blends, and Interfaces*; Noda, I. and Rubingh, D. N., Ed.; Elsevier Science Publishers B.V., 1992, pp 151-172.

(22) Lele, A. K.; Shine, A. D. *AICHE J.* **1992**, 38, 742-752.

(23) Lele, A. K.; Shine, A. D. *Ind. Eng. Chem. Res.* **1994**, 33, 1476-1485.

(24) Mawson, S.; Johnston, K. P.; Combes, J. R.; DeSimone, J. M. *Macromolecules* **1995**, 28, 3182-3191.

(25) Alessi, P.; Cortesi, A.; Kikic, I.; Foster, N. R.; Macnaughton, S. J.; Colombo, I. *Industrial and Engineering Chemistry Research* **1996**, 35, 4718-4726.

(26) Kim, J. H.; Paxton, T. E.; Tomasko, D. L. *Biotechnology Progress* **1996**, 12, 650-61.

(27) Debenedetti, P. G.; Tom, J. W.; Yeo, S. D.; Lim, G. B. *Journal of Controlled Release* **1993**, 24, 27-44.

(28) Gallagher, P. M.; Coffey, M. P.; Krukonis, V. J.; Klasuts, N. In *Supercritical Fluid Science and Technology*; Johnston, K. P. and Penninger, J. M. L., Ed.; American Chemical Society: Washington, D.C., 1989; Vol. 406, pp 334-354.

(29) Randolph, T. W.; Randolph, A. J.; Mebes, M.; Yeung, S. *Biotechnology Progress* **1993**, 9, 429-435.

(30) Chou, Y. H.; Tomasko, D. L. *GAS Crystallization of Polymer-Pharmaceutical Composite Particles*; International Society for the Advancement of Supercritical Fluids: Sendai, Japan, 1997; Vol. A, pp 55-7.

(31) Dixon, D. J. *Formation of Polymer Materials by Precipitation with a Compressed Fluid Antisolvent*; University of Texas at Austin: Austin, Texas 1992.

(32) Dixon, D. J.; Johnston, K. P.; Bodmeier, R. P. *AIChe Journal* **1993**, 39, 127-139.

(33) Dixon, D. J.; Johnston, K. P. *Journal of Applied Polymer Science* **1993**, 50, 1929-1942.

(34) Dixon, D. J.; Luna-Barcenas, G.; Johnston, K. P. *Polymer* **1994**, 35, 3998 - 4005.

(35) Yeo, S. D.; Lim, G. B.; Debenedetti, P. G.; Bernstein, H. *Biotechnology and Bioengineering* **1993**, 41, 341-346.

(36) Yeo, S.-D.; Debenedetti, P. G.; Radosz, M.; Schmidt, H.-W. *Macromolecules* **1993**, 26, 6207-6210.

(37) Luna-Barcenas, G.; Kanakia, S. K.; Sanchez, I. C.; Johnston, K. P. *Polymer* **1995**, 36, 3173-3182.

(38) Bodmeier, R. P.; Wang, H.; Dixon, D. J.; Mawson, S.; Johnston, K. P. *Pharmaceutical Research* **1995**, 12, 1211-1217.

(39) Mawson, S.; Johnston, K. P.; Betts, D. E.; McClain, J. B.; DeSimone, J. M. *Macromolecules* **1997**, 30, 71-77.

(40) Mawson, S. *The Formation and Characterization of Polymeric Materials Precipitated by CO2-Based Spray Processes*; University of Texas at Austin: Austin,Texas 1996.

(41) Mawson, S.; Kanakia, S.; Johnston, K. P. *Journal of Applied Polymer Science* **1997**.

(42) Mawson, S.; Kanakia, S.; Johnston, K. P. *Polymer* **1997**, 38, 2957-2967.

(43) Falk, R.; Randolph, T.; Meyer, J. D.; Kelly, R. M.; Manning, M. C. *Journal of Controlled Release* **1997**, 44, 77-85.

(44) Winters, M. A.; Knutson, B. L.; Debenedetti, P. B.; Sparks, H. G.; Przybycien, T. M.; Stevenson, C. L.; Prestrelski, S. J. *Journal of Pharmaceutical Sciences* **1996**, 85, 586-594.

(45) Bleich, J.; Kleinebudde, P.; Müller, B. W. *International Journal of Pharmaceutics* **1994**, 106, 77-84.

(46) Bleich, J.; Müller, B. W. *Journal of Microencapsulation* **1996**, 13, 131-9.

(47) Fischer, W.; Müller, B. W. United States 5043280, 1991

(48) McHugh, M. A.; Krukonis, V. In *Encyclopedia of Polymer Science and Engineering*; 2nd ed.; Mark, H. F., Bikales, N. M., Overberger, C. G. and Menges, G., Ed.; John Wiley: NY, 1988; Vol. 16.

(49) McHugh, M. A. *Polymers in Supercritical Fluids*; International Society for the Advancement of Supercritical Fluids: Sendai, Japan, 1997; Vol. C, pp 785-8.

(50) Steckel, H.; Thies, J.; Müller, B. W. *International Journal of Pharmaceutics* **1997**, 152, 99-110.

(51) Ruchatz, F.; Kleinebudde, P.; Müller, B. W. *Journal of Pharmaceutical Sciences* **1997**, 86, 101-5.

(52) Falk, R. F.; Randolph, T. W. *Pharmaceutical Research* **1998**, 15, 1233-7.

(53) Condo, P. D.; Paul, D. R.; Johnston, K. P. *Macromolecules* **1994**, 27, 365-371.

(54) Fong, J. W. United States 4166800, 1979

(55) Schwendeman, S. P.; Cardamone, M.; Klibanov, A.; Langer, R.; Brandon, M. R. In *Microparticulate Systems for the Delivery of Proteins and Vaccines*; Cohen, S. and Bernstein, H., Ed.; Marcel Dekker, Inc.: New York, 1996; Vol. 77, pp 1-49.

(56) Yeo, S. D.; Debenedetti, P. G.; Patro, S. Y.; Przybycien, T. M. *Journal of Pharmaceutical Sciences* **1994**, 83, 1651-1656.

(57) Winters, M. A.; Debenedetti, P. G.; Barey, J.; Sparks, H. G.; Sane, S. U.; Przybycien, T. M. *Pharmaceutical Research* **1997**, 14, 1370-8.

(58) Kissel, T.; Koneberg, R. In *Microparticulate Systems for the Delivery of Proteins and Vaccines*; Cohen, S. and Bernstein, H., Ed.; Marcel Dekker, Inc.: New York, 1996; Vol. 77, pp 51-87.

(59) Bleich, J.; Müller, B. W.; Wabmus, W. *International journal of pharmaceutics* **1993**, 97, 111-7.

(60) Lemert, R. M.; Fuller, R. A.; Johnston, K. P. *J. Phys. Chem.* **1990**, 94, 6021-28.

(61) Bailey, P. D. *An Introduction To Peptide Chemistry*; John Wiley & Sons: New York, 1990.

(62) Hamaguchi, K.; Hayashi, K. In *Proteins: Structure and Function*; Funatsu, M., Hiromi, K., Imahori, K., Murachi, T. and Narita, K., Ed.; John Wiley & Sons: New York, 1972; Vol. 1, pp 85-222.

CHAPTER 3

Rapid Expansion from Supercritical to Aqueous Solution to Produce Suspensions of Water-Insoluble Drugs

3.1 INTRODUCTION

A large number of drugs are insoluble or poorly soluble in water. Hence, the clinical utility of the available pharmaceutical dosage forms can be limited by this insolubility. An alternative approach for the formulation of water-insoluble biologically active compounds is surface-stabilized micron- or submicron-size particulate preparations. The pharmacokinetic properties of both oral and injectable formulations are dependent on the particle size. Small particles are often needed in order to maximize surface area, to improve bioavailability, and for dissolution requirements. Pace *et al.* have reviewed the usefulness of microparticulate preparations of water-insoluble or poorly soluble injectable drugs.[1] Current techniques for micronizing solids include spray drying[2-3], emulsion-solvent-extraction[4-6], and processes based on high shear, cavitation, attrition, and/or impaction (microfluidization, high pressure homogenization, ball milling, media milling, air jet milling).[7-11] There can be several drawbacks associated with these techniques, including broad particle size distributions and

denatured products caused by exposure to high temperatures (observed in jet milling), lengthy periods for residual solvent extraction (in the spray drying process), and separation of processing agents that may be undesirable in the final formulation (in ball milling or media milling processes).

The overall objective of this work is to use an alternative method for particle size reduction based on rapid expansion from supercritical fluids, especially CO_2. CO_2 is an environmentally benign solvent that is non-flammable, inexpensive, and essentially non-toxic. It has relatively mild critical conditions, T_c = 31 °C and P_c = 73.8 bar, allowing processing of thermally labile materials in a medium which has gas-like transport properties at liquid-like densities. CO_2 has no dipole moment and a very low polarizability per volume. Therefore, only certain water-insoluble pharmaceutical compounds are soluble, particularly those with low melting points. A recent review[12] summarizes the solubility of many pharmaceutical compounds of interest in supercritical CO_2. In some cases, the solubility was enhanced by the addition of a cosolvent, such as an alcohol.

In rapid expansion from supercritical solution (RESS), nucleation and crystallization are triggered by reducing the solvent density, or solvent strength, through expansion to atmospheric conditions.[12-23] Typically, the solution is sprayed through a 10-50 μm i.d. nozzle with an aspect ratio (L/D) of 5-100. This process has been used successfully to form a variety of microparticles and microfibrils from polymers, drugs, and inorganic compounds. An example of a highly soluble polymer, which has been used in RESS to form submicron particles and fibers, is poly(1,1,2,2-tetrahydroperfluorodecylacrylate).[15] Most

particle sizes reported have been between 5-100 μm. From theoretical calculations, it should be possible to form particles as small as 20-50 nm.[24] The inability to approach the theoretical lower limit is likely due to particle growth during collisions in the free jet.[24] Nanoparticles of beta-carotene (300 nm) were formed by expansion within a valve of an ethylene solution, which then flowed into a 10% (w/w) viscous gelatin solution in order to inhibit post-expansion particle agglomeration.[19] Phospholipids and other surface modifiers in aqueous solution have been utilized to stabilize aqueous suspensions produced by RESAS of CO_2 solutions.[25] In both of these studies, the suspensions were much less concentrated than those in the present study.

The goal of this work was to produce aqueous suspensions of water-insoluble drugs by RESS with an average particle size of less than 1 μm at substantial drug concentrations, *e.g.* above 20 mg/mL. High concentrations of water-insoluble drugs are of great interest for parenteral administration. The supercritical solutions were sprayed directly into an aqueous surfactant solution in order to stabilize small particles by minimizing flocculation and agglomeration resulting from particle collisions. The surfactant was chosen to be active at the drug-water interface, but need not be active at the CO_2-drug interface. Tween-80, a non-ionic surfactant (polyoxyethylene sorbitan monooleate $C_{64}H_{124}O_{26}$), was chosen to sterically stabilize the drug particles. It is approved by the US Food and Drug Administration for use as an excipient in either oral or parenteral delivery formulations. If the surfactant can rapidly adsorb to the surface of the growing particles in the free jet, it may stabilize submicron particles. The solubilities of

several drugs in CO_2 were measured to determine if they were large enough for RESAS. Cyclosporine, a water-insoluble immunosuppressant for organ transplantation, was used as a model drug for this study, since it is soluble in CO_2 and is of interest in parenteral administration. To evaluate the effectiveness of the process, the concentration of drug in the suspension was measured by high performance liquid chromatography (HPLC) and particle sizes were measured by dynamic light scattering (DLS).

3.2 EXPERIMENTAL

3.2.1 Materials and Analytical Methods

Cyclosporine A was obtained from North China Pharmaceutical Corporation. Flurbiprofen was obtained from Sigma and Piroxicam from Cipla. These drugs were used without further purification. Instrument Grade CO_2 was used for all experiments. Tween-80 was purchased from Fisher Scientific. The aqueous solutions consisted of 1.0 and 5.0 % (w/w) Tween-80, and these concentrations are higher than the critical micelle concentration. Water was purified to Type 1 reagent grade by passing it through a Barnstead (NANOpure II) filtration system.

Separation and quantification of drug concentrations in the aqueous solutions were achieved by high performance liquid chromotography (HPLC) with a 250 mm long C-18 column (SGE ODS - 5μm). Five mL of methanol was added to 0.5 mL of each sample, 9.6 μL of which was injected into the system. Methanol was used as the mobile phase, and the detection wavelength was 210

nm. The solubility of drug in aqueous Tween-80 solutions was determined from the saturated solutions at 10 °C and 22 °C. An excess amount of drug was added to 1-20 % (w/w) aqueous Tween-80 solutions, stirred for 1 hr., and then allowed to equilibrate for 1 week at 10 °C and 22 °C. The dissolved amount of drug was determined from a filtrate of these saturated solutions by the above-mentioned HPLC method.

Dynamic light scattering (DLS) measurements were conducted with a Brookhaven Zetaplus (Brookhaven Instruments Corporation, New York) to determine particle sizes in terms of number-weighted, mass-weighted, and intensity-weighted size distributions. The time between the formation of the drug suspensions and analysis was 1-3 days.

3.2.2 Phase Behavior and Rapid Expansion from Supercritical Solution

The drug phase behavior in CO_2 was determined with a high-pressure variable-volume cell that is discussed in detail elsewhere.[26] The cell was equipped with a sapphire window, allowing visual observation of the phase behavior. A predetermined amount of drug was loaded into the front of the cell, and then the cell was sealed. CO_2 was metered into the front of the cell and then the back side of the cell was pressurized with CO_2, by a computer-controlled syringe pump (ISCO 260D). The cell was immersed in a thermostated water bath with polycarbonate shielding. Cloud points were determined visually by noting the pressure when the drug precipitated out of solution as the pressure was slowly reduced at 0.1 bar/sec. Phase separation was defined as the point when a light,

directed into the view cell, no longer reflected off the smooth stainless steel face of the piston. Each cloud point determination was repeated three times giving a reproducibility within ± 2 bar.

The RESS apparatus is shown in Figure 3.1. The solution cell consists of a 4 ft. long 11/16 in. I.D. by 1 in. O.D. stainless steel tube equipped with a piston. The cell is loaded and pressurized in a similar fashion as discussed with the phase behavior apparatus. Heating tape and a temperature controller were used to control the temperature of the solution to within ± 0.3 °C. The preheater consisted of a 16 in. long, 1/4 in. O.D. x 1/8 in. I.D. tube. This section was heated with heating tape and another temperature controller.

The nozzle consisted of a 10 in. long 1/16 in. O.D. x 0.010 in. I.D. stainless steel tube. The nozzle tip was cut with a pair of wire cutters to produce a crimped thin slit orifice at the end of the tube. The tapered section of the tube was only 0.5 mm long. The tip was then filed back until the desired flowrate was achieved for a given pressure drop across the restriction. The depressurization profile inside the tapered nozzle tip may be expected to be much sharper compared to that for a capillary tube or a 30 μm laser-drilled orifice plate. The crimped nozzle never plugged with drug during the sprays, whereas plugging was prevalent with the 30 μm orifice. Also, in all cases, the preheater and nozzle assemblies were pre-pressurized by means of a CO_2 bypass line to insure there was no initial pressure drop inside the lines which could cause plugging. The flowrate through the nozzle was compared with that through the well-defined laser-drilled orifice. A 30 μm diameter orifice plate, with a thickness of 0.254

mm, produces a flowrate of ~5 mL/min at a ΔP of 345 bar. Several different nozzles were made allowing flowrate ranges from 0.15 to 1.25 mL/min for the same ΔP of 345 bar, suggesting that the cross section of the orifice was considerably smaller than 30 μm. Also, it was observed that the orifice was not circular but rather in the shape of a thin slit. All of the experiments conducted in this work were performed at the same ΔP of 345 bar.

The nozzle was submerged 1 cm below the surface of the aqueous surfactant solution, which was contained in an 80 mL, 2.2 cm diameter, side-arm test tube. This was done to bring the jet, and hence the particles being formed, into intimate contact with the suspending medium. The test tube was submerged in a temperature-controlled water bath to maintain a constant temperature within the trapping solution. The temperature of the receiving solution was measured using a thermocouple submerged in the liquid. The vigorous expansion of the CO_2 spray into the aqueous solution caused considerable foaming. To alleviate this problem, N_2 was sprayed at 7.8 L/min and 2 bar into the tube above the foam through three, 1/16 in. O.D. x 0.030 in. I.D. tubes to break the foam and allow drainage back into the bulk liquid phase.

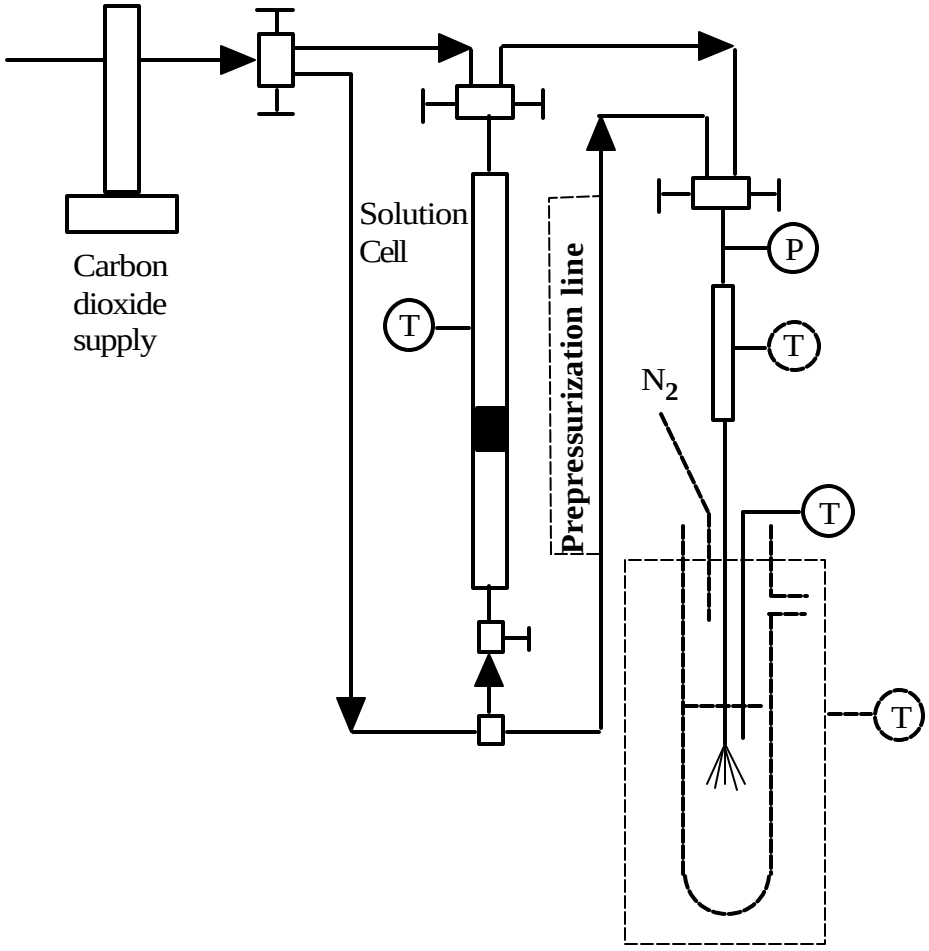

Figure 3.1. RESS apparatus for producing suspensions of submicron, water-insoluble drugs.

3.3 RESULTS AND DISCUSSION

3.3.1 Phase Behavior

To determine the applicability of the RESS process for micronizing certain drugs, their solubility in CO_2 was determined. Known amounts of drug and CO_2 were loaded into the phase behavior apparatus as described previously. The temperature and pressure were varied from 25-90 °C and 69-345 bar, respectively.

The solubilities of a few hydrophobic drugs in compressed CO_2 are summarized in Table 3.1. The structures of these drugs are shown in Table 3.2. Piroxicam is only slightly soluble in CO_2. At 0.053 % (w/w), Piroxicam was soluble in CO_2 at 331 bar and 35 °C. 0.06 % (w/w) Flurbiprofen was soluble at 83 bar and 35 °C. Cyclosporine A was the most soluble drug studied, with a solubility of up to 1.0 % (w/w) for the range of conditions studied. The solubility behavior of cyclosporine in CO_2 is provided in more detail in Figure 3.2. The minimum temperature required for complete solubility of 1.0 % (w/w) cyclosporine in CO_2 was 30 °C, while lower concentrations were easily soluble at room temperature. The data show an increase in cloud point pressure with temperature, a characteristic of lower critical solution temperature (LCST) phase behavior.[27] This type of behavior is entropically driven and is often observed in systems with supercritical fluid solvents. Because of cyclosporine's high solubility in CO_2, it was chosen as the model drug for the RESS experiments.

Table 3.1. Solubility of hydrophobic drugs in compressed CO_2.

Solute	Concentration (%, w/w)	Temperature (°C)	Cloud point (bar)
Cyclosporine A	0.25	25	Soluble <83
		30	128
		35	142
	1.0	30	238
		50	285
		70	330
Flurbiprofen	0.06	35	78
Piroxicam	0.053	35	331

Figure 3.2. Effect of temperature and pressure on cyclosporine A solubility in compressed CO_2. The drug precipitates below the cloud point pressure.

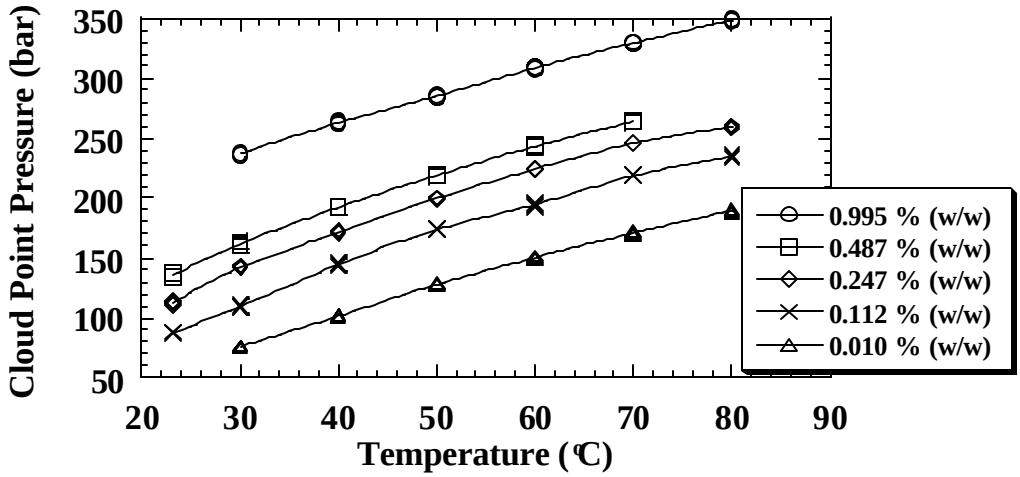

Table 3.2. Structures of the hydrophobic drugs and surfactant used in this study.

Compound	Structure
Cyclosporine MW=1201 Mp=148-151°C	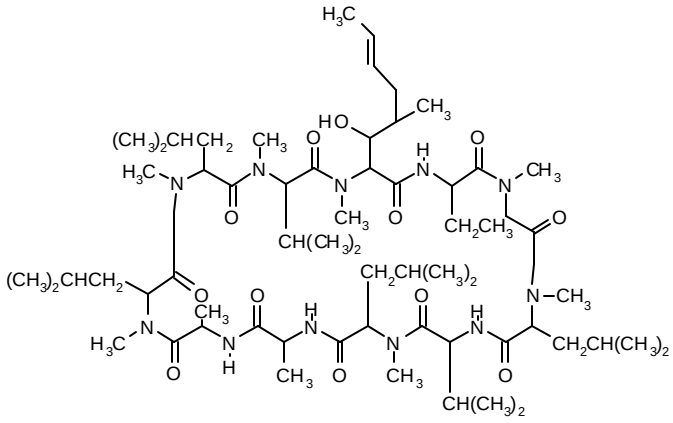
Piroxicam MW=331 Mp=198-200°C	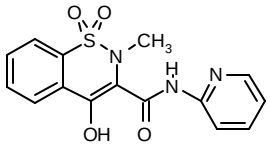
Flurbiprofen MW=244 Mp=110-111°C	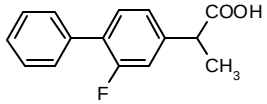
Tween-80	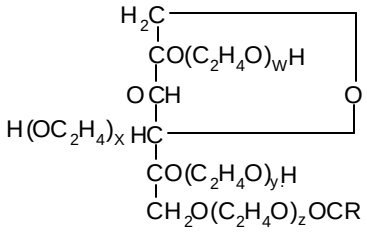 w+x+y+z = 20 R = oleic acid

A

.n increase in the amount of surfactant aids stabilization of the particle suspensions. However, if the surfactant concentration becomes too large, the formation of a large number of micelles could lead to substantial solubilization of drug in the cores of the micelles. To check this possibility, the equilibrium solubility of the drugs in the micellar solutions was measured as a control experiment. In the next section, it will be seen that the concentrations of drug in the aqueous suspensions significantly exceeded the amount that dissolves in the micellar solutions for surfactant concentrations up to 5.0 % (w/w).

The effects of temperature and Tween-80 concentration on the solubility of cyclosporine in the micellar solutions are shown in Figure 3.3. At 22 °C, the solubility of the drug is 0.55 mg/mL in a 1.0 % (w/w) solution and increases with increasing surfactant concentration to a level of 12.77 mg/mL at 20.0 % (w/w) surfactant. Similarly, at 10 °C, the solubility increases from 2.1 mg/mL at 1.0 % (w/w) to 18.1 mg/mL at 20.0 % (w/w) surfactant. The results indicate that the drug:surfactant ratio (g/g) was relatively constant with an average and standard deviation of 0.065 ± 0.011 at 22 °C, and 0.134 ± 0.043 at 10 °C for surfactant concentrations up to 5.0 % (w/w).

To put the micellar solubilities in perspective, consider a 50 mg drug/mL solution. This concentration would require drug:surfactant ratios of 4.95 in a 1.0 % (w/w) surfactant solution, and 0.95 in a 5.0 % (w/w) solution. These ratios far exceed the values for micelle solubility alone at either of the two temperatures

studied. The same would be true for a 20 mg/mL solution, but at drug concentrations below 10 mg/mL the micellar solubility becomes significant.

Figure 3.3. Effect of temperature and concentration on solubility of cyclosporine A in micellar aqueous solution of Tween-80.

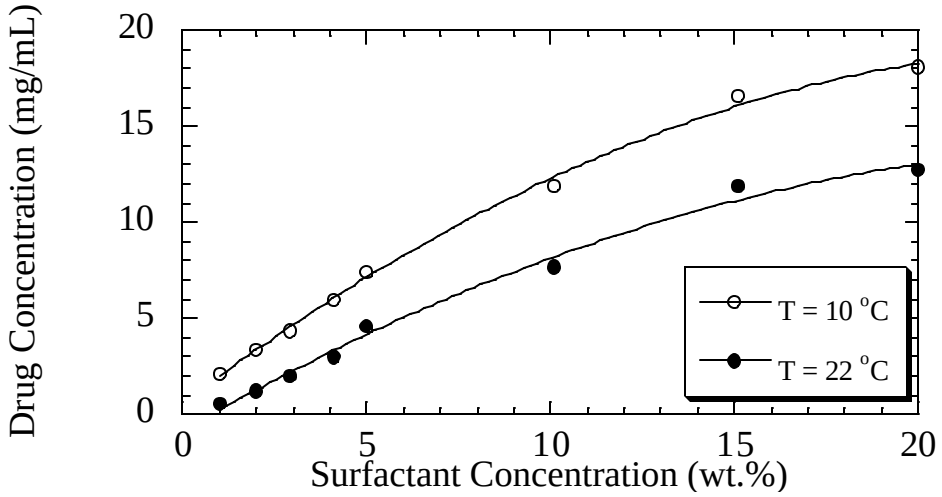

3.3.2 RESS of Cyclosporine into Aqueous Solutions of Tween-80

First, for comparison, cyclosporine processed by RESS was collected in a test tube with no aqueous trapping solution. The cyclosporine in CO_2 solution was held at a temperature of 30 °C to achieve solubilization at 345 bar. The pre-expansion temperature and pressure were 60 °C and 345 bar, respectively. The particles collected were 3-50 μm in diameter and were non-spherical and highly

irregular in shape when examined by scanning electron microscopy. The rapid collisions between the particles in the free jet led to excessive particle growth.

The results of spraying a 1.0 % (w/w) solution of cyclosporine in CO_2 into a 1.0 % (w/w) aqueous solution of Tween-80 are summarized in Table 3.3. The cyclosporine in CO_2 solution was again held at a temperature of 30 °C. In all cases, the pre-expansion temperature and pressure were 60 °C and 345 bar. At this condition, the cyclosporine was completely soluble as determined in Figure 3.2. The receiving solution was heated to maintain a constant temperature of 25 °C. The pre-expansion temperature and the receiving solution temperature were chosen to prevent water from freezing at the tip of the nozzle.

Table 3.3 is organized in order of increasing drug:surfactant ratio. A minimum ratio of approximately 0.065 is required to be above the micellar solubility of the drug at 25 °C. The concentration shown is the measured amount of drug in the suspension according to HPLC. In each run, a measured volume of a known concentration of cyclosporine in CO_2 was sprayed. Hence, the yield is the percentage of the recovered drug, according to HPLC, relative to the amount of drug sprayed. The particle size range as measured by DLS is also given in Table 3.3. Before addition of the cyclosporine, the Tween-80 micellar solutions were clear, and hence the micelles were too small to scatter light and were not measurable by DLS.

Table 3.3. Cyclosporine microparticles prepared by RESS of a 1.0 % (w/w) solution into 20.0 mL of 1.0 % (w/w) Tween-80 aqueous solution. $T_{sol'n}$ = 30.0 °C, $T_{preheater}$ = 60.0 °C, ΔP = 345 bar.

#	Solution Flowrate (mL/min)	Spray Time (min)	Drug Concentration (mg/mL)	Yield (%)	Particle Size (nm)	Drug:Surfact-ant Ratio
1	0.25[a,b]	15	2.93		230-4100	
2	0.35	6.5	0.91	82	410-540	0.090
3	0.31	16	2.08	86	420-560	0.206
4	0.51[c]	20	3.09	63	250-890	0.306
5	0.35	29	5.92	100	410-600	0.586
6	0.56	18	6.20	100	440-670	0.614
7	0.20[b]	141	17.60	66	440-1600	1.74

[a] No surfactant present

[b] 10.0 mL receiving solution

[c] Foam overflowed leading to low yield

As a control experiment (1), the drug solution was sprayed into pure water. In this case, the aqueous phase became slightly turbid and also foamed. Spraying pure CO_2 into H_2O does not cause foaming; thus cyclosporine is surface active at the H_2O-CO_2 interface. According to the DLS measurements, the particles ranged in size from 230 to 4100 nm, as there is no surfactant present to

provide stabilization. Significantly larger particles were also observed visually, which were too large for measurement by DLS.

Cyclosporine in CO_2 was sprayed into 1.0 % (w/w) Tween-80 solutions to attempt to stabilize submicron particles. In experiment (2) the drug:surfactant ratio was 0.090 mg/mL, and the stabilized particles ranged in size from 410-540 nm. In this case, the foaming was adequately controlled, and the yield was approximately 82%. This experiment, with a low drug loading, demonstrates that the initial small particles can be stabilized within the expanding jet, without excessive growth due to particle collisions, unlike the cases where there was no trapping solution or surfactant stabilizer.

The suspensions in experiments (2), (3), and (5) were formed by spraying at a constant flowrate but for increasing amounts of time to achieve higher drug loadings. Significant change in the particle size distribution was not observed as the drug loading was increased from 0.91 to 5.92 mg/mL, indicating the surfactant limits particle growth. Also, the yield was high in all cases, suggesting that the drug was not entrained by the rising gaseous CO_2. Experiments (4) and (6) were conducted at higher flowrates for the same ΔP with a larger nozzle slit. In experiment (4), some overflowing of the foam occurred and led to a lower drug trapping efficiency and a broader particle size distribution due to less thorough surfactant stabilization. A comparison of (5) and (6) demonstrates that increasing the flowrate from 0.35 to 0.56 mL/min does not have a significant impact on the particle size, for similar aqueous drug concentrations. In all of these examples,

the surfactant diffuses rapidly enough to the particle surfaces to prevent excessive growth.

In most cases, submicron particles were stabilized even at the higher drug loadings. In some cases, extreme foaming caused surfactant depletion and resulted in broader particle size distributions, for example in (4). The reason for the foam overflow was insufficient N_2 flow to break the foam, a problem that was easily overcome in the other experiments. Also, in cases where the drug concentration was very high, like (7), the number of particle collisions in the aqueous solution was high, leading to larger particle sizes. Furthermore, the surfactant levels available to adsorb to particle surfaces decrease as the drug:surfactant ratio reaches 1.74. Concentrations of drug in 1.0 % (w/w) Tween-80 solutions as high as 6.20 mg/mL could be stabilized with particle diameters in the range of 500 nm. With a higher drug loading and drug:surfactant ratio, size distributions became broader. It was observed that the surfactant level was insufficient to stabilize the particles for a drug:surfactant ratio significantly above 0.6.

Table 3.4 summarizes the results of spraying 1.0 % (w/w) solutions of cyclosporine in CO_2 into more concentrated 5.0 % (w/w) aqueous Tween-80 solutions. The drug levels ranged from 3.97 to 45.9 mg/mL. The pressure of the solution was held at 345 bar and several flow rates were studied by using different nozzle sizes. The higher surfactant concentration in these cases led to stabilization of submicron particles (~500 nm) at concentrations of up to 37.5 mg/mL at a drug:surfactant ratio of 0.713. Experiments (9) - (11) demonstrate

reasonable reproducibility for these experiments. Also, a comparison of (5) from Table 3.3 with (9) – (11) in Table 3.4 indicates the change in particle size is insignificant when changing from 1.0 to 5.0 % (w/w) surfactant solutions. At drug loadings of ~ 6 mg/mL both solutions can stabilize the particles. Drug concentrations in the suspensions as high as 37.5 mg/mL could be stabilized efficiently in a 5.0 % (w/w) Tween-80 solution, as seen in (13). Such high concentrations could not be achieved in a 1.0 % (w/w) solution, because the drug:surfactant ratios become excessive for particle stabilization.

The significantly higher flowrate in (8) seems to produce smaller particles than in (9) and (10). This is possibly due to several factors: more vigorous stirring within the receiving cell due to the high-velocity CO_2 stream, a change in expansion characteristics due to the larger nozzle slit used for the higher flowrate, and/or the lower drug loading and drug:surfactant ratio. In (12) and (14), the lower trapping efficiency is a result of spraying into only 10 mL of the trapping solution. While the foam produced during the spray was suppressed, i.e. kept at a constant level so as to avoid overflowing, it was not completely eliminated. Therefore, a greater percentage of the surfactant and H_2O were lost to the foam for an initial 10 mL of solution compared to 20 mL, since the foam heights were equal. However, the particle size was not affected by changing the receiving solution volume, only the yield. At a drug loading higher than 37.5 mg/mL, the particles were stabilized much less effectively, as seen in (14). In this case, the drug:surfactant ratio was up to 0.873 and the particle size distribution was broad.

As in the experiments shown in Table 3.3, the particle size distribution becomes much broader above a threshold drug:surfactant ratio of about 0.6-0.7.

Table 3.4. Cyclosporine microparticles prepared by RESS of a 1.0 % (w/w) solution into 20.0 mL of 5.0 % (w/w) Tween-80 aqueous solution. $T_{sol'n}$ = 30.0 °C, $T_{preheater}$ = 60.0 °C, ΔP = 345 bar.

#	Solution Flowrate (mL/min)	Spray Time (min)	Drug Conc. (mg/mL)	Yield (%)	Particle Size (nm)	Drug:Surfactant Ratio
8	1.25	8	3.97	82	15-560	0.075
9	0.57	19	5.55	95	340-500	0.105
10	0.55	19	5.58	99	490-600	0.106
11	0.56	20	6.10	96	410-520	0.116
12	0.24 [a]	112	23.8	64	410-545	0.452
13	0.55	70	37.5	100	500-660	0.713
14	0.37 [a]	122	45.9	64	380-550, 970-1550 [b]	0.873

[a] 10.0 mL receiving solution

[b] Two peaks - 37% in lower peak by intensity averaging, 63% in lower peak by weight

3.4 CONCLUSIONS

Aqueous stabilizing solutions have been successfully incorporated into the RESS process to trap 500 nm particles of a water-insoluble pharmaceutical compound. In RESAS, the surfactant diffuses rapidly to the particle surface to

impede particle agglomeration and growth. Cyclosporine microparticles were formed by spraying a 1.0 % (w/w) solution (in CO_2) into 1.0 and 5.0 % (w/w) Tween-80 solutions to prevent microparticle flocculation and agglomeration. By RESAS, cyclosporine particles 500-700 nm in diameter were stabilized for drug concentrations as high as 6.20 mg/mL and 37.5 mg/mL in 1.0 and 5.0 % (w/w) Tween-80 solutions, respectively. At a drug:surfactant ratio above 0.6-0.7 the surfactant can no longer stabilize the particles, resulting in broader size distributions. RESAS may be expected to be a general process to produce smaller particle sizes of organic and inorganic water-insoluble materials than in the case of RESS into air.

3.5 REFERENCES

(1) Pace, S. N.; Pace, G. W.; Parikh, I.; Mishra, A. K. *Pharmaceutical Technology* **1999**, *23*, 116-34.

(2) Broadhead, J.; Rouan, S. K. E.; Rhodes, C. T. *Drug Development and Industrial Pharmacy* **1992**, *18*, 1169-1206.

(3) Masters, K. *Spray Drying Handbook*; Third ed.; John Wiley and Sons: New York, **1979.**

(4) Puisieux, F.; Barratt, G.; Couarraze, G.; Couvreur, P.; Devissaguet, J. P.; Dubernet, C.; Fattal, E.; Fessi, H.; Vauthier, C.; Benita, S. in *Polymeric Biomaterials*; Dumitrius, S., Ed.; Marcel Dekker, Inc.: New York, **1994**, pp 749-94.

(5) Chasin, M.; Langer, R. *Biodegradable Polymers as Drug Delivery Systems*; Swarbick, J., Ed.; Marcel Dekker, Inc.: New York, **1990**; Vol. 45, pp 347.

(6) Bakan, J. A. in *Encyclopedia of Pharmaceutical Technology*; Swarbrick, J. and Boylan, J. C., Ed.; Marcel Dekker, Inc.: New York, **1994**; Vol. 9, pp 423-41.

(7) Byers, J. E.; Peck, G. E. *Drug Development and Industrial Pharmacy* **1990**, *16*, 1761-79.

(8) Rubinstein, M. H.; Gould, P. *Drug Development and Industrial Pharmacy* **1987**, *13*, 81-92.

(9) Parrott, E. L. in *Encyclopedia of Pharmaceutical Technology*; Swarbrick, J. and Boylan, J. C., Ed.; Marcel Dekker, Inc.: New York, **1994**; Vol. 3, pp 101-21.

(10) Aiache, J. M.; Beyssac, E. in *Encyclopedia of Pharmaceutical Technology*; Swarbrick, J. and Boylan, J. C., Ed.; Marcel Dekker, Inc.: New York, **1994**; Vol. 12, pp 389-420.

(11) Illig, K. J.; Mueller, R. L.; Ostrander, K. D.; Swanson, J. R. *Pharmaceutical Technology* **1996**, *20*, 78-88.

(12) Subramaniam, B.; Rajewski, R. A.; Snavely, K. *Journal of Pharmaceutical Sciences* **1997**, *86*, 885-90.

(13) Phillips, E. M.; Stella, V. J. *International Journal of Pharmaceutics* **1992**, *94*, 1-10.

(14) Tom, J. W.; Debenedetti, P. G. *The Journal of Supercritical Solutions* **1994**, *7*, 9-29.

(15) Mawson, S.; Johnston, K. P.; Combes, J. R.; DeSimone, J. M. *Macromolecules* **1995**, *28*, 3182-3191.

(16) Alessi, P.; Cortesi, A.; Kikic, I.; Foster, N. R.; Macnaughton, S. J.; Colombo, I. *Industrial and Engineering Chemistry Research* **1996**, *35*, 4718-4726.

(17) Mohamed, R. S.; Halverson, D. S.; Debenedetti, P. G.; Prud'homme, R. K. in *Supercritical Fluid Science and Technology*; Johnston, K. P. and Penninger, J. M. L., Ed.; American Chemical Society: Washington D.C., **1989**; Vol. 406, pp 355-78.

(18) Matson, D. W. *Chemtech* **1989**, *19*, 480-6.

(19) Chang, C. J.; Randolph, A. D. *AIChE Journal* **1989**, *35*, 1876-82.

(20) Domingo, C.; Berends, E.; van Rosmalen, G. M. *Journal of Supercritical Fluids* **1997**, *10*, 39-55.

(21) Lele, A. K.; Shine, A. D. *Ind. Eng. Chem. Res.* **1994**, *33*, 1476-1485.

(22) Krukonis, V. J. in *Supercritical Fluid Extraction and Chromatography: Techniques and Applications*; Chapentier, B. A. and Sevenants, M. R., Ed.; American Chemical Society: Washington, D.C., **1988**; Vol. 366, pp 26-43.

(23) Kim, J. H.; Paxton, T. E.; Tomasko, D. L. *Biotechnology Progress* **1996**, *12*, 650-61.

(24) Debenedetti, P. G. in *Supercritical Fluids: Fundamentals for Application*; Kiran, E. and Levelt Sengers, J. M. H., Ed.; Kluwer Academic Publishers: Boston, **1994**; Vol. 273, pp 719-29.

(25) Henrikson, I. B.; Mishra, A. K.; Pace, G. W.; Johnston, K. P.; Mawson, S. *Insoluble Drug Delivery.* U.S., # US96/16841. pending, 1996.

(26) Lemert, R. M.; Fuller, R. A.; Johnston, K. P. *J. Phys. Chem.* **1990**, *94*, 6021-28.

(27) McHugh, M. A.; Krukonis, V. J. *Supercritical Fluid Extraction Principles and Practice*; 2nd ed.; Butterworths: Stoneham, MA, **1994**.

CHAPTER 4

Phopholipid-Stabilized Nanoparticles of Cyclosporine A by Rapid Expansion from Supercritical to Aqueous Solution

4.1 INTRODUCTION

The often low bioavailability of water-insoluble drugs leads to poor pharmacokinetic performance in the body. Techniques to improve bioavailability in oral or parenteral applications of water-insoluble drugs include powder micronization, the formation of micron- and submicron-size dispersions, and solubility enhancement in aqueous solution by addition of appropriate surfactants, organic solvents or buffers, or drug-carrier systems such as liposomes. The payloads for drugs in liposomes are often limited due to the low volume fraction of hydrophobic regions.[1] The use of surfactants or organic solvents in parenteral administration can lead to phlebitis, anaphylaxis, hypotension, or even vasodilation.[1] Traditional micronization techniques such as spray-drying[2,3], emulsion-solvent extraction[4-6], and processes based on high shear, for example, microfluidization, high-pressure homogenization, ball milling, and air jet milling[7-11] can have certain drawbacks. With many of these techniques, particle size distributions tend to be broad, products can be denatured by exposure to high

temperatures or organic solvents, residual solvent concentrations can be high without lengthy periods for additional extraction/evaporation, or undesirable processing agents will need to be separated from the final products. Yields can be well below 100% due to losses in solids handling in milling and spray drying. Milling techniques also require cumbersome solids handling. Hence, processing techniques that do not rely on organic solvents, high temperatures, and that can provide small particles with narrow distributions are highly desirable.

Dissolution rates of poorly-water soluble drugs may be increased by reducing the particle size, to increase the surface area, and by inhibiting crystallization to form amorphous particles. Both of these factors may be achieved by phase separation techniques that include rapid nucleation rates and prevention of particle growth. The process rapid expansion from supercritical solution (RESS) may be used to accomplish these goals according to theoretical models of nucleation. The expansion from the supercritical state to atmospheric pressure reduces the solvent density (or strength) and initiates intense nucleation.[12-22] The particle formation steps include nucleation, condensation of solute molecules about the nuclei and coagulation of particles in the free jet expansion. Recent work by Charoenchaitrakool et al.[23] has produced 2.5 μm particles by RESS with enhanced dissolution rates for the poorly water-soluble compound ibuprofen, likely due to both the reduction in particle size and crystallinity.[23] If coagulation can be minimized, it should be possible to produce 20-50 nm drug particles.[24,25]

A novel process, rapid expansion from supercritical to aqueous solution (RESAS) has been developed to reduce the coagulation rate in the free jet expansion of RESS.[26] The supercritical solution is expanded through an orifice or tapered nozzle into an aqueous solution containing a stabilizer to minimize particle aggregation during free jet expansion. Previously, Young, et al. demonstrated the ability for Tween 80, a non-ionic polysorbitan ester, to stabilize 400-700 nm cyclosporine particles produced by RESAS.[26] CO_2 was chosen as the supercritical fluid of interest since it is an environmentally benign solvent that is nonflammable, inexpensive, and essentially non-toxic. It also has relatively mild critical conditions, Tc = 31 °C, Pc = 73.8 bar, and so allows processing at moderate temperatures to prevent thermal degradation. Sun, et al. have demonstrated a technique to form PbS nanoparticles by expanding a supercritical fluid containing one reactant, $Pb(NO_3)_2$, into a liquid solution containing a second reactant, Na_2S.[27]

Here, we focus on phospholipids to minimize coagulation in RESAS. Phospholipids are amphiphilic molecules, usually consisting of two lipophilic tails, which, when added to water, rapidly aggregate and form liposomes. Depending on the chemical compositions of the phospholipids, concentration, and method of formation, a variety of sizes and structures can be formed such as 1-10 μm multi-lamellar vesicles (MLVs), 0.1-1 μm large unilamellar vesicles (LUVs), and <0.1 μm small unilamellar vesicles (SUVs).[28,29] In this work, the focus is on SUVs. High drug:lipid ratios with particle sizes <1 μm have been achieved by micronizing drugs while in the presence of phospholipid stabilizers.[1] It is

suggested that in these systems the drug not only partitions into the bilayers of the SUVs employed, but colloidal drug particles are stabilized by a monolayer of phospholipid and either successive bilayers or small loosely associated vesicles.

The goal of this work was to use phospholipid vesicle solutions to stabilize nanoparticle aqueous dispersions of cyclosporine, a water-insoluble immunosuppressant, with substantial payloads, e.g. above 20 mg/mL by RESAS. To place these experiments in perspective, we begin by presenting briefly new RESAS results for stabilization by a series of micelle-forming surfactants (without phospholipids). We then demonstrate that higher drug loadings and smaller drug particles (<500 nm) may be produced with the phospholipid vesicles. The phospholipids are mixed with small amounts of micelle-forming surfactants to enhance fluidity of the surfactant bilayers. The results are compared for aqueous solutions stabilized with vesicles with only micelle-forming surfactants to provide mechanistic insight into the stabilization processes. The effects of several variables, such as drug concentration in the suspension, stabilizing solution temperature, preheater temperature, and flowrate are examined. The products are evaluated by measuring drug loading with high performance liquid chromatography (HPLC), particle sizing by dynamic light scattering (DLS), and particle morphology by transmission electron microscopy (TEM) and x-ray diffraction.

4.2 EXPERIMENTAL

4.2.1 Materials and methods.

Cyclosporine was obtained from North China Pharmaceutical Corporation and used without any further purification. Lipoid E80 (Vernon Walden, Inc.) Phospholipon 100H (American Lecithin Co.), Myrj 52 (ICI Americas), Pluronic F127(BASF), methanol (HPLC grade, EM Science), and Tween 80 (Aldrich) were used without further purification. Mannitol, sodium lauryl sulfate, and sodium deoxycholate were purchased from Sigma and used without further purification. Water was purified to Type I reagent grade by passing it through a Barnstead (NANOpure II) filtration system. Instrument grade CO_2 (Matheson) was used for all of the experiments. The structures of the various surfactants used in this study are shown in Table 4.1.

High performance liquid chromatography (HPLC) combined with UV detection was used to quantify the drug concentration from the aqueous suspensions. The column used for HPLC was a 250 mm long C-18 column (SGE ODS, 5 μm). Samples were prepared by withdrawing 0.5 mL of the suspension and adding to 5 mL of methanol, of which 9.6 μL was actually injected onto the column. The mobile phase consisted of pure methanol, and the detection wavelength was 210 nm.

The solubility of cyclosporine in the surfactant solutions was determined from a saturated solution at 25 °C. Excess drug was added to 10 mL of each surfactant solution and allowed to equilibrate with stirring for 1 week at 25 °C.

The dissolved drug content was determined by the above-mentioned HPLC method by analyzing a filtrate of each saturated solution.

The intensity-weighted particle size distribution was determined by Dynamic Light Scattering (DLS) via a Brookhaven Zetaplus (Brookhaven Instruments Corporation, New York). Particle size measurements were made within 24 hours of preparation and at 1-month time intervals. Multimodal size distributions were determined by a non-negative least squares method and the mean diameters and size ranges reported.

Table 4.1. Structures of the surfactants used in this study.

Surfactant	Structure
Myrj 52	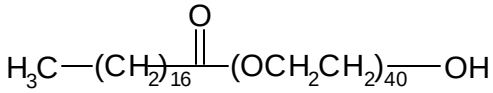
Pluronic F127	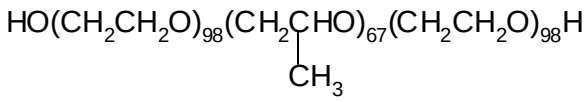
Tween 80	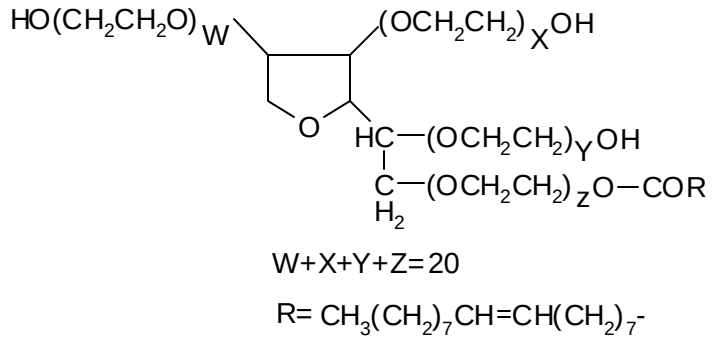
SLS	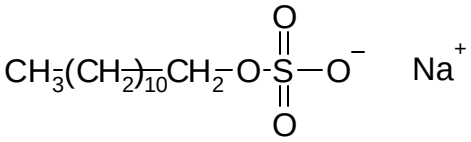

X-ray diffraction data was taken with a PW1720 X-ray generator (Philips). Suspensions examined were frozen, lyophilized, and the dry powder remaining was examined. Samples containing liquid surfactants, like Tween 80, could not be examined by this technique, only those that form a dry powder.

Differential scanning calorimetry was used to determine the phase transitions of the phospholipids. A TA Instruments DSC 2920 calorimeter was used. Typically, 8-15 mg of sample was loaded into the pan. A heating rate of 1 °C/min was used to scan over the temperature range desired.

Confirmation of vesicle and particle size and structure was determined by transmission electron microscopy using a Philips EM208 microscope. Diluted samples were dropped onto copper grids coated with Formvar. The grid was allowed to stand for 5 minutes, before the negative stain was dropped onto the grid. The stain used was a 1.0 % (w/w) solution of uranyl acetate, which had been brought to a neutral pH to prevent damage to vesicle structure.[30] After staining for 5 minutes, the grid was washed lightly (3 drops) with pure water and then the excess water was removed by touching the edge of the grid to an absorbent cloth.

4.2.2 Preparation of phospholipid vesicles.

Phospholipid solution "A" was typically made with an overall aqueous batch size of 200 g. First, Tween 80 and mannitol were added to the requisite amount of water and stirred until completely dissolved. The solution was chilled in an ice water bath, and then the phospholipid added. The solution was stirred

and sonicated (Branson Sonifier 250) while still chilled to break up any large clumps. At this time the pH was adjusted to 7.0 by adding 0.1 M NaOH. This solution was then passed 30 times through a high-pressure homogenizer (Avestin Emulsiflex C-5) at a shear pressure drop of 15000 psig to produce small unilamellar vesicles. The outlet flow from the pump was passed through a chilling tube, which was submerged in an ice bath, before returning to the pump feed supply to keep the temperature of the phospholipid solution entering the pump at 10 °C. At the end of the run, the pH was again checked and, if necessary, 0.1 M NaOH was added to bring the final pH to between 7.5 and 8.0. This solution was then refrigerated at 4 °C until ready for use.

4.2.3 Rapid Expansion from Supercritical to Aqueous solution.

The RESAS apparatus is shown in Figure 4.1. The carbon dioxide was supplied to the system by means of a high-pressure computer-controlled syringe pump (ISCO). The two solution cells are comprised of 4 ft long, 11/16 in. i.d. x 1 in. o.d. stainless steel tubes set up in parallel and equipped with pistons. Each cell was loaded with a predetermined mass of drug above the piston, sealed, and then loaded with a known volume of CO_2. The back side (or bottom) of the piston was subsequently pressurized by CO_2 to the desired pressure. Each cell was heated by 4, 2' long strips of heating tape connected to heating controllers to maintain the temperature to within ± 0.3 °C. For initial solution equilibration and mixing, only 2 of the heating tape strips were heated (the second and fourth from the top) to produce density fluctuations within the fluid to aid mixing. At the same time, the

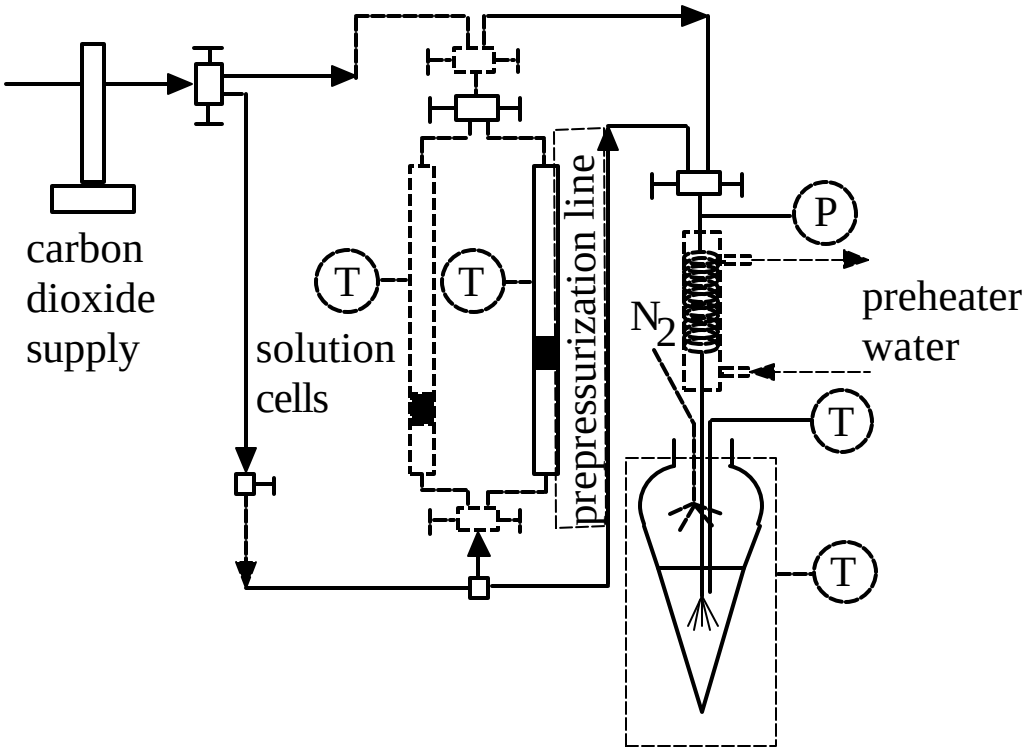

Figure 4.1. Schematic of apparatus used for rapid expansion from supercritical to aqueous solution (RESAS).

pressure within the cell was cycled via the syringe pump to create further mixing by moving the piston up and down. Typically, the solution would come to the equilibrium concentration within 24 hours. The solution concentration was checked by spraying the solution into pure methanol to collect dissolved drug, and the sample was analyzed by HPLC. If the aforementioned mixing technique was not utilized it could take the solution up to a week to reach equilibrium. The preheater consisted of a 30 ft. long piece of 1/16 in. o.d. x 0.03 in. i.d. stainless steel tubing coiled within a 1 ½" dia. x 20" long tube (column heater - Alltech) with heated water circulating through it at a rate of 2.4 L/min. This allowed very uniform heating of the preheater coil, preventing hot spots, which could otherwise produce crystallization of the drug within the coil.

For most of the experiments, the nozzle was made from a 10 inch long, 1/16 in. o.d. x 0.03 in. i.d. stainless steel tube, in a similar manner to that previously described. [26] Two sizes of nozzle were made by filing the end of the nozzle, allowing flowrates of 0.88 mL/min or 2.5 mL/min at a constant pressure drop of 345 bar. Figure 4.2 provides an example of what the spray pattern looks like exiting the 2.5 mL/min nozzle operated at a pressure drop of 345 bar. For comparison purposes, a 10 in. long piece of 50 μm i.d. fused silica capillary tubing (Polymicro Technologies, Inc.) was used as the nozzle for a few experiments.

The aqueous stabilizing solution was held in a 125 mL separatory funnel. The expanding diameter of the funnel helps to destabilize foam formation created by CO_2 bubbling through the solution, while providing sufficient depth for small

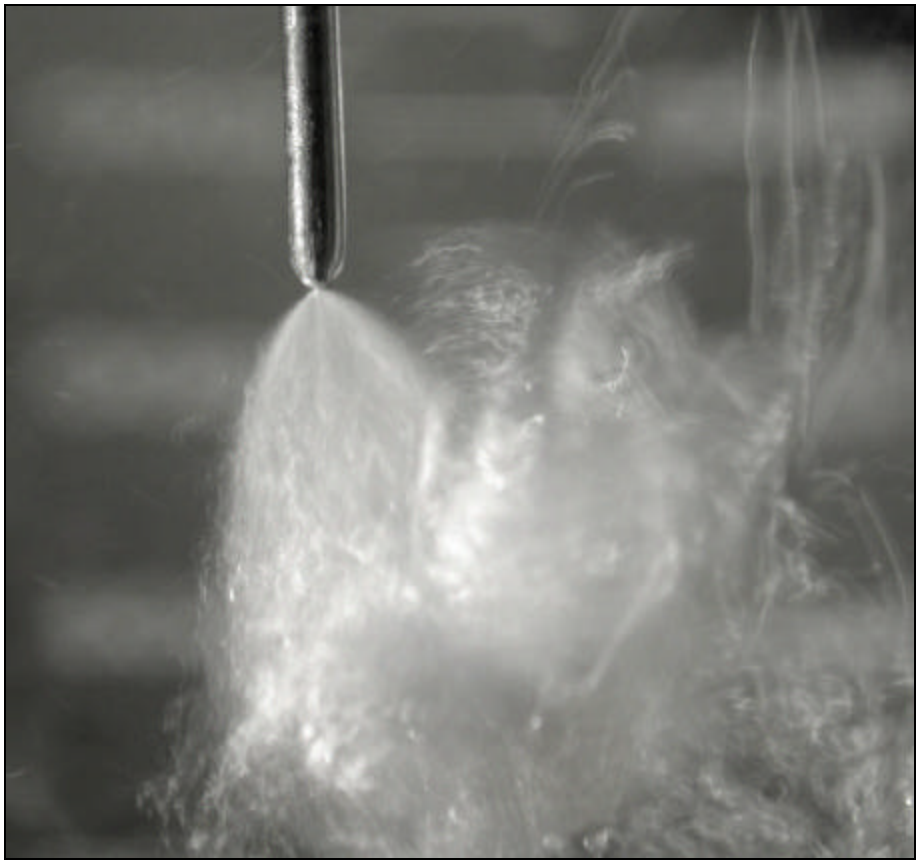

Figure 4.2 Spray profile for a CO_2 solution expanding through a tapered elliptical nozzle with a flow rate of 2.5 mL/min at 345 bar.

volumes of liquid to allow the nozzle to be submerged. The nozzle was submerged approximately 1 cm below the surface of the aqueous solution. In this way, the particles that are being formed are brought into close contact with the stabilizing solution. The separatory funnel was submerged within a temperature-controlled water bath. A thermocouple was submerged next to the nozzle in the stabilizing solution to measure the local temperature of the solution. To suppress and drain any foam produced during RESAS, N_2 gas was blown down on top of the foam at 7.8 L/min and 2 bar into the funnel approximately 4 cm above the foam through four, 1/16 in. o.d. x 0.03 in. i.d. stainless steel tubes. Prior to each experiment, 10 mL of the stabilizing solution was filtered with a 0.2 μm PES sterile disposable syringe filter (Whatman) and then added to the funnel. Immediately prior to collecting the particles, the stabilizing solution in the funnel was submerged in the heated water bath to bring it to the desired collection temperature.

To produce the suspensions, first the preheater and nozzle assemblies were prepressurized with CO_2. The prepressurization prevented plugging of the nozzle. Once the flow of CO_2 had equilibrated, the flow was switched so as to push the solution out of the cell and through the nozzle. Initially, the spray was conducted by spraying into a separatory funnel containing pure water. Once drug particles began to accumulate in the water, the separatory funnel was switched to one of the prepared and preheated stabilizing solutions. A measured volume (as measured by the syringe pump) of solution was sprayed to produce a suspension of a desired concentration. Upon completing the spray, the stabilizing solution

was replaced by pure water again, and the flow switched back to pure CO_2. Sufficient CO_2 was allowed to spray through the nozzle to insure all drug was swept out of the system to prevent nozzle plugging upon depressurization. For all of the samples using phospholipid-based surfactants the pH of the suspension was adjusted again, after the spray was completed, to 7.0 by adding sufficient 0.1 M NaOH. Typically the pH of the phospholipid solution would go from 7.5 $\rightarrow$ 3.5 during the course of the spray. pH neutralization was required to insure long-term stability of the phospholipids. The samples were stored with a N_2 headspace by purging the air from the sample vial through a septum in the vial cap to prevent oxidation of the phospholipid components. The samples were refrigerated at 4°C.

4.3 RESULTS AND DISCUSSION

4.3.1 Cyclosporine solubility.

The phase behavior of cyclosporine in CO_2 has previously been reported.[26] At 30 °C and 345 bar, 1.0 % (w/w) of cyclosporine is readily soluble in CO_2. All of the RESAS experiments in this work were performed with an initial solution concentration of 1.0 % (w/w). It is important to note that the solubility of cyclosporine in CO_2 decreases with temperature at constant pressure (cloud point increases). The solubilities of cyclosporine in the surfactant solutions used for stabilization were measured to serve as a control, as shown in Table 4.2 at 25 ^{o}C. The goal of RESAS was to produce suspensions with a drug/surfactant ratio much higher, and at least twice as high, as is obtained from the equilibrium solubility in

the surfactant solution. As a result, SLS was not chosen as one of the surfactants to examine since the solubility of cyclosporine in this solution is quite high.

Table 4.2. Solubility of cyclosporine in various surfactant systems at 25.0 °C.

Surfactant name	Surfactant conc. in H_2O % (w/w)	Drug solubility mg/mL	Drug/surf. ratio w/w
Tween 80[a]	1	0.56	0.056
	2	1.2	0.060
Myrj 52	2	1.7	0.085
SLS	2	27.0	1.4
Pluronic F127	2	0.01	0.0005
Lipoid E80/Tween 80/mannitol	10/2/5.5	4.75	0.04
	1/0.2/0.55	0.32	0.03

[a] Young, et al. *Biotechnol. Prog*., **2000**, 16(3), 402-7

4.3.2 Effect of surfactant type on particle size.

While the bulk of the RESAS experiments will focus on phospholipid-based systems, micelle-forming surfactants including Tween 80, Poloxamer F127, and Myrj 52 were studied for comparison, as shown in Table 4.3. All of the experiments conducted in the table had the following initial conditions: a drug concentration of 1.0 % (w/w) in CO_2, a solution temperature of 30.0 °C, a preheater temperature of 60.0 °C, a pressure drop of 345 bar with a nozzle that

Table 4.3. Effect of surfactant type on cyclosporine microparticles prepared by RESAS of a 1.0 % (w/w) solution into 10.0 mL of 2.0 % (w/w) aqueous surfactant solution.[a]

Surfactant type	Drug conc. (mg/mL)	Yield % (w/w)	Particle mean (nm)	Particle size distribution (nm)	Drug/surf. ratio @ max sol.	Drug/surf. ratio (g/g)
Tween 80[b]	6.1	68	970	210-320(21%), 500-760(59%), 2200-3400(20%)	0.056	0.61
Tween 80[b]	5.4	64	660	220-290(25%), 700-940(75%)		0.54
F127	4.0	46	1010	140-250(12%), 400-860(75%), 3400-5400(13%)	0.0005	0.20
F127	4.7	48	1200	180-310(7%), 520-870(66%), 2100-4100(27%)		0.24
Myrj 52	4.6	49	840	90-120(2%), 310-590(58%), 1100-2100(40%)	0.085	0.23
Myrj 52	3.2	38	1240	150-270(9%), 410-850(79%), 4800-7500(13%)		0.16
SLS	------	------	-----	-------	1.4	

[a] $T_{sol'n}$ = 30.0 °C, $T_{preheater}$ = 60.0 °C, ΔP = 345 bar, T_{bath} = 25.0 °C, solution flowrate = 2.5 mL/min

[b] 1.0 % (w/w)

produced a flow rate of 2.5 mL/min, and a stabilizing solution bath temperature of 25 °C. The table shows the final concentration of drug in the suspension as measured by HPLC, the mean particle size, the particle size distribution (with the relative percentage of particles found in each peak for multi-peak distributions), and the drug to surfactant ratio for the equilibrium solubility as well as for the actual suspension.

As seen in Table 4.2, Tween 80 stabilized particles with mean diameters from 660 – 970 nm with fairly broad distributions at relatively high drug/surfactant ratios of nearly 0.6, which was 10 times the equilibrium solubility. These results agree reasonably well with previous work.[26] The new experiments utilize smaller aqueous stabilizer volumes and higher flow rates that did not seem to modify the particle size. To minimize aggregation resulting from particle collisions, the surfactant must reach the surface of the primary particle rapidly and orient such that it can provide steric stabilization. Previously,[26] the particle size increased markedly for a drug:surfactant ratio >0.6, due to insufficient surface coverage. In contrast, using Pluronic F127 led to substantially larger particles, despite the lower drug/surfactant ratio of approximately 0.25. It appears that this surfactant has a lower affinity for the particle surface, which would be consistent with the low equilibrium solubility. The lipophilic propylene oxide group makes up only 30 % (w/w) of the surfactant molecule, which might not be enough for sufficient adsorption at the particle surface. The use of Myrj 52 also yielded larger cyclosporine particles than Tween 80. While this surfactant has a modestly different lipophilic group than Tween (stearate compared to oleate), it also has a

more linear, or less bulky, hydrophilic group. Tween 80 has several ethylene oxide side chains providing greater steric repulsion in the continuous aqueous phase.

Table 4.4. Compositions of the various phospholipid surfactant systems used in this study.

Designation	Components	Concentrations % (w/w)	Vesicle size mean nm	Vesicle size range nm
Phospholipid "A"	Lipoid E80/ Tween 80/ Mannitol	10/2/5.5 1/0.2/0.55	39.6 35.1	20-50 10-50
Phospholipid "B"	Phospholipon 100H/ Tween 80/ Mannitol	2/2/5.5	90.2	70-280
Phospholipid "C"	Phospholipon 100H/ Myrj52/ Sodium Deoxycholate/ Mannitol	2/1/0.25/5.5	131.2	60-360
Phospholipid "D"	Phospholipon 100H/ Myrj52/ Mannitol	2/2/5.5	140.5	70-440

Results are shown in Table 4.5 for several phospholipid-based surfactant mixtures, whose compositions are given in Table 4.4. The two phospholipids included commercially available compounds Lipoid E80 (from chicken egg-white) and Phospholipon 100H (hydrogenated soybean), which both consist primarily of dipalmitoylphosphatidylcholine (DPPC), and include small amounts of impurities such as phosphatidylethanolamine, sphingomyelin, and lyso-

phosphatidylcholine. Each of these systems was prepared so as to have initial structures consisting of small unilamellar vesicles < 1 μm in water. Preparations made with Lipoid E80 had starting vesicle sizes of 10-50 nm, while those made with Phospholipon 100H were slightly larger, as confirmed by DLS. The nonionic surfactants can act to make the vesicle bilayer more fluid[31], facilitating transport across the bilayer. All of these systems included Mannitol to enhance vesicle stability, and also to act as a cryoprotectant to prevent loss of structure during lyophilization.[32-34] Sodium deoxycholate was utilized in system "C" to supplement the steric stabilization with electrostatic stabilization.

Results are shown in Table 4.5 for the various phospholipid-based surfactant systems. The table shows the final concentration of drug in the suspension as measured by HPLC, the mean particle size, the particle size distribution (with the relative percentage of particles found in each peak for multi-peak distributions), and the drug to surfactant ratio for the equilibrium solubility as well as at the final suspension concentration. In order to be able to distinguish between vesicles and particles in the final solutions, a few control experiments were performed. First, in the range of 10 – 50 °C, it was found that the size of the SUVs does not change when measured by DLS. Second, if pure CO_2 is sprayed into the solution for a time similar to that in the rest of the experiments (up to an hour), there is also no change in the vesicle size even with the change in pH from $7 \rightarrow 3$ that results. pH is known to affect vesicles by increasing DPPC hydrolysis rates, and pH gradients have been utilized in the formation of SUVs.[35] Therefore, it's reasonable to

Table 4.5. Effect of surfactant type on cyclosporine microparticles prepared by RESAS for a stabilizing solution bath temperature of 25 °C.[a]

Phospholipid surfactant composition	Drug conc. (mg/mL)	Yield % (w/w)	Particle mean (nm)	Particle size distribution (nm)	Drug/surf. ratio (g/g)
A[b]	6.5	93	220	30-50(4%), 100-160(66%), 330-560(30%)	0.54
A[b]	6.9	100	220	80-120(32%), 250-300(68%)	0.58
B	4.6	54	660	80-420(91%), 3300-6300(9%)	0.12
B	5.1	62	640	80-420(93%), 5100-7100(7%)	0.13
C	4.1	26	2740	140-300(16%), 720-1740(60%), 7500-10000(34%)	0.13
C	4.2	34	4110	280-470(56%), 7700-10000(44%)	0.13
D	7.7	63	390	150-200(54%), 560-750(46%)	0.19
D	6.9	59	460	110-180(54%), 320-560(27%), 1180-2060(19%)	0.17

[a] $T_{sol'n}$ = 30.0 °C, $T_{preheater}$ = 60.0 °C, ΔP = 345 bar, T_{bath} = 25.0 °C, solution flowrate = 2.5 mL/min

[b] 1.0 % Lipoid E80/ 0.2 % Tween 80/ 0.55 % Mannitol (w/w); T_{bath} = 45.0 °C

believe that any change in particle size distribution as measured by DLS after RESAS with a drug would correspond to the presence of stabilized drug particles.

The low concentration solution "A" was able to stabilize cyclosporine particles at concentrations of ~7 mg/mL (~0.6 drug:surfactant ratio) with mean diameters of 220-230 nm and relatively narrow size distributions as seen in Table 4.5. The distributions are bimodal. The smaller peak is somewhat larger than the initial drug-free vesicles suggesting that the drug induces modest aggregation of these vesicles. The larger peak is 5-10 times the size of the initial vesicles. It is likely that most of the drug is contained in these larger aggregates. The drug/surfactant ratios are over 20 times the equilibrium solubility in the vesicles. While the examples discussed here were made with the lower concentration of formulation A, these suspensions tended to be less stable (discussed in more detail later) and were incapable of stabilizing drug payloads up to 50 mg/mL. Therefore, the majority of the rest of the work detailed herein was conducted using the higher concentration of formulation A.

Figure 4.3 shows TEM micrographs taken of several of the suspensions formed in this study. The top picture shows the initial empty SUVs of phospholipid formulation A before RESAS with particle sizes that are between 10-80 nm. Upon exposure of the aqueous vesicles to CO_2, there was no noticeable change in the TEM micrographs. Note that in some regions, the vesicles associate loosely to form aggregates. Also, the vesicle shape appears distorted from a spherical shape. Some distortion can occur due to collapse or close packing of the vesicles upon water evaporation.[28,35] The negative staining

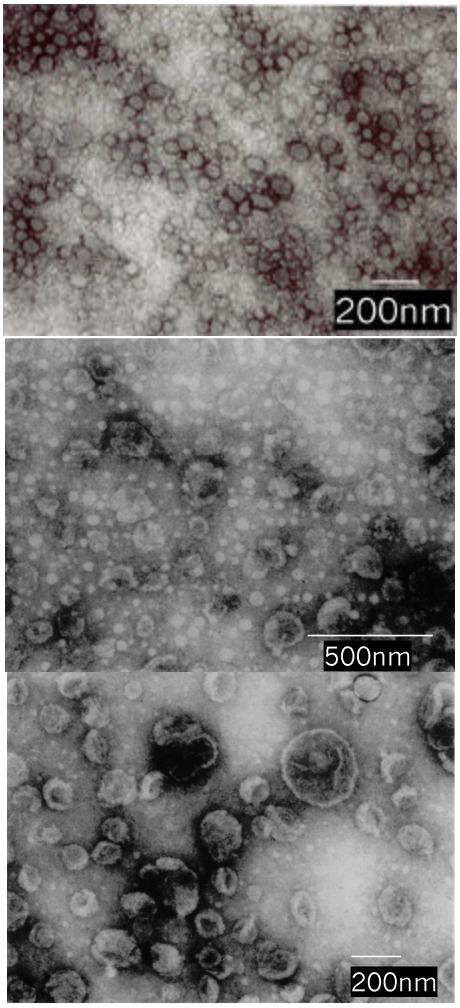

Figure 4.3 TEM micrographs of: a) initial SUVs made from phospholipid formulation A before RESAS, b) drug loaded vesicles of phospholipid formulation A at a concentration of 17.6 mg/mL and stabilizing solution temperature of 31.1 °C; operating conditions: T_{soln} = 30.0 °C, $T_{preheater}$ = 60.0 °C, ΔP = 345 bar, T_{bath} = 45.0 °C, solution flowrate = 2.5 mL/min, c) drug loaded vesicles of phospholipid formulation A at a concentration of 54.0mg/mL and stabilizing solution temperature of 50.3 °C; operating conditions: T_{soln} = 30.0 °C, $T_{preheater}$ = 60.0 °C, ΔP = 345 bar, T_{bath} = 80.0 °C, solution flowrate = 2.5 mL/min

technique can be used to observe multilamellar structures, if present. MLVs could be seen (not shown) before homogenization to form SUVs. The middle micrograph shows the particles at a drug:surfactant ratio of 0.15, showing both the large stabilized drug particles (~200 nm) as well as small vesicles. The DLS results showed particles as large as 400 nm, so there may be some aggregation occurring within the suspension between the larger drug particles and the remaining SUVs. Unfortunately, with this staining technique, we were unable to visualize the monolayer of surfactant on the particles, as the stain simply deposits around the outside of the particle. Also, we saw no evidence of successive bilayers surrounding the particles. While it was somewhat difficult to distinguish between drug particles and vesicles, the larger objects seen in this micrograph never appeared when inspecting phospholipid vesicles with no drug. Also, the entities we believe to be the drug particles have highly non-uniform surfaces, which was also something not observed with unloaded vesicles. The bottom micrograph shows the particles formed at a high drug:surfactant ratio of 0.45, depicting very few small vesicles remaining with numerous large stabilized drug particles, approaching 300 nm. The DLS results in this case indicated three size ranges, 40-60, 100-200, and 500-920, with the bulk of the material present in the last peak. This distribution again suggests that some of the particles in the TEM associate or aggregate.

The particle diameters of the phospholipid-stabilized suspensions are markedly lower than those produced with micellar-forming surfactants for similar surfactant concentrations and drug/surfactant ratios. To stabilize such small

particles, the surfactant must be able to rapidly adsorb onto the particle surfaces as they precipitate and hinder growth in the jet. Since the bulk of the surfactant is now in the structure of a vesicle, the stabilization mechanism may be expected to be different than for the micelle-forming surfactants in Table 4.3. In the case of vesicles, the aggregation number of surfactant is much larger than for micelles. Thus, the local concentration of surfactant in a single vesicle that can coat a growing drug particle is higher than for a single micelle. The preferred curvature of the surfactant is more favorable for vesicles than micelles. For vesicles, the interface with water is less curved than for the much smaller micelles and will more closely match that of the drug particles. The better match in curvature may be expected to favor particle stability. The growing drug nuclei may collide with a bilayer of the vesicle and dissolve. The presence of the non-ionic surfactant Tween can aid the transport through the bilayer. Since vesicles tend to be relatively stable, growth of drug particles by collision/coagulation is minimized. Thus, the particle may be expected to grow mostly due to a condensation mechanism[25] within the bilayer as additional drug nuclei enter. When the drug particle size becomes large enough, it can disrupt the vesicle structure and essentially cause an "unzipping" of the bilayer as the vesicle breaks. The rearrangement of the surfactant may be expected, leaving a monolayer of the phospholipid on the particle surface with the polar heads solvated by water. SUVs may then become loosely associated with the hydrophilic groups on the outside surface of this monolayer. Previous work has demonstrated the ability of phospholipid surfactants to adsorb on a hydrophobic surface as a monolayer.[1]

Unfortunately, in all the cases where Phospholipon 100H was used, the solutions foamed extensively and quickly became very viscous, or in the case of solution "C" even gelled, during the spray. Changing the temperature of these solutions from 25 °C to 75 °C had no observable or measurable effect on the particles collected or the nature of the solution during RESAS. When the solution becomes too thick, any further spraying yields large particles, as the surfactant can no longer diffuse to the particle surfaces as they precipitate and grow. In the case of phospholipid solution "B," particles were stabilized with mean diameters from 370-660 nm with broad distributions from 30 nm to 7 μm. Phospholipid solution "C" quickly gelled during the spray, yielding the largest particles of any of the phospholipid combinations with approximate mean particle sizes of 2-4 μm and broad size distributions. Phospholipid solution "D" stabilized particles moderately well, with mean sizes of 290-460 nm and particles ranging from 70 nm to 3 μm. Solutions "B, C, and D" also each had low trapping yields as the solutions became too viscous. Likely, the difference between the performance of Lipoid E80 and Phospholipon 100H lies in the source (egg vs. soybean), and resulting differences in impurities. Since phospholipid solution "A" produced the smallest particles, it will be the focus of the experiments in later sections concerning the effects of temperature, drug concentration, etc.

In Figure 4.4, we show the x-ray diffraction patterns for cyclosporine before RESAS (lower curve), and for cyclosporine stabilized by Pluronic F127 (upper curve). Prior to processing, the cyclosporine is crystalline, showing multiple sharp peaks. After processing by RESAS and stabilization by F127, the

cyclosporine crystal peaks have disappeared, suggesting the drug is now trapped in an amorphous state. The two large peaks seen are due to the surfactant, Pluronic F127. Since the entire sample produced with F127 was dried and analyzed (including the large particles), and the entire sample was amorphous, it is not unreasonable that the smaller drug particles trapped with the other surfactant systems could also be amorphous.

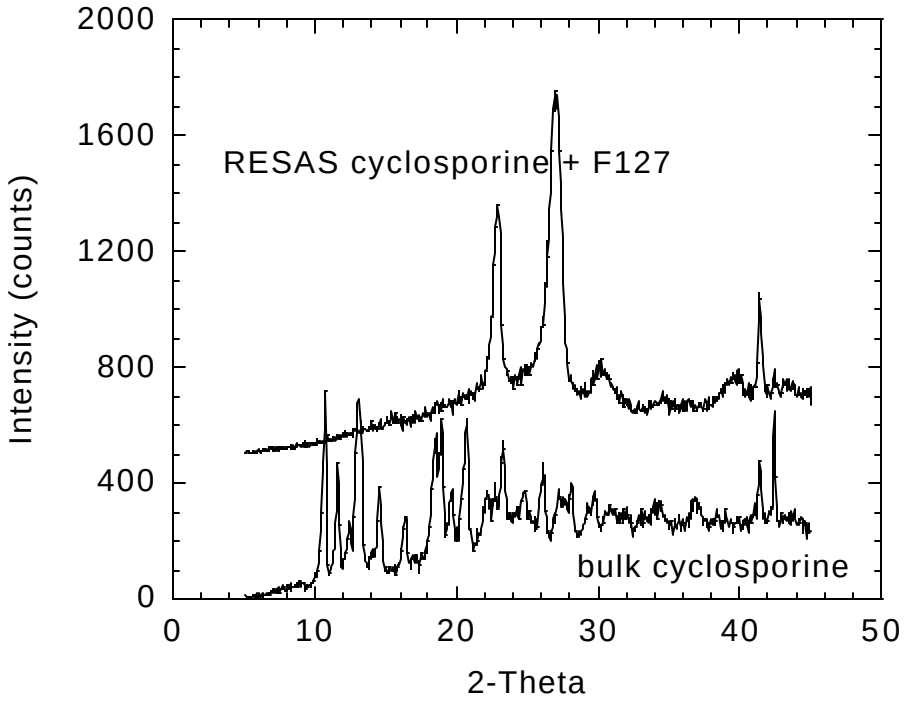

Figure 4.4 X-ray diffraction patterns for bulk cyclosporine (bottom) and cyclosporine processed by RESAS and stabilized by poloxamer F127 (drug/surfactant ratio= 0.2).

4.3.3 Effect of suspension concentration

Tables 6,7,8 illustrate the effect of the drug concentration, which is a function of spray time, on the particle size for bath temperatures of 25, 45, and 80 °C, respectively. In all of the experiments, the stabilizing solution was phospholipid formulation "A" at the higher concentration levels as shown in Table 4.4. The starting vesicle size in the solution, as listed in Table 4.4, was 10-50 nm and they are likely SUVs. Upon examination with TEM, the vesicles appeared similar to those shown in Figure 4.3a. The tables show the actual stabilizing solution temperature measured within the separatory funnel in addition to the same entries found in Table 4.5.

Table 4.6 shows the particle size for a bath temperature of 25.0 °C. At a drug concentration of ~20 mg/mL, particles collected had a mean diameter of 500-650 nm with sizes ranging from 70 nm – 2 μm. At ~40 mg/mL the mean particle size increased to 730 nm with very broad distributions. The average particle size grew by as much as 50% when doubling the drug concentration. A further increase in drug concentration to 46 mg/mL produced a substantial increase in particles larger than 1 micron indicating loss of stabilization against aggregation.

In Table 4.7 versus Table 4.6 the only difference in experimental conditions was the stabilizing solution bath temperature, which was 45.0 °C. Initially, at a drug:surfactant ratio of ~0.1 (roughly 2 times the equilibrium solubility) the particle mean diameters were only 160-180 nm with narrow size

Table 4.6. Effect of suspension concentration on cyclosporine microparticles prepared by RESAS for a stabilizing solution bath temperature of 25 °C.[a]

Stabilizing sol'n temp. °C	Drug conc. (mg/mL)	Yield % (w/w)	Particle mean (nm)	Particle size distribution (nm)	Drug/surf. ratio (g/g)
14	18.4	89	650	70-140 (28%), 240-450 (36%), 1000-1900(36%)	0.15
13.3	19.4	96	500	90-190 (45%), 530-1260 (55%)	0.16
14.8	24.2	110	630	120-210 (47%), 760-1440 (53%)	0.20
15.8	39.0	110	730	50-80 (4%), 160-290 (33%), 750-1500 (63%)	0.33
13.7	39.8	80	960	80-160 (14%), 480-910 (74%), 2700-5200 (12%)	0.33
13.6	45.9	94	1700	80-160 (12%), 500-1150 (74%), 5000-10000 (14%)	0.38

[a] T_{soln} = 30.0 °C, $T_{preheater}$ = 60.0 °C, ΔP = 345 bar, T_{bath} = 25.0 °C, solution flowrate = 2.5 mL/min

Table 4.7. Effect of suspension concentration on cyclosporine microparticles prepared by RESAS for a stabilizing solution bath temperature of 45 °C.[a]

Stabilizing sol'n temp. °C	Drug conc. (mg/mL)	Yield % (w/w)	Particle mean (nm)	Particle size distribution (nm)	Drug/surf. ratio (g/g)
32	10.3	70	160	80-110 (67%), 260-350 (33%)	0.09
33	13.0	87	180	80-110 (47%), 220-290 (53%)	0.11
31.2	15.8	89	280	40-70 (6%), 140-220 (67%), 450-760 (27%)	0.13
29.8	17.5	95	290	110-160 (44%), 370-470 (56%)	0.15
31.1	17.6	93	260	90-120 (33%), 290-400 (67%)	0.15
30.3	26.2	72	380	40-80 (10 %), 200-370 (71%), 690-1100 (19%)	0.22
31.2	24.4	74	310	40-100 (13%), 200-520 (87%)	0.20
30.5	31.7	83	390	30-50 (2%), 140-230 (44%), 430-820 (54%)	0.26

[a] T_{soln} = 30.0 °C, $T_{preheater}$ = 60.0 °C, ΔP = 345 bar, T_{bath} = 45.0 °C, solution flowrate = 2.5 mL/min

Table 4.8. Effect of suspension concentration on cyclosporine microparticles prepared by RESAS for a stabilizing solution bath temperature of 80 °C.[a]

Stabilizing sol'n temp. °C	Drug conc. (mg/mL)	Yield % (w/w)	Particle mean (nm)	Particle size distribution (nm)	Drug/surf. ratio (g/g)
56.8	12.6	88	220	60-90 (45%), 270-380 (55%)	0.11
54.3	14.8	88	230	60-90 (40 %), 290-390 (60%)	0.12
57.2	17.6	72	320	60-100 (28%), 310-600 (72%)	0.15
53.7	23.8	62	390	80-120 (34%), 440-650 (66%)	0.20
53.8	27.0	72	460	100-140 (31%), 500-750 (69%)	0.23
52.7	39.8	99	480	50-100 (48%), 170-360 (18%), 860-1770 (34%)	0.33
50.3	54.0	139	500	40-60 (26%), 100-200 (11%), 500-920 (63%)	0.45

[a] T_{soln} = 30.0 °C, $T_{preheater}$ = 60.0 °C, ΔP = 345 bar, T_{bath} = 80.0 °C, solution flowrate = 2.5 mL/min

distributions. At a drug surfactant ratio of ~0.15, the particle mean increased to 260-290 nm, and at 0.25, it reached 310-390 nm with a slightly broader size distribution. In all cases the particles were much smaller than those produced with Tween 80.

In Table 4.8, the stabilizing solution bath temperature was 80 °C. For a given drug loading, each of the properties of the particles was similar to that for a bath temperature of 45 ^{o}C. In all three cases, the particle size increased substantially with drug concentration, which increases with spray time. Figure 4.5 demonstrates the trends in particle growth more clearly. For the two higher stabilizing solution temperatures, the particle size increases approximately linearly with drug concentration, with only a small increase in size with temperature. For a temperature of 14 °C, the size is larger by a factor of about two and the scatter about the linear correlation with drug concentration is much larger.

Several factors may be expected to cause the increase in particle size with drug concentration. The first factor is surfactant depletion in the aqueous solution as the SUVs coat the particles and form drug-surfactant aggregates. As the spray time and drug concentration increase, fewer of the initial SUVs are available for stabilizing incoming particles. Another factor is that the particle collision rate increases approximately with the square of the particle concentration. In addition, an increase in the drug concentration raises the drug/surfactant ratio in the aqueous solution. The resulting increase in total drug surface area and decrease in surfactant coverage of this drug surface area may lead to greater aggregation of

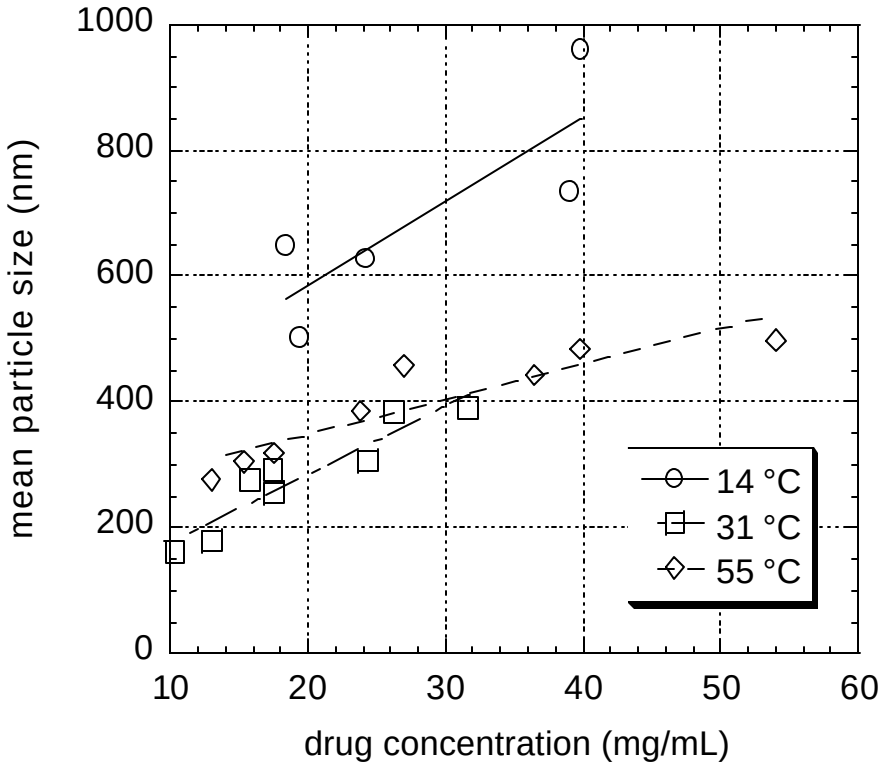

Figure 4.5 Effect of drug concentration and stabilizing solution temperature on cyclosporine particles produced by RESAS with phospholipid solution "A" as the stabilizer. T_{soln} = 30.0 °C, $T_{preheater}$ = 60.0 °C, ΔP = 345 bar, T_{bath} = 25, 45, 80.0 °C, solution flowrate = 2.5 mL/min

the surfactant coated drug particles. Another factor is simply the greater time for particle growth due to shear-induced aggregation caused by the flowing carbon dioxide. Once removed from the process, however, the drug suspensions were extremely stable with little change in particle size measurable by DLS even after weeks of storage, as discussed in greater detail below.

4.3.4 Effect of stabilizing solution temperature

The ability for the phospholipid-based surfactants to stabilize the particles may be expected to depend upon the temperature of the medium within the receiving vessel. Most phospholipid vesicles exhibit a transition temperature from a rigid gel-like state to a fluid liquid-crystalline state. As temperature increases, the phospholipid chains within the vesicles go from a very rigid, ordered state, to one that is more flexible and can allow diffusion across the bilayer. The rigidity of the phospholipid tails, and hence the vesicles, could affect the surfactant's ability to rearrange in order to stabilize the drug particles as they precipitate. The effect of lipid chain melting behavior, and hence the lipid's ability to orient at the surface of emulsion droplets has been studied.[28] Dry Lipoid E80 powder was analyzed by DSC to determine the chain melting point, as shown in Figure 4.6. The melting transition appears slightly above room temperature, at 24-29 °C. While the location of the transition agrees with previous studies,[28] the transition enthalpy is lower here. This difference is likely due to adsorbed water. When 10 % (w/w) of lipoid E80 was added to water, however, the DSC thermogram was dominated by the water melting peak, and since the transition

enthalpy was already low, it could no longer be detected. This effect was seen previously.[28] Also, the fact that it is hard to detect a clear transition in solution is not unexpected for lipid samples that are not made of pure components or that have additives such as cholesterol.[36] While the presence of Tween 80, mannitol, and even the drug in the vesicles would be expected to further broaden/shift the transition point,[28,36-41] this effect could unfortunately not be demonstrated with this system.

Note that in each of the tables, the actual stabilizing solution temperature near the nozzle is significantly lower than that of the water bath used to heat the medium. This cooling is due to the expanding CO_2 gas. As seen in Fig. 3, the particle sizes measured when the stabilizing solution temperature was above 30 °C were nearly the same at similar drug loadings, regardless of the stabilizing solution bath temperature. However, a large increase in particle size was noted for the cases where the stabilizing solution was only 14 °C. It's likely that at this temperature the phospholipid chains are too rigid to rearrange and stabilize the growing particles as rapidly as at the higher temperatures. The increase in the viscosity of water at locally low temperatures could further inhibit diffusion and rearrangement of surfactant. There could also be an effect of locally colder temperatures in the vicinity of the nozzle tip decreasing supersaturation based on the phase diagram[26], slowing particle nucleation and producing larger particles. This supersaturation effect is discussed in greater detail in the next section on the effect of preheater temperature for a constant stabilizing solution temperature.

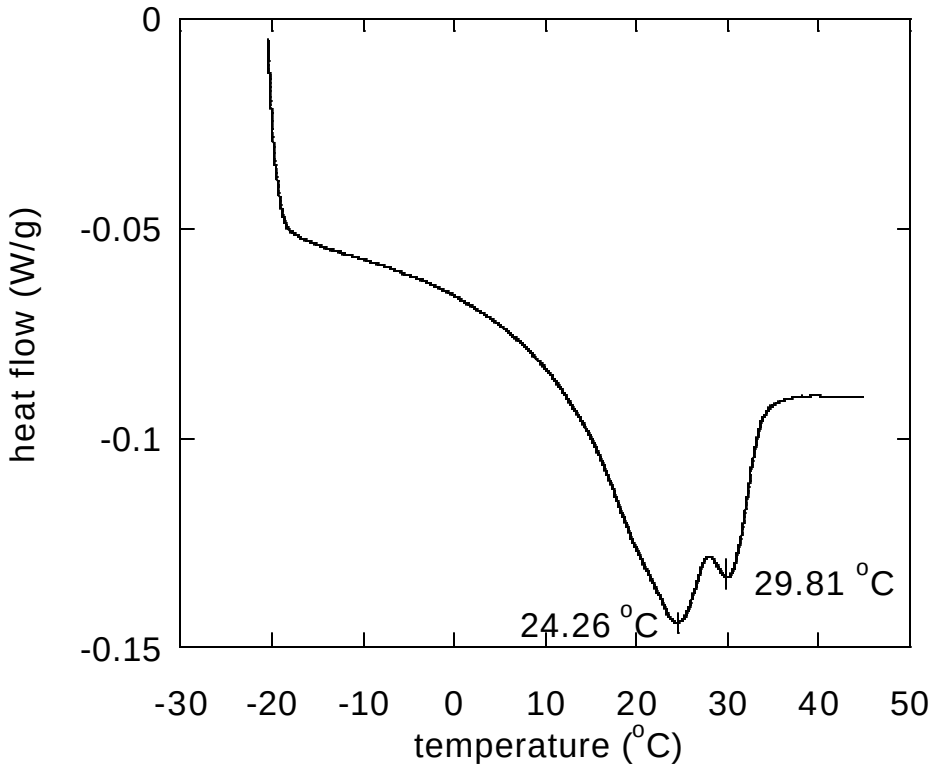

Figure 4.6 DSC thermogram of bulk Lipoid E80.

4.3.5 Effect of preheater temperature

Cyclosporine becomes less soluble in CO_2 as temperature increases.[26] Therefore it is expected that at higher preheater temperatures, the depressurization in the nozzle will cause the solution to pass through the phase boundary more quickly than at lower temperatures, leading to higher levels of supersaturation.[15,25,26,42] The greater supersaturation, in turn, leads to higher rates of nucleation, which would lead to the formation of smaller particles, if aggregation may be controlled.

Table 4.9 illustrates the effects of the preheater temperature on the cyclosporine particle size. The first two entries show the results through a nozzle at a flow rate of 0.88 mL/min at a ΔP of 345 bar. At a low preheater temperature of 30 °C, the particles produced at this flowrate were larger than 10 μm and quickly settled out, leaving only drug solubilized in the SUVs. With a bath temperature of only 30 °C, the stabilizing solution temperature became too cold for adequate stabilization as discussed above. At a higher preheater temperature of 60 °C, and at a drug:surfactant ratio of 0.24 the particles had a mean size of 530 nm. The higher preheater temperature resulted in less local cooling for this nozzle flowrate, and allowed the stabilization of particles.

Table 4.9. Effect of preheater temperature on cyclosporine microparticles prepared by RESAS of a 1.0 % (w/w) solution into 10.0 mL of phospholipid mixture A.[a]

T_{pre} °C	Stabilizing sol'n temp. °C	Drug conc. (mg/mL)	Yield % (w/w)	Particle mean (nm)	Particle size distribution (nm)	Drug/surf. ratio (g/g)
30[b]	22.0	2.5	30		30-130, >10 μm	0.02
60[b]	21.2	24.0	80	530	190-290 (82%), 1500-2500 (18%)	0.24
30	32.1	27.8	100	400	50-240 (40%), 440-720 (60%)	0.23
30	31.7	19.3	82	380	90-170 (15%), 270-590 (85%)	0.16
60	32.2	14.3	98	280	40-180 (68%), 420-770 (32%)	0.12
60	31.8	11.9	84	320	110-150 (41%), 400-540 (59%)	0.10
80	31.6	11.7	79	110	70-100 (90%), 280-380 (10%)	0.10
80	32.0	13.1	78	190	20-140 (70%), 280-380 (30%)	0.11

[a] T_{soln} = 30.0 °C, T_{bath} = 45.0 °C, ΔP = 345 bar, solution flowrate = 2.5 mL/min

[b] T_{soln} = 30.0 °C, T_{bath} = 40.0 °C, ΔP = 345 bar, solution flowrate = 0.88 mL/min

In the remainder of the results in Table 4.9, the solution flowrate was 2.5 mL/min at the same ΔP of 345 bar. As the preheater temperature was changed from 30 to 80 °C, the mean particle size decreased. The drug/surfactant ratio was fairly constant, especially for the higher two preheater temperatures. Notice that the preheater temperature had essentially no effect on the stabilizing solution temperature due to the efficient heat transfer in the nozzle and the jet, and the large change in latent heat for compressed CO_2 relative to the sensible heat. Consequently, the rigidity of the phospholipids in the aqueous solutions was essentially constant. Thus, the decrease in particle size is most likely due to the faster nucleation rate produced by the higher supersaturation at the higher preheater temperatures.

4.3.6 Effect of nozzle size

Table 4.9 also illustrates the effect of nozzle size on the particle size. Two crimped nozzles were compared with similar operating pressures, ΔP = 345 bar, but with flow rates of 0.88 mL/min and 2.5 mL/min. The greater restriction for the slower flowrate nozzle indicates that the crimping and filing process produced a smaller elliptical orifice. The smaller, low flowrate, nozzle appears to produce larger particles than the high flowrate nozzle. While smaller droplet sizes would be expected with the smaller nozzle due to more intense atomization, the dominating factor on particle stability in this system appears to be the conditions of the stabilizing solution. At the lower flowrate, the jet is less forceful and creates less mixing/turbulence within the stabilizing solution. The weaker mixing

is evident in the lower local temperature within the stabilizing solution. At the higher flowrates, the solution is agitated more intensely, and heat is transferred throughout the fluid within the separatory funnel more efficiently, producing a higher local temperature. Since the lower flowrate nozzle creates less turbulence, the particles and surfactant are not mixed as well leading to less effective stabilization. Also, the particles are not carried away from the jet as quickly, allowing for potentially more collisions prior to complete stabilization. In the future, this limitation could be overcome by stirring the solution.

The use of a much larger 50 μm i.d. x 10 cm long straight capillary nozzle in RESAS led to low yields (<35%) and the formation of >10 μm particles. Also, this nozzle tended to plug easily as compared to the crimped nozzle design, which never plugged during a spray. In the case of the capillary nozzle, the depressurization profile occurs over the entire length of the nozzle, resulting to some particle nucleation and growth within the nozzle where it cannot be stabilized.

4.3.7 Long term stability

For all of the samples produced, initial particle size measurements were made within 24 hours of the RESAS spray. Also, the stability of the particle size after 1 month of storage at 4 ^{o}C and under nitrogen was examined and the data is shown in Table 4.10. Each sample was gently inverted 5-10 times and then allowed to sit for 1 hour prior to analysis. For each of the non-phospholipid surfactants, the particles settled completely and caked at the bottom of the vial.

These samples were not redispersible, even by sonication. The samples produced by RESAS with phospholipid solution "A" had good stability, with no settling observed for most of the suspensions without shaking. Even in cases where there was some settling present, the samples were easily redispersed by the gentle inversions. Most of the samples experienced some growth, or small broadening in the size distribution. In one case, the particle size grew considerably during the one month period, likely due to the very high drug:surfactant ratio (>0.5) in this system due to the low amount of surfactant and also showed instability in the form of settling. In the case where the particle size appears to decrease, it's likely that some of the larger particles have settled out (not visible to eye) and were simply not captured in the sample analyzed by DLS.

Table 4.10. Suspension stability after 1 month of storage at 4°C for phospholipid mixture A - 10/2/5.5 % (w/w) Lipoid E80/Tween 80/mannitol.

Original mean nm	Mean after 1 mo. nm	Distribution after 1 mo. nm	% change
260	320	30-50(25%), 120-190(16%), 410-710(59%)	20
220	750[a]	50-230(17%), 660-1200(83%)	240
1700	720	100-160(10%), 650-1000(90%)	-40
390	700	80-140(29%), 200-300(6%), 820-1230(65%)	80
460	560	50-240(47%), 560-1780(53%)	20
400	740	60-90(41%), 170-350(16%), 1200-2000(43%)	85
320	420	50-150(46%), 220-410(15%), 680-1120(39%)	30

[a] settling height was 7% of the total; 1.0/0.2/0.55 % (w/w) Lipoid E80/Tween 80/mannitol

4.4 CONCLUSIONS

Phospholipid vesicles mixed with nonionic surfactants stabilize cyclosporine particles produced by RESAS with mean diameters as small as 200-300 nm. This size range is several hundred nanometers smaller than produced by RESAS for particles stabilized by Tween 80. Many of the size distributions are bimodal, according to DLS measurements and TEM, consisting of vesicles with very low drug concentrations and drug particle aggregates stabilized with vesicles. As the local temperature of the aqueous stabilizing solution is increased above 25 ^{o} C, the vesicles become less rigid and stabilize the drug particles more effectively leading to smaller particles. For a given stabilizing solution temperature, the particle size also decreases with an increase in preheater temperature due to greater supersaturation in the nozzle and more rapid nucleation. High drug loadings in the aqueous suspensions, as high as 54 mg/mL, could be achieved with particle sizes of ~500 nm. This concentration is ~10 times the equilibrium solubility in the aqueous surfactant solution. From X-ray diffraction data of dry powder samples it was observed that the particles are stabilized rapidly enough to trap the drug in an amorphous state. Long-term stability studies of the suspensions stored at 4 °C indicate only modest particle growth, over 1 month.

4.5 REFERENCES

(1) Pace, S.N. et al. *Pharmaceutical Technology* **1999**, 23, 116-134

(2) Broadhead, J. et al. *Drug Development and Industrial Pharmacy* **1992**, 18 (11-12), 1169-1206

(3) Masters, K. *Spray Drying Handbook*, **1979** John Wiley and Sons

(4) Chasin, M. and Langer, R., eds *Biodegradable Polymers as Drug Delivery Systems*, **1990**, Marcel Dekker, Inc.

(5) Bakan, J.A. In *Encyclopedia of Pharmaceutical Technology* (Vol. 9) (Swarbrick, J. and Boylan, J.C., eds.), **1994**, pp. 423-441, Marcel Dekker, Inc.

(6) Puisieux, F. et al. In *Polymeric Biomaterials* (Dumitrius, S., ed.), **1994**, pp. 749-794, Marcel Dekker, Inc.

(7) Byers, J.E. and Peck, G.E. *Drug Development and Industrial Pharmacy* **1990**, 16 (11), 1761-1779

(8) Aiache, J.M. and Beyssac, E. In *Encyclopedia of Pharmaceutical Technology* (Vol. 12) (Swarbrick, J. and Boylan, J.C., eds.), **1994**, pp. 389-420, Marcel Dekker, Inc.

(9) Illig, K.J. et al. *Pharmaceutical Technology* **1996**, 20, 78-88

(10) Parrott, E.L. In *Encyclopedia of Pharmaceutical Technology* (Vol. 3) (Swarbrick, J. and Boylan, J.C., eds.), **1994**, pp. 101-121, Marcel Dekker, Inc.

(11) Rubinstein, M.H. and Gould, P. *Drug Development and Industrial Pharmacy* **1987**, 13 (1), 81-92

(12) Subramaniam, B. et al. *Journal of Pharmaceutical Sciences* **1997**, 86 (8), 885-890

(13) Phillips, E.M. and Stella, V.J. *International Journal of Pharmaceutics* **1992**, 94, 1-10

(14) Tom, J.W. et al. *The Journal of Supercritical Fluids* **1994**, 7, 9-29

(15) Mawson, S. et al. *Macromolecules* **1995**, 28 (9), 3182-3191

(16) Alessi, P. et al. *Industrial and Engineering Chemistry Research* **1996**, 35, 4718-4726

(17) Mohamed, R.S. et al. In *Supercritical Fluid Science and Technology* (Vol. 406) (Johnston, K.P. and Penninger, J.M.L., eds.), **1989**, pp. 355-378, American Chemical Society

(18) Matson, D.W. *Chemtech* **1989**, 19 (8), 480-486

(19) Chang, C.J. and Randolph, A.D. *AIChE Journal* **1989**, 35 (11), 1876-1882

(20) Domingo, C. et al. *Journal of Supercritical Fluids* **1997**, 10, 39-55

(21) Lele, A.K. and Shine, A.D. *Ind. Eng. Chem. Res.* **1994**, 33, 1476-1485

(22) Krukonis, V.J. In *Supercritical Fluid Extraction and Chromatography: Techniques and Applications* (Vol. 366) (Chapentier, B.A. and Sevenants, M.R., eds.), **1988**, pp. 26-43, American Chemical Society

(23) Charoenchaitrakool, M. et al. *Ind. Eng. Chem. Res.* **2000**, 39 (4794-802)

(24) Debenedetti, P.G. In *Supercritical Fluids: Fundamentals for Application* (Vol. 273) (Kiran, E. and Levelt Sengers, J.M.H., eds.), **1994**, pp. 719-729, Kluwer Academic Publishers

(25) Weber, M. and Thies, M. **2001,** *Personal Communication*

(26) Young, T.J. et al. *Biotech. Progress* **2000**, 16 (3), 402-407

(27) Sun, Y.P. et al. *Ind. Eng. Chem. Res.* **2000**, 39, 5663-5669

(28) Wabel, C. Thesis In *Dept. of Pharmaceutics*, University of Erlangen-Nurnberg, **1998**

(29) Lieberman, H.A. et al., eds *Pharmaceutical dosage forms: disperse systems*, **1998**, Marcel Dekker, Inc.

(30) New, R.R.C., ed. *Liposomes: a practical approach*, **1990**, Oxford University Press

(31) Sujatha, J. and Mishra, A.K. *Journal of Photochemistry and Photobiology A: Chemistry* **1997**, 104, 173-178

(32) Weiner, N. et al. *Drug Development and Industrial Pharmacy* **1989**, 15 (10), 1523-1554

(33) Crowe, J.H. et al. *Biochemical Journal* **1987**, 242, 1-10

(34) Talsma, H. et al. *International Journal of Pharmaceutics* **1991**, 77, 119-126

(35) Cevc, G., ed. *Phospholipids Handbook*, **1993**, Marcel Dekker

(36) Socaciu, C. et al. *Chemistry and Physics of Lipids* **2000**, 106, 79-88

(37) Yang, J. and Appleyard, J. *J. Phys. Chem. B* **2000**, 104, 8097-8100

(38) Grau, A. et al. *Archives of Biochemistry and Biophysics* **2000**, 377 (2), 315-323

(39) Fresta, M. et al. *Journal of Colloid and Interface Science* **2000**, 226, 222-230

(40) Moya, S. et al. *Macromolecules* **2000**, 33, 4538-4544

(41) Shobini, J. and Mishra, A.K. *Spectrochimica Acta Part A* **2000**, 56, 2239-2248

(42) Shine, A.D. U.S.A. 5290827, **1994**, pp. 8, University of Delaware

CHAPTER 5

Conclusions and Recommendations

5.1 CONCLUSIONS

1. The Vapor-over-Liquid PCA (V/L PCA) process was successfully used to encapsulate a protein into PGLA. The PGLA particles had to be large enough to encapsulate the protein and should not agglomerate. In contrast, the primary particles (0.5 to 5 μm) were too small for encapsulation when the solution was sprayed directly into liquid or supercritical CO_2; furthermore, the particles were highly agglomerated. By delaying precipitation in a vapor CO_2 phase over a liquid CO_2 phase, much larger primary particles were formed, from 5 to 70 μm.

2. The amorphous polymer PGLA is highly plasticized by CO_2. Dissolution of CO_2 into PGLA depresses the T_g from the normal value of 45 °C to approximately -40 °C at 276 bar, based upon observation of particle agglomeration. Below -40°C, the polymer remains as a non-sticky free-flowing powder in the presence of CO_2 at 276 bar. Below -30°C, the rate of mixing between CH_2Cl_2 and liquid CO_2 decreases appreciably. At an optimal temperature of -20 °C, the highly viscous PGLA microspheres do not

agglomerate, yet the temperature is high enough to achieve adequate mixing between liquid CO_2 and the organic solution. An additional benefit of operating at colder temperatures is the relatively low pressure. At -20°C, the saturation pressure of CO_2 is 19.7 bar, compared to 61.4 bar at 23 °C. Experimental temperatures of 0 °C or above, or below -30°C yielded only large (>1000 µm) agglomerates. At high temperatures the particles are too sticky due to dissolved CO_2, and at low temperatures, the organic solution and CO_2 mix too slowly.

3. The vapor-over-liquid PCA process forms microspheres in the 5-70 µm range when a 5.0 % solution of PGLA in dichloromethane is sprayed at 0.22 mL/min through a 100 µm diameter nozzle into static CO_2 at -20 °C. Lower concentrations yielded smaller primary particles whereas, highly viscous, concentrated solutions above 10.0 wt. % led to skin formation in the vapor phase and subsequent agglomeration in the liquid CO_2 phase. The thin skin is weak due to low molecular weight and dissolved CO_2, and hence rupturing occurs upon impact at the liquid interface, leading to agglomeration. Particle sizes did not change appreciably with solution flow rate in the "dripping" regime. At the onset of streaming flow, there was a higher percentage of large particles, while the particle size range remained the same. The most spherical and uniform particles ranging in size from 3-25 µm in diameter were produced by flowing CO_2 at high velocity through an annular region in a coaxial nozzle to provide mixing at the interface.

4. Encapsulation of 1-10 μm lysozyme particles proved successful for the 5-70 μm PGLA microspheres for a 1:10 ratio by weight of protein to polymer and a 5 wt % polymer solution. The presence of lysozyme in the particles was demonstrated by SEM analysis, optical microscopy, and EDS. A high encapsulation efficiency for this process is favored by the fact that the protein and polymer precipitate together in small droplets. The use of protein suspensions extends the applicability of the PCA process substantially, since many proteins are insoluble in organic solvents and are less likely to be denatured when suspended.

5. Rapid Expansion from Supercitical to Aqueous Solution (RESAS) incorporates an aqueous stabilizing solution to trap submicron particles of a water-insoluble pharmaceutical compound. In RESAS, the surfactant diffuses rapidly to the particle surface to impede particle agglomeration and growth. Cyclosporine microparticles ~ 0.5 μm in diameter were formed by spraying a 1.0 % (w/w) solution (in CO_2) into 1.0 and 5.0 % (w/w) Tween-80 solutions to prevent microparticle flocculation and agglomeration. RESAS may be expected to be a general process to produce smaller particle sizes of organic and inorganic water-insoluble materials than in the case of RESS into air.

6. By RESAS, cyclosporine particles 500-700 nm in diameter were stabilized for drug concentrations as high as 6.20 mg/mL and 37.5 mg/mL in 1.0 and 5.0 %

(w/w) Tween-80 solutions, respectively. At a drug:surfactant ratio above 0.6-0.7 the surfactant can no longer stabilize the particles, resulting in broader size distributions.

7. Phospholipid vesicles mixed with nonionic surfactants stabilize cyclosporine particles produced by RESAS with mean diameters as small as 200-300 nm. Many of the size distributions are bimodal, according to DLS measurements and TEM, consisting of vesicles with very low drug concentrations and drug particle aggregates stabilized with vesicles. As the local temperature of the aqueous stabilizing solution is increased above 25 ^{o} C, the vesicles become less rigid and stabilize the drug particles more effectively leading to smaller particles. For a given stabilizing solution temperature, the particle size also decreases with an increase in preheater temperature due to greater supersaturation in the nozzle and more rapid nucleation.

8. Using phospholipid stabilizers, high drug loadings in the aqueous suspensions (as high as 54 mg/mL) could be achieved with particle sizes of ~500 nm. This concentration is ~10 times the equilibrium solubility in the aqueous surfactant solution. From X-ray diffraction data of dry powder samples it was observed that the particles are stabilized rapidly enough to trap the drug in an amorphous state. Long-term stability studies of the suspensions stored at 4 °C indicate only modest particle growth, over 1 month.

5.2 RECOMMENDATIONS

1. It is recommended that alternative supercritical fluids should be examined for use in the RESAS process. Since drugs may have limited solubility in SC CO_2, others such as pentane or diethyl ether could be tried. Also, the supercritical solvents could be blended. Also, the possibility of adding cosolvents, such as methanol or acetone, exists.

2. It is recommended that addition of surfactant to the supercritical fluid phase in RESAS be examined. This could enhance solubility in the CO_2 phase if the surfactants chosen form micelles in CO_2. Also, this may allow even faster stabilization of the particles formed since the surfactant and drug are more likely to be in intimate contact during precipitation. Depending on the solubility of surfactant in CO_2, perhaps the total surfactant necessary for particle stabilization could be split between the CO_2 and aqueous phases.

3. It is recommended that other means of testing the particle-surfactant structure in water be evaluated. A possibility includes freeze-fracture SEM, where the solution is frozen and cut providing cross-sectional views of the suspension.

4. It is recommended that other stabilizing surfactants for RESAS be examined. The phenomenon of critical surface area coverage for suspension stability vs. surfactant type and size could be examined more thoroughly.

5. It is recommended that further testing be conducted on drug-active suspensions be performed such as dissolution rates. The rate vs. stabilizer type could be examined. Also, the rate vs. particle size could be examined.

6. It is recommended that method should be developed for the capture of larger quantities of powder from PCA. Powders formed could then be tested for multiple purposes. Encapsulated products could be dissolution rate tested. Drug powders could be tested for crystallinity. Polymer blends could be tested for film-forming and other mechanical properties.

Bibliography

Aiache, J.M. and Beyssac, E. In *Encyclopedia of Pharmaceutical Technology* (Vol. 12) (Swarbrick, J. and Boylan, J.C., eds.), Marcel Dekker, Inc.: New York, **1994**, 389-420.

Alessi, P.; Cortesi, A.; Kikic, I.; Foster, N. R.; Macnaughton, S. J.; Colombo, I. *Industrial and Engineering Chemistry Research* **1996**, *35*, 4718-4726.

Alonso, M. J. In *Microparticulate Systems for the Delivery of Proteins and Vaccines*; Cohen, S. and Bernstein, H., Ed.; Marcel Dekker, Inc.: New York, 1996; Vol. 77, 203-242.

Bailey, P. D. *An Introduction To Peptide Chemistry*; John Wiley & Sons: New York, **1990**.

Bakan, J.A. In *Encyclopedia of Pharmaceutical Technology* (Vol. 9) (Swarbrick, J. and Boylan, J.C., eds.), Marcel Dekker, Inc.: New York, **1994**, 423-441.

Bleich, J.; Kleinebudde, P.; Müller, B. W. *International Journal of Pharmaceutics* **1994**, 106, 77-84.

Bleich, J.; Müller, B. W.; Wabmus, W. *International journal of pharmaceutics* **1993**, 97, 111-7.

Bleich, J.; Müller, B. W. *Journal of Microencapsulation* **1996**, 13, 131-9.

Bodmeier, R. P.; Wang, H.; Dixon, D. J.; Mawson, S.; Johnston, K. P. *Pharmaceutical Research* **1995**, 12, 1211-1217.

Boen, S. N.; Bruch, M. D.; Lele, A. K.; Shine, A. D. In *Polymer Solutions, Blends, and Interfaces*; Noda, I. and Rubingh, D. N., Ed.; Elsevier Science Publishers B.V., **1992**, 151-172.

Broadhead, J. et al. *Drug Development and Industrial Pharmacy* **1992**, 18 (11-12), 1169-1206.

Byers, J.E. and Peck, G.E. *Drug Development and Industrial Pharmacy* **1990**, 16 (11), 1761-1779.

Cavalier, M.; Benoit, J. P.; Thies, C. *Journal of Pharmacy and Pharmacology* **1986**, 38, 249-53.

Cevc, G., ed. *Phospholipids Handbook*, Marcel Dekker, Inc.: New York, **1993**.

Chang, C. J.; Randolph, A. D. *AIChE Journal* **1989**, *35*, 1876-82.

Charoenchaitrakool, M. et al. *Ind. Eng. Chem. Res.* **2000**, 39, 4794-802.

Chasin, M. and Langer, R., eds *Biodegradable Polymers as Drug Delivery Systems*, Marcel Dekker, Inc.: New York, **1990**.

Chou, Y. H.; Tomasko, D. L. *GAS Crystallization of Polymer-Pharmaceutical Composite Particles*; International Society for the Advancement of Supercritical Fluids: Sendai, Japan, **1997**; Vol. A, 55-7.

Condo, P. D.; Paul, D. R.; Johnston, K. P. *Macromolecules* **1994**, 27, 365-371.

Crowe, J.H. et al. *Biochemical Journal* **1987**, 242, 1-10.

Debenedetti, P. G.; Tom, J. W.; Yeo, S. D.; Lim, G. B. *Journal of Controlled Release* **1993**, 24, 27-44.

Debenedetti, P.G. In *Supercritical Fluids: Fundamentals for Application* (Vol. 273) (Kiran, E. and Levelt Sengers, J.M.H., eds.), Kluwer Academic Publsishers, **1994**, pp. 719-729.

Dixon, D. J. *Formation of Polymer Materials by Precipitation with a Compressed Fluid Antisolvent*; University of Texas at Austin: Austin, Texas **1992.**

Dixon, D. J.; Johnston, K. P.; Bodmeier, R. P. *AIChe Journal* **1993**, 39, 127-139.

Dixon, D. J.; Johnston, K. P. *Journal of Applied Polymer Science* **1993**, 50, 1929-1942.

Dixon, D. J.; Luna-Barcenas, G.; Johnston, K. P. *Polymer* **1994**, 35, 3998 - 4005.

Domb, A. J.; Amselem, S.; Maniar, M. In *Polymeric Biomaterials*; Dumitrius, S., Ed.; Marcel Dekker, Inc.: New York, **1994**, 399-433.

Domingo, C.; Berends, E.; van Rosmalen, G. M. *Journal of Supercritical Fluids* **1997**, *10*, 39-55.

Falk, R. F.; Randolph, T. W. *Pharmaceutical Research* **1998**, 15, 1233-7.

Falk, R.; Randolph, T.; Meyer, J. D.; Kelly, R. M.; Manning, M. C. *Journal of Controlled Release* **1997**, 44, 77-85.

Fischer, W.; Müller, B. W. United States 5043280, **1991.**

Fong, J. W.. United States 4384975, **1983.**

Fong, J. W. United States 4166800, **1979.**

Fresta, M. et al. *Journal of Colloid and Interface Science* **2000**, 226, 222-230.

Gallagher, P. M.; Coffey, M. P.; Krukonis, V. J.; Klasuts, N. In *Supercritical Fluid Science and Technology*; Johnston, K. P. and Penninger, J. M. L., Ed.; American Chemical Society: Washington, D.C., 1989; Vol. 406, 334-354.

Grau, A. et al. *Archives of Biochemistry and Biophysics* **2000**, 377 (2), 315-323

Hamaguchi, K.; Hayashi, K. In *Proteins: Structure and Function*; Funatsu, M., Hiromi, K., Imahori, K., Murachi, T. and Narita, K., Ed.; John Wiley & Sons: New York, 1972; Vol. 1, 85-222.

Illig, K.J. et al. *Pharmaceutical Technology* **1996**, 20, 78-88.

Johnston, K. P.; Kim, S.; Combes, J. *Am. Chem. Soc. Symp. Ser.* **1989**, 406, 52-71.

Kim, J. H.; Paxton, T. E.; Tomasko, D. L. *Biotechnology Progress* **1996**, *12*, 650-61.

Kissel, T.; Koneberg, R. In *Microparticulate Systems for the Delivery of Proteins and Vaccines*; Cohen, S. and Bernstein, H., Ed.; Marcel Dekker, Inc.: New York, 1996; Vol. 77, 51-87.

Knutson, B. L.; Debenedetti, P. G.; Tom, J. W. In *Microparticulate Systems for the Delivery of Proteins and Vaccines*; Cohen, S. and Bernstein, H., Ed.; Marcel Dekker, Inc.: New York, 1996, 89-125.

Krukonis, V. J. in *Supercritical Fluid Extraction and Chromatography: Techniques and Applications*; Chapentier, B. A. and Sevenants, M. R., Ed.; American Chemical Society: Washington, D.C., **1988**; Vol. 366, 26-43.

Langer, R. *Chemical Engineering Communications* **1980**, 6, 1-48.

Larson, et al. *Biotechnol. Prog*. **1996.**

Leelarasamee, N.; Howard, S. A.; Malanga, C. J.; Ma, J. K. H *Journal of Microencapsulation* **1988**, 5, 147-57.

Lele, A. K.; Shine, A. D. *AICHE J*. **1992**, 38, 742-752.

Lele, A. K.; Shine, A. D. *Ind. Eng. Chem. Res.* **1994**, *33*, 1476-1485.

Lemert, R. M.; Fuller, R. A.; Johnston, K. P. *J. Phys. Chem.* **1990**, 94, 6021-28.

Lewis, D. H. In *Biodegradable Polymers as Drug Delivery Systems*; Chasin, M. and Langer, R., Ed.; Marcel Dekker, Inc.: New York, 1990; Vol. 45, 1-41.

Lieberman, H.A. et al., eds *Pharmaceutical dosage forms: disperse systems*, Marcel Dekker, Inc.: New York, **1998.**

Luna-Barcenas, G.; Kanakia, S. K.; Sanchez, I. C.; Johnston, K. P. *Polymer* **1995**, 36, 3173-3182.

McHugh, M. A.; Krukonis, V. In *Encyclopedia of Polymer Science and Engineering*; 2nd ed.; Mark, H. F., Bikales, N. M., Overberger, C. G. and Menges, G., Ed.; John Wiley: NY, **1988**; Vol. 16.

McHugh, M. A. *Polymers in Supercritical Fluids*; International Society for the Advancement of Supercritical Fluids: Sendai, Japan, **1997**; Vol. C, 785-8.

McHugh, M. A.; Krukonis, V. J. *Supercritical Fluid Extraction Principles and Practice*; 2nd ed.; Butterworths: Stoneham, MA, **1994.**

Masters, K. *Spray Drying Handbook*, John Wiley and Sons: New York, **1979**.

Mathiowitz, E.; Jacob, J. S.; Jong, Y. S.; Carino, G. P.; Chickering, D. E.; Chaturvedi, P.; Santos, C. A.; Vijayaraghavan, K.; Montgomery, S.; Bassett, M.; Morrell, C. *Nature* **1997**, 386, 410-4.

Matson, D. W.; Petersen, R. C.; Smith, R. D. *J. Mater. Sci.* **1987**, 22, 1919-1928.

Matson, D. W.; Fulton, J. L.; Peterson, R. C.; Smith, R. D. *Ind. Eng. Chem. Res.* **1987**, 26, 2298-2306.

Matson, D. W. *Chemtech* **1989**, *19*, 480-6.

Mawson, S.; Johnston, K. P.; Combes, J. R.; DeSimone, J. M. *Macromolecules* **1995**, *28*, 3182-3191.

Mawson, S.; Johnston, K. P.; Betts, D. E.; McClain, J. B.; DeSimone, J. M. *Macromolecules* **1997**, 30, 71-77.

Mawson, S. *The Formation and Characterization of Polymeric Materials Precipitated by CO2-Based Spray Processes*; University of Texas at Austin: Austin,Texas **1996**.

Mawson, S.; Kanakia, S.; Johnston, K. P. *Journal of Applied Polymer Science* **1997**.

Mawson, S.; Kanakia, S.; Johnston, K. P. *Polymer* **1997**, 38, 2957-2967.

Mohamed, R. S.; Halverson, D. S.; Debenedetti, P. G.; Prud'homme, R. K. in *Supercritical Fluid Science and Technology*; Johnston, K. P. and Penninger, J. M. L., Ed.; American Chemical Society: Washington D.C., **1989**; Vol. 406, 355-78.

Moya, S. et al. *Macromolecules* **2000**, 33, 4538-4544.

New, R.R.C., ed. *Liposomes: a practical approach*, Oxford University Press, **1990**.

Pace, S.N. et al. *Pharmaceutical Technology* **1999**, 23, 116-134Park, T. G.; Alonso, M. J.; Langer, R. *Journal of Applied Polymer Science* **1994**, 52, 1797-1807.

Parrott, E.L. In *Encyclopedia of Pharmaceutical Technology* (Vol. 3) (Swarbrick, J. and Boylan, J.C., eds.),Marcel Dekker, Inc.: New York, **1994**, 101-121.

Phillips, E. M.; Stella, V. J. *International Journal of Pharmaceutics* **1992**, *94*, 1-10.

Puisieux, F. et al. In *Polymeric Biomaterials* (Dumitrius, S., ed.), Marcel Dekker, Inc.: New York, **1994**, 749-794.

Randolph, T. W.; Randolph, A. J.; Mebes, M.; Yeung, S. *Biotechnology Progress* **1993**, 9, 429-435.

Reverchon, et al. *J. Supercrit. Fluids* **1993**, *6*, 241-8

Rubinstein, M.H. and Gould, P. *Drug Development and Industrial Pharmacy* **1987**, 13 (1), 81-92.

Ruchatz, F.; Kleinebudde, P.; Müller, B. W. *Journal of Pharmaceutical Sciences* **1997**, 86, 101-5.

Schwendeman, S. P.; Cardamone, M.; Klibanov, A.; Langer, R.; Brandon, M. R. In *Microparticulate Systems for the Delivery of Proteins and Vaccines*; Cohen, S. and Bernstein, H., Ed.; Marcel Dekker, Inc.: New York, **1996**; Vol. 77, 1-49.

Shine, A.D. U.S.A. 5290827, **1994**, pp. 8, University of Delaware.

Shobini, J. and Mishra, A.K. *Spectrochimica Acta Part A* **2000**, 56, 2239-2248.

Socaciu, C. et al. *Chemistry and Physics of Lipids* **2000**, 106, 79-88.

Spenlehauer, G.; Veillard, M.; Benoit, J. P. *Journal of Pharmaceutical Sciences* **1986**, 75, 750-5.

Steckel, H.; Thies, J.; Müller, B. W. *International Journal of Pharmaceutics* **1997**, 152, 99-110.

Subra, et al. *High Pressure Chemical Engineering* **1996**, *12* 49-54.

Subramaniam, B.; Rajewski, R. A.; Snavely, K. *Journal of Pharmaceutical Sciences* **1997**, *86*, 885-90.

Sujatha, J. and Mishra, A.K. *Journal of Photochemistry and Photobiology A: Chemistry* **1997**, 104, 173-178.

Sun, Y.P. et al. *Ind. Eng. Chem. Res.* **2000**, 39, 5663-5669.

Talsma, H. et al. *International Journal of Pharmaceutics* **1991**, 77, 119-126.

Thanoo, B. C.; Doll, W. J.; Mehta, R. C.; Digenis, G. A.; DeLuca, P. P. *Pharmaceutical Research* **1995**, 12, 2060-4.

Tom, J. W.; Debenedetti, P. G. *Biotechnolgy Progress* **1991**, 7, 403-411.

Tom, J. W.; Debenedetti, P. G. *Journal of Aerosol Science* **1991**, 22, 555-584.

Tom, J. W.; Debenedetti, P. G. *The Journal of Supercritical Solutions* **1994**, *7*, 9-29.

Wabel, C. Thesis In *Dept. of Pharmaceutics*, University of Erlangen-Nurnberg, **1998.**

Weber, M. and Thies, M. **2001,** *Personal Communication.*

Weiner, N. et al. *Drug Development and Industrial Pharmacy* **1989**, 15 (10), 1523-1554.

Winters, M. A.; Debenedetti, P. G.; Barey, J.; Sparks, H. G.; Sane, S. U.; Przybycien, T. M. *Pharmaceutical Research* **1997**, 14, 1370-8.

Winters, M. A.; Knutson, B. L.; Debenedetti, P. B.; Sparks, H. G.; Przybycien, T. M.; Stevenson, C. L.; Prestrelski, S. J. *Journal of Pharmaceutical Sciences* **1996**, 85, 586-594.

Yang, J. and Appleyard, J. *J. Phys. Chem. B* **2000**, 104, 8097-8100.

Yeo, S. D.; Lim, G. B.; Debenedetti, P. G.; Bernstein, H. *Biotechnology and Bioengineering* **1993**, 41, 341-346.

Yeo, S.-D.; Debenedetti, P. G.; Radosz, M.; Schmidt, H.-W. *Macromolecules* **1993**, 26, 6207-6210.

Yeo, S. D.; Debenedetti, P. G.; Patro, S. Y.; Przybycien, T. M. *Journal of Pharmaceutical Sciences* **1994**, 83, 1651-1656.

Young, T.J. et al. *Biotech. Progress* **2000**, 16 (3), 402-407.